J Elast (2013) 112:139–183
DOI 10.1007/s10659-012-9404-3

Tangent Second-Order Estimates for the Large-Strain, Macroscopic Response of Particle-Reinforced Elastomers

Reza Avazmohammadi · Pedro Ponte Castañeda

Received: 15 March 2012 / Published online: 5 September 2012

Abstract An approximate homogenization method is proposed and used to obtain estimates for the effective constitutive behavior and associated microstructure evolution in hyperelastic composites undergoing finite-strain deformations. The method is a modified version of the "tangent second-order" procedure (Ponte Castañeda and Tiberio in J. Mech. Phys. Solids 48:1389, 2000), and can be used to provide estimates for the nonlinear elastic composites in terms of corresponding estimates for suitably chosen "linear comparison composites". The method makes use of the "tangent" moduli of the phases, evaluated at suitable averages of the deformation gradient, and yields a constitutive relation accounting for the evolution of characteristic features of the underlying microstructure in the composites, when subjected to large deformations. Satisfaction of the exact, macroscopic incompressibility constraint is ensured by means of an energy decoupling approximation splitting the elastic energy into a purely "distortional" component, together with a "dilatational" component. The method is applied to elastomers containing random distributions of aligned, rigid, ellipsoidal inclusions, and explicit analytical estimates are obtained for the special case of spherical inclusions distributed isotropically in an incompressible neo-Hookean matrix. In addition, the method is also applied to two-dimensional composites with random distributions of aligned, elliptical fibers, and the results are compared with corresponding results of earlier homogenization estimates and finite element simulations.

Keywords Composite materials · Reinforced rubbers · Particle rotations · Homogenization · Ellipsoidal inclusions

Mathematics Subject Classification 49S05 · 74B20 · 74Q15 · 74Q05

R. Avazmohammadi · P. Ponte Castañeda (✉)
Department of Mechanical Engineering and Applied Mechanics, University of Pennsylvania, Philadelphia, PA 19104-6315, USA
e-mail: ponte@seas.upenn.edu

1 Introduction

The study of the effective response of hyperelastic composites with *random* or *periodic* microstructures has found renewed attention in the literature due to its practical relevance for soft materials, such as, for example, biological tissues [8, 12], thermoplastic elastomers [17, 31], and reinforced rubbers [5, 6]. Because of the considerable flexibility of these materials in the elastic regime, their microstructure evolves with the deformation, and this is expected to have a significant impact on their macroscopic response. It follows that accurate models for the constitutive behavior of such materials must account for the *geometric* nonlinearities associated with the evolution of microstructure, as well as the *constitutive* nonlinearities associated with the constitutive response of the constituent phases. With this goal in mind, two different nonlinear homogenization methods have been developed recently for hyperelastic composites by means of variational principles [33] for the properties of suitably chosen "linear comparison composites" (LCC). Both methods have the distinguishing feature of being exact to second order in the heterogeneity contrast of the phases, and for this reason they are known as "second-order" methods. The first method, which was proposed by Ponte Castañeda and Tiberio [36] building on earlier work for viscoplastic composites [35, 38], identifies the modulus tensors of the phases in the LCC with the tangent modulus tensors of the hyperelastic phases, evaluated at the phase averages of the deformation fields in the LCC, and is known as the "tangent second-order" (TSO) method. The second method, which was developed by Lopez-Pamies and Ponte Castañeda [23, 25] building on earlier work for viscoplastic composites [36], makes use of additional information about the second moments of the fluctuations of the deformation gradients in the LCC to define an alternative linearization of the nonlinear constitutive response of the hyperelastic phases leading to more accurate predictions, especially at higher concentration of the phases, and goes by the label of "generalized second-order" (GSO) homogenization method. Applications for two-dimensional composites containing periodic and random distributions of aligned, rigid, elliptical fibers in an elastomeric matrix have been given by Lahellec et al. [20] and Lopez-Pamies and Ponte Castañeda [24, 26], using a modified version of the TSO and GSO methods, respectively. More general results for fiber-reinforced elastomers subjected to three-dimensional loading conditions with periodic and random distributions of fibers have been provided by Brun et al. [7] and Agoras et al. [2, 3], respectively, by means of the GSO method. In addition, Bouchart et al. [6] have presented an application of the TSO method for three-dimensional reinforced rubbers, while Racherla et al. [39] provided an application of the TSO method for polydomain thermoplastic elastomers with lamellar microstructures. Finally, it should be mentioned that a novel homogenization approach for hyperelastic composites has been proposed recently by deBotton [9], and developed further by deBotton et al. [10] and Lopez-Pamies and Idiart [22], building on earlier work for nonlinear composites with "sequentially laminated" microstructures [15, 18, 34].

In spite of the significant progress that has been made to date, there are still significant barriers for the general implementation of all the presently available nonlinear homogenization methods for hyperelastic composites. The TSO method is the easiest to use, but it can give unreliable estimates for large concentrations and strongly nonlinear behavior of the constituent phases, including the failure to capture (unless appropriately modified) the overall incompressibility constraint for incompressible phases. The GSO method seems to provide the most reliable predictions, but it is more difficult to use than the TSO method and thus far has only been used for continuous fiber composites. On the other hand, the "sequentially laminated" homogenization is the most recent, and thus far it has only been used successfully for neo-Hookean phases, requiring the solution of difficult nonlinear PDE more generally.

The main goal of this work is to develop a general, three-dimensional model based on the TSO method of Ponte Castañeda and Tiberio [36] for the effective behavior of elastomeric composite materials subjected to finite deformations. Thus, we provide analytical estimates for the effective behavior of dilute and non-dilute composites that are capable of accounting for general (ellipsoidal) particle shapes and distribution, as well as general three-dimensional loading conditions (including nonaligned loadings). In addition, evolution laws can be obtained for the relevant microstructural variables, including particle orientations. It is also worth emphasizing that the new estimates recover the exact overall incompressibility constraint for the special case of rigidly reinforced elastomers with incompressible matrix phases. Furthermore, the resulting constitutive model can be used to detect macroscopic material failure in the form of loss of strong ellipticity (or rank-one convexity) of the associated homogenized behavior [14], although this will not be pursued in detail in this work.

The paper is organized as follows. Sections 2 and 3 describe in some detail the tangent second-order homogenization method. Section 4 presents the main results of the paper, namely, the derivation of the homogenized constitutive relation for particle-reinforced elastomers with general ellipsoidal microstructures and incompressible matrix behavior, including the development of evolution laws for the average orientation of the particles with the deformation. The principal features of this model are examined within the context of 2-D and 3-D examples, respectively, in Sects. 5 and 6. Thus, Sect. 5 deals with the application to elastomers reinforced with cylindrical fibers of elliptical cross-section under (transverse) plane-strain loading. More specific results are presented and compared with corresponding GSO estimates for composites with circular fibers, as well as with FEM results from the literature. In Sect. 6, the results of Sect. 4 are applied to the class of statistically isotropic composites consisting of an incompressible, elastomeric matrix reinforced by rigid spherical inclusions. In both examples, the influence of the particle volume fraction, matrix properties and loading conditions on the macroscopic behavior of the composite is investigated. Finally, some conclusion are drawn in Sect. 7.

2 Hyperelastic Composites

Consider a material consisting of N different (homogeneous) phases, which are assumed to be distributed *randomly* in a specimen occupying a volume Ω_0 with boundary $\partial\Omega_0$ in the undeformed configuration. Furthermore, the characteristic length-scale of the inhomogeneities (e.g., particles, or voids) is much smaller than the size of the specimen and the scale of variation of the loading conditions. Let the position vector of a material point in the undeformed configuration Ω_0 be denoted by $\mathbf{X}$, with Cartesian components X_i, $i \in \{1, 2, 3\}$ and the corresponding position vector in the deformed configuration Ω be denoted by $\mathbf{x}$, with components x_i. The deformation gradient tensor represented by $\mathbf{F}$ has components $F_{ij} = \partial x_i/\partial X_j$ and is required to satisfy the material *impenetrability* condition: $J = \det\mathbf{F}(\mathbf{X}) > 0$ for all $\mathbf{X} \in \Omega_0$. In addition, let $\mathbf{F} = \mathbf{RU}$ where $\mathbf{U}$ and $\mathbf{R}$ stand for the stretch and (*rigid-body*) rotation tensors, respectively, and let $\mathbf{C} = \mathbf{F}^T\mathbf{F} = \mathbf{U}^2$ denote the right Cauchy–Green deformation tensor.

We assume that the constitutive behavior of the phases is purely elastic and characterized by the stored-energy functions $W^{(r)}(\mathbf{F})$ $(r = 1, \ldots, N)$, which are taken to be *nonconvex* functions of the deformation gradient tensor $\mathbf{F}$, such that the local energy function of the composite may be written as

$$W(\mathbf{X}, \mathbf{F}) = \sum_{r=1}^{N} \chi^{(r)}(\mathbf{X})\, W^{(r)}(\mathbf{F}). \tag{1}$$

In the above equation, the characteristic functions $\chi^{(r)}$, describing the distribution of the phases in the reference configuration, are such that they equal 1 if the position vector $\mathbf{X}$ is inside the phase r (i.e., $\mathbf{X} \in \Omega_0^{(r)}$) and zero otherwise. The stored-energy functions $W^{(r)}(\mathbf{F})$ are assumed to be objective, namely, $W^{(r)}(\mathbf{QF}) = W^{(r)}(\mathbf{F})$ for all proper orthogonal tensors $\mathbf{Q}$ and arbitrary deformation gradients $\mathbf{F}$, so that $W^{(r)}(\mathbf{F}) = W^{(r)}(\mathbf{U})$. The local or microscopic constitutive relation for the composite is then given by

$$\mathbf{S} = \frac{\partial W(\mathbf{X}, \mathbf{F})}{\partial \mathbf{F}}, \tag{2}$$

where $\mathbf{S}$ stands for the first Piola-Kirchhoff stress tensor.

Following Hill [16], the effective stored-energy function $\widetilde{W}$ of the composite elastomer is defined by

$$\widetilde{W}(\bar{\mathbf{F}}) = \min_{\mathbf{F} \in K(\bar{\mathbf{F}})} \big\langle W(\mathbf{X}, \mathbf{F}) \big\rangle = \min_{\mathbf{F} \in K(\bar{\mathbf{F}})} \sum_{r=1}^{N} c_0^{(r)} \big\langle W^{(r)}(\mathbf{F}) \big\rangle^{(r)}, \tag{3}$$

where $K(\bar{\mathbf{F}})$ denotes the set of kinematically admissible deformation gradients:

$$K(\bar{\mathbf{F}}) = \big\{ \mathbf{F} | \exists \mathbf{x} = \mathbf{x}(\mathbf{X}) \text{ with } \mathbf{F} = \operatorname{Grad} \mathbf{x} \text{ and } J > 0 \text{ in } \Omega_0, \mathbf{x} = \bar{\mathbf{F}}\mathbf{X} \text{ on } \partial\Omega_0 \big\}. \tag{4}$$

In the above expressions, the triangular brackets $\langle \cdot \rangle$ and $\langle \cdot \rangle^{(r)}$ denote volume averages (in the undeformed configuration) over the domains Ω_0 and $\Omega_0^{(r)}$, respectively, so that the scalar $c_0^{(r)} = \langle \chi^{(r)} \rangle$ indicates the initial volume fraction of the phase r.

In the neighborhood of $\bar{\mathbf{F}} = \mathbf{I}$ (where $\mathbf{I}$ is the second-order identity tensor), the solution of the Euler-Lagrange equations associated with the variational problem (3) is unique, and gives the minimum energy. As the deformation progresses into the finite deformation regime, the composite may reach a point at which this "principal" solution bifurcates into lower energy solutions. This point corresponds to the onset of an instability, beyond which the applicability of the "principal" solution becomes questionable. However, it is still possible to extract useful information from the principal solution by computing the associated macroscopic instabilities from the loss of strong ellipticity of the homogenized behavior. Based on these remarks, in this work, we will estimate the overall behavior of composite elastomers by means of the effective stored-energy function

$$\widehat{W}(\bar{\mathbf{F}}) = \operatorname*{stat}_{\mathbf{F} \in K(\bar{\mathbf{F}})} \sum_{r=1}^{N} c_0^{(r)} \big\langle W^{(r)}(\mathbf{F}) \big\rangle^{(r)}, \tag{5}$$

instead of solving the variational problem (3). From its definition, it is clear that $\widetilde{W}(\bar{\mathbf{F}}) = \widehat{W}(\bar{\mathbf{F}})$ from $\bar{\mathbf{F}} = \mathbf{I}$ up to the onset of the first instability, beyond which $\widetilde{W}(\bar{\mathbf{F}}) \leq \widehat{W}(\bar{\mathbf{F}})$. Moreover, it is often the case [14] that the first instability is indeed a long wavelength instability, as characterized by the loss of strong ellipticity of $\widetilde{W}(\bar{\mathbf{F}})$. Furthermore, it is worth stating that $\widehat{W}(\bar{\mathbf{F}})$ is an *objective* function of the macroscopic deformation gradient $\bar{\mathbf{F}}$, by virtue of its definition (5) and of the objectivity assumption for the $W^{(r)}$.

Noting that under the affine boundary condition $\langle \mathbf{F} \rangle = \bar{\mathbf{F}}$, and defining the average stress $\bar{\mathbf{S}} = \langle \mathbf{S} \rangle$, the effective constitutive relation for the composite is given by [16]

$$\bar{\mathbf{S}} = \frac{\partial \widetilde{W}}{\partial \bar{\mathbf{F}}}(\bar{\mathbf{F}}). \tag{6}$$

In the next section, we present a concise review of the "tangent second-order" homogenization procedure, including its specialization for the case of two-phase elastomeric composites.

3 Tangent Second-Order Method

In this section, we recall the tangent second-order (TSO) method of Ponte Castañeda and Tiberio [36] (see also [35, 38]) in order to generate *new* estimates for the effective stored-energy function $\widetilde{W}(\bar{\mathbf{F}})$ for the above-described elastomeric composite. The main concept behind the TSO method is the construction of a fictitious "linear comparison composite" (LCC), with the same microstructure (i.e., same characteristic functions $\chi^{(r)}(\mathbf{X})$) as the actual (nonlinear) composite material (in the undeformed configuration). The constituent phases of the LCC are identified with appropriate linearizations of the given nonlinear phases resulting from suitable variational principles. This allows the use of already available methods to estimate the effective behavior of linear composites to generate corresponding estimates for nonlinear composites.

Similar to relation (1), the local stored-energy function of the LCC can be formally expressed as

$$W_T(\mathbf{X},\mathbf{F}) = \sum_{r=1}^{N} \chi^{(r)}(\mathbf{X}) W_T^{(r)}(\mathbf{F}), \tag{7}$$

where $W_T^{(r)}(\mathbf{F})$ is the energy potential of phase r in the LCC, which may in turn be rewritten in the form

$$W_T^{(r)}(\mathbf{F}) = f^{(r)} + \mathbf{T}^{(r)} \cdot \mathbf{F} + \frac{1}{2}\mathbf{F} \cdot \mathbf{L}^{(r)}\mathbf{F}, \tag{8}$$

where the "thermal stress" $\mathbf{T}^{(r)}$ and "specific heat" $f^{(r)}$ are defined as

$$\begin{aligned} \mathbf{T}^{(r)} &= \mathbf{S}^{(r)}\big(\mathbf{F}^{(r)}\big) - \mathbf{L}^{(r)}\mathbf{F}^{(r)}, \\ f^{(r)} &= W^{(r)}\big(\mathbf{F}^{(r)}\big) - \mathbf{T}^{(r)} \cdot \mathbf{F}^{(r)} - \frac{1}{2}\mathbf{F}^{(r)} \cdot \mathbf{L}^{(r)}\mathbf{F}^{(r)}. \end{aligned} \tag{9}$$

In these expressions, the $\mathbf{F}^{(r)}$ are constant, reference, second-order tensors, while the $\mathbf{L}^{(r)}$ are uniform, (major) symmetric, fourth-order tensors, which are usually identified with the tangent modulus tensors of the phases, evaluated at the corresponding reference deformations $\mathbf{F}^{(r)}$, i.e.,

$$\mathbf{L}^{(r)} = \mathbf{L}_t^{(r)}\big(\mathbf{F}^{(r)}\big) = \frac{\partial^2 W^{(r)}}{\partial \mathbf{F}\, \partial \mathbf{F}}\big(\mathbf{F}^{(r)}\big). \tag{10}$$

In addition, use has been made of the notation

$$\mathbf{S}^{(r)} = \frac{\partial W^{(r)}}{\partial \mathbf{F}}\big(\mathbf{F}^{(r)}\big). \tag{11}$$

If all the phases in the LCC are characterized by potentials of the form (8), it follows from the linearity of the problem that the effective potential of the LCC can be written as [36]

$$\widetilde{W}_T(\mathbf{F}) = \tilde{f} + \tilde{\mathbf{T}} \cdot \bar{\mathbf{F}} + \frac{1}{2}\bar{\mathbf{F}} \cdot \tilde{\mathbf{L}}\bar{\mathbf{F}}, \tag{12}$$

where $\tilde{\mathbf{L}}$ is the effective modulus tensor of the linear-elastic comparison composite, and $\tilde{\mathbf{T}}$ and $\tilde{f}$ are the effective thermal stress and specific heat, respectively. For two-phase composites, the expressions for $\tilde{\mathbf{T}}$ and $\tilde{f}$ are given by [21, 36]

$$\tilde{\mathbf{T}} = \bar{\mathbf{T}} + (\tilde{\mathbf{L}} - \bar{\mathbf{L}})(\Delta\mathbf{L})^{-1}\Delta\mathbf{T}, \tag{13}$$

$$\tilde{f} = \bar{f} + \frac{1}{2}\Delta\mathbf{T}(\Delta\mathbf{L})^{-1} \cdot (\tilde{\mathbf{L}} - \bar{\mathbf{L}})(\Delta\mathbf{L})^{-1}\Delta\mathbf{T}, \tag{14}$$

where $\Delta\mathbf{T} = \mathbf{T}^{(1)} - \mathbf{T}^{(2)}$, and $\Delta\mathbf{L} = \mathbf{L}^{(1)} - \mathbf{L}^{(2)}$. Furthermore, $\bar{f}$, $\bar{\mathbf{T}}$, and $\bar{\mathbf{L}}$ are the volume averages of f, $\mathbf{T}$ and $\mathbf{L}$. Using Eqs. (13) and (14) in (12), the effective potential associated with the LCC for two-phase composites can be written as

$$\begin{aligned}\widetilde{W}_T = \bar{f} + \frac{1}{2}(\Delta\mathbf{L}_0)^{-1}\Delta\mathbf{T} \cdot (\tilde{\mathbf{L}} - \bar{\mathbf{L}})(\Delta\mathbf{L})^{-1}\Delta\mathbf{T} \\ + \big[\bar{\mathbf{T}} + (\tilde{\mathbf{L}} - \bar{\mathbf{L}})(\Delta\mathbf{L})^{-1}\Delta\mathbf{T}\big] \cdot \bar{\mathbf{F}} + \frac{1}{2}\bar{\mathbf{F}} \cdot \tilde{\mathbf{L}}\bar{\mathbf{F}}.\end{aligned} \tag{15}$$

Within the context of the *tangent* second-order theory, Ponte Castañeda and Tiberio [36] made use the prescriptions $\mathbf{F}^{(r)} = \bar{\mathbf{F}}^{(r)}$ for the LCC and obtained the following estimate for the stored-energy function of N-phase, *hyperelastic composites*

$$\widehat{W}(\bar{\mathbf{F}}) = \sum_{r=1}^{N} c^{(r)} \left\{ W^{(r)}\big(\bar{\mathbf{F}}^{(r)}\big) + \frac{1}{2}\big(\bar{\mathbf{F}} - \bar{\mathbf{F}}^{(r)}\big) \cdot \mathbf{S}^{(r)}\big(\bar{\mathbf{F}}^{(r)}\big) \right\}, \tag{16}$$

where the variables $\bar{\mathbf{F}}^{(r)}$ are the phase averages of the deformation gradient field in the LCC. For two-phase composites, $\bar{\mathbf{F}}^{(1)}$ and $\bar{\mathbf{F}}^{(2)}$ are determined by means of the system of equations [36]

$$\bar{\mathbf{F}} = c_0^{(1)}\bar{\mathbf{F}}^{(1)} + c_0^{(2)}\bar{\mathbf{F}}^{(2)}, \tag{17}$$

$$\bar{\mathbf{F}}^{(2)} = \bar{\mathbf{F}} - \frac{1}{c_0^{(2)}}(\Delta\mathbf{L})^{-1}(\tilde{\mathbf{L}} - \bar{\mathbf{L}})(\Delta\mathbf{L})^{-1}\big[\Delta\mathbf{S} + \mathbf{L}^{(1)}\big(\bar{\mathbf{F}} - \bar{\mathbf{F}}^{(1)}\big) - \mathbf{L}^{(2)}\big(\bar{\mathbf{F}} - \bar{\mathbf{F}}^{(2)}\big)\big], \tag{18}$$

where $\Delta\mathbf{S} = \mathbf{S}^{(1)}(\bar{\mathbf{F}}^{(1)}) - \mathbf{S}^{(2)}(\bar{\mathbf{F}}^{(2)})$, and the first equation describes as the overall average deformation condition. After some algebra, Eq. (18) can alternatively be written in the form

$$\bar{\mathbf{F}} - \bar{\mathbf{F}}^{(2)} = \big[c_0^{(2)}\big(\tilde{\mathbf{L}} - \mathbf{L}^{(1)}\big)^{-1} + (\Delta\mathbf{L})^{-1}\big]\big[\mathbf{L}^{(1)}\big(\bar{\mathbf{F}}^{(1)} - \bar{\mathbf{F}}^{(2)}\big) - \Delta\mathbf{S}\big]. \tag{19}$$

In this work, we make use of the generalized estimate of the Willis type [37, 40] for the effective modulus tensor $\tilde{\mathbf{L}}$ of the LCC. This type of estimate is known to be quite accurate for the type of "particulate" random microstructures, up to moderate concentrations of inclusions. For two-phase composites, this estimate is given by

$$\tilde{\mathbf{L}} = \mathbf{L}^{(1)} + c_0^{(2)}\big[c_0^{(1)}\mathbf{P} - (\Delta\mathbf{L})^{-1}\big]^{-1} \tag{20}$$

where the microstructural tensor $\mathbf{P}$ contains information about the shape and distribution of the particles in the undeformed configuration [37]. The general expression for the components of the tensor $\mathbf{P}$ associated with an ellipsoidal inclusion, defined by

$$D_0 = \big\{\mathbf{X} : \mathbf{X}^T\big(\mathbf{Z}_0^T\mathbf{Z}_0\big)\mathbf{X} < 1\big\}, \tag{21}$$

in an infinite matrix with the elastic modulus tensor $\mathbf{L}^{(1)}$, is given by

$$P_{ijkl} = \frac{1}{4\pi |\mathbf{Z}_0|} \int_{|\boldsymbol{\xi}|=1} H_{ijkl}(\boldsymbol{\xi}) \left[\boldsymbol{\xi}^T \left(\mathbf{Z}_0^T \mathbf{Z}_0\right)^{-1} \boldsymbol{\xi}\right]^{\frac{-3}{2}} dS, \tag{22}$$

where the symmetric, second-order tensor $\mathbf{Z}_0$ serves to characterize the shape and orientation of the inclusion. In addition, $\mathbf{H}$ is a fourth-order tensor with components $B_{ik}(\boldsymbol{\xi})\xi_j\xi_l$, and $\mathbf{B}$ denotes the inverse of the acoustic tensor $\mathbf{K}$ with components

$$K_{ik} = L^{(1)}_{ijkl}\xi_j\xi_l. \tag{23}$$

Making use of the Willis estimate (20), the *implicit* tensorial equation (19) for the variable $\bar{\mathbf{F}}^{(2)}$ may be re-written as

$$\bar{\mathbf{F}} - \bar{\mathbf{F}}^{(2)} = \left(1 - c_0^{(2)}\right)\mathbf{P}\left[\mathbf{L}^{(1)}\left(\bar{\mathbf{F}}^{(1)} - \bar{\mathbf{F}}^{(2)}\right) - \Delta\mathbf{S}\right]. \tag{24}$$

In summary, the variational estimate (16) for two-phase composites depends explicitly only on the variables $\bar{\mathbf{F}}^{(1)}$ and $\bar{\mathbf{F}}^{(2)}$ corresponding to the average values of the deformation gradient over the phases of the chosen LCC with the strain energies defined in (8). Hence, the implementation of this estimate, in general, requires the calculation of the 18 unknown components of $\bar{\mathbf{F}}^{(1)}$ and $\bar{\mathbf{F}}^{(2)}$ using the relations (24) and (17), which constitute a system of 18 scalar, algebraic equations. Having computed these components for given macroscopic loading, phases characteristics and microstructure, the second-order estimate for the effective stored-energy function $\widehat{W}(\bar{\mathbf{F}})$ for particle-reinforced elastomers can be, in turn, obtained from (16).

4 Rigidly Reinforced Composites

4.1 Tangent Second-Order Estimates

In this section, we confine our attention to the special case of rigid particles, and our objective is to obtain a simplified form for the effective stored-energy function (16) and the associated kinematical equation (19) in this case. In order to characterize the constitutive response of the rigid particles, we assume without loss of generality that the stored-energy function of the particle phase is given by

$$W^{(2)}(\mathbf{F}) = \frac{1}{2}\mu^{(2)}\left[\mathrm{tr}\left(\mathbf{F}^T\mathbf{F}\right) - 3 - 2\ln(\det\mathbf{F})\right] + \frac{1}{2}\mu'^{(2)}(\det\mathbf{F} - 1)^2, \tag{25}$$

such that the rigid behavior of the particles is obtained by taking the limit as the Lamé moduli $\mu^{(2)}$ and $\mu'^{(2)}$ tend to infinity. It should be remarked that the stored-energy function (25) is zero if and only if $\mathbf{F} = \mathbf{R}$, where $\mathbf{R}$ stands for a rotation tensor. This indicates that the particles can only undergo a rigid-body rotation in the limit $\mu^{(2)}, \mu'^{(2)} \to \infty$.

Introducing the small parameter ι, defined by

$$\iota = 1/\mu^{(2)} = \alpha/\mu'^{(2)}, \tag{26}$$

in which α is an arbitrary constant, we consider the following regular expansion for $\bar{\mathbf{F}}^{(2)}$ as ι tends to zero

$$\bar{\mathbf{F}}^{(2)} = \bar{\mathbf{F}}^{(2)}_0 + \iota\bar{\mathbf{F}}^{(2)}_1 + O\left(\iota^2\right). \tag{27}$$

The corresponding asymptotic expansions for $(\bar{\mathbf{F}}^{(2)})^{-1}$ and $\bar{J}^{(2)} = \det \bar{\mathbf{F}}^{(2)}$ are given by

$$\begin{aligned}\big(\bar{\mathbf{F}}^{(2)}\big)^{-1} &= \big[\bar{\mathbf{F}}_0^{(2)} + \iota\bar{\mathbf{F}}_1^{(2)} + O\big(\iota^2\big)\big]^{-1} \\ &= \big(\bar{\mathbf{F}}_0^{(2)}\big)^{-1} - \iota\big(\bar{\mathbf{F}}_0^{(2)}\big)^{-1}\bar{\mathbf{F}}_1^{(2)}\big(\bar{\mathbf{F}}_0^{(2)}\big)^{-1} + O\big(\iota^2\big), \qquad (28)\\ \bar{J}^{(2)} &= \bar{J}_0^{(2)} + \iota\bar{J}_1^{(2)} + O\big(\iota^2\big), \qquad (29)\end{aligned}$$

where

$$\bar{J}_0^{(2)} = \det\bar{\mathbf{F}}_0^{(2)}, \qquad (30)$$

$$\bar{J}_1^{(2)} = \mathrm{tr}\big[\big(\bar{\mathbf{F}}_0^{(2)}\big)^{*}\bar{\mathbf{F}}_1^{(2)}\big], \qquad (31)$$

in which the superscript $*$ refers to the adjugate tensor.

Next, using the strain energy (25), along with the expansions (27)–(29), the nominal stress expansion in phase 2 is written as

$$\mathbf{S}^{(2)}\big(\bar{\mathbf{F}}^{(2)}\big) = \iota^{-1}\mathbf{S}_{-1}^{(2)} + \mathbf{S}_0^{(2)} + O(\iota), \qquad (32)$$

where

$$\mathbf{S}_{-1}^{(2)} = \bar{\mathbf{F}}_0^{(2)} - \big(\bar{\mathbf{F}}_0^{(2)}\big)^{-T} + \alpha\bar{J}_0^{(2)}\big(\bar{J}_0^{(2)} - 1\big)\big(\bar{\mathbf{F}}_0^{(2)}\big)^{-T}, \qquad (33)$$

and

$$\begin{aligned}\mathbf{S}_0^{(2)} = \bar{\mathbf{F}}_1^{(2)} &+ \big[1 - \alpha\bar{J}_0^{(2)}\big(\bar{J}_0^{(2)} - 1\big)\big]\big(\bar{\mathbf{F}}_0^{(2)}\big)^{-T}\big(\bar{\mathbf{F}}_1^{(2)}\big)^{T}\big(\bar{\mathbf{F}}_0^{(2)}\big)^{-T} \\ &+ \alpha\bar{J}_1^{(2)}\big(2\bar{J}_0^{(2)} - 1\big)\big(\bar{\mathbf{F}}_0^{(2)}\big)^{-T}. \qquad (34)\end{aligned}$$

Moreover, the average rotational balance equation in phase 2 (which is a consequence of the objectivity of the chosen strain energy)

$$\big(\bar{\mathbf{F}}^{(2)}\big)^{T}\mathbf{S}^{(2)} = \big(\mathbf{S}^{(2)}\big)^{T}\bar{\mathbf{F}}^{(2)}, \qquad (35)$$

reduces to

$$\big[\big(\bar{\mathbf{F}}_0^{(2)}\big)^{T} - \big(\bar{\mathbf{F}}_0^{(2)}\big)^{-1}\big]\bar{\mathbf{F}}_1^{(2)} + \big(\bar{\mathbf{F}}_1^{(2)}\big)^{T}\big[\big(\bar{\mathbf{F}}_0^{(2)}\big)^{-T} - \bar{\mathbf{F}}_0^{(2)}\big] + O(\iota) = \mathbf{0}, \qquad (36)$$

by means of Eqs. (27) and (32)–(34).

In addition, making use of the overall average deformation condition (17), it follows that the average deformation gradient in the matrix is given by

$$\bar{\mathbf{F}}^{(1)} = \bar{\mathbf{F}}_0^{(1)} + O(\iota) \qquad (37)$$

where $\bar{\mathbf{F}}_0^{(1)} = (1 - c_0^{(2)})^{-1}(\bar{\mathbf{F}} - c_0^{(2)}\bar{\mathbf{F}}_0^{(2)})$. (Note that higher-order contributions will not be needed, and will therefore not be detailed here.)

Noting the asymptotic expansion $W^{(2)}(\bar{\mathbf{F}}^{(2)}) = W^{(2)}(\bar{\mathbf{F}}_0^{(2)}) + O(\iota)$ for the stored-energy function of particles, and making use of relations (27), (32) and (37), the second-order estimate (16) for the rigidly reinforced elastomers can be shown to reduce to

$$\widehat{W}(\bar{\mathbf{F}}) = \frac{1}{2}\iota^{-1}c_0^{(2)}\big(\bar{\mathbf{F}} - \bar{\mathbf{F}}_0^{(2)}\big)\cdot\mathbf{S}_{-1}^{(2)} + \big(1-c_0^{(2)}\big)W^{(1)}\big(\bar{\mathbf{F}}_0^{(1)}\big) + c_0^{(2)}W^{(2)}\big(\bar{\mathbf{F}}_0^{(2)}\big) + \frac{1}{2}c_0^{(2)}\big\{\big(\bar{\mathbf{F}} - \bar{\mathbf{F}}_0^{(2)}\big)\cdot\big[\mathbf{S}_0^{(2)} - \mathbf{S}^{(1)}\big(\bar{\mathbf{F}}_0^{(1)}\big)\big] - \bar{\mathbf{F}}_1^{(2)}\cdot\mathbf{S}_{-1}^{(2)}\big\} + O(\iota). \tag{38}$$

Remembering that the computation of $\bar{\mathbf{F}}_0^{(1)}$ and $\mathbf{S}_{-1}^{(2)}$ requires the evaluation of the tensor $\bar{\mathbf{F}}_0^{(2)}$, and that the variable $\bar{\mathbf{F}}_1^{(2)}$ can be eliminated in favor of $\mathbf{S}_0^{(2)}$ by means of Eq. (34), the calculation of the above expression requires the determination of the variables $\bar{\mathbf{F}}_0^{(2)}$ and $\mathbf{S}_0^{(2)}$. To this end, we consider next the expansion of Eq. (19) to obtain a tensorial equation for the deformation gradient $\bar{\mathbf{F}}_0^{(2)}$.

Thus, setting $\mathbf{L}^{(2)}$ equal to the tangent modulus tensor [36] of the particle phase, $\mathbf{L}^{(2)} = \mathbf{L}_t^{(2)}(\bar{\mathbf{F}}^{(2)}) = \partial^2 W^{(2)}/\partial\mathbf{F}\partial\mathbf{F}(\bar{\mathbf{F}}^{(2)})$, it follows from the definition of the strain energy (25) that $\mathbf{L}^{(2)}$ can be expanded as

$$\mathbf{L}^{(2)} = \iota^{-1}\mathbf{L}_{-1}^{(2)} + O\big(\iota^0\big), \tag{39}$$

where

$$\mathbf{L}_{-1}^{(2)} = \big\{(\boldsymbol{\mathcal{I}} - \boldsymbol{\mathcal{X}}) + \alpha\big[J(2J-1)\mathbf{F}^{-T}\otimes\mathbf{F}^{-T} + J(J-1)\boldsymbol{\mathcal{X}}\big]\big\}\big|_{\mathbf{F}=\bar{\mathbf{F}}_0^{(2)}}. \tag{40}$$

In this last expression, $\boldsymbol{\mathcal{I}}$ is the fourth-order identity tensor with components $\mathcal{I}_{ijkl} = \delta_{ik}\delta_{jl}$ and the components of the fourth-order tensor $\boldsymbol{\mathcal{X}}$ read as

$$\mathcal{X}_{ijkl} = -F_{li}^{-1}F_{jk}^{-1}. \tag{41}$$

Next, assuming that $\mathbf{L}^{(1)}$ is of order one and making use of the expression (39), $\Delta\mathbf{L} = \mathbf{L}^{(1)} - \mathbf{L}^{(2)}$ can be expanded as $(\Delta\mathbf{L})^{-1} = -\iota(\mathbf{L}_{-1}^{(2)})^{-1} + O(\iota^2)$. Substituting this expansion, along with relations (27), (32) and (37), into (19), it reduces after some algebra to

$$c_0^{(2)}\mathbf{S}_{-1}^{(2)}\iota^{-1} + \mathbf{T}\big(\bar{\mathbf{F}} - \bar{\mathbf{F}}_0^{(2)}\big) + c_0^{(2)}\big[\mathbf{S}^{(1)}\big(\bar{\mathbf{F}}_0^{(1)}\big) - \mathbf{S}_0^{(2)}\big] - \big(\tilde{\mathbf{L}}_0 - \mathbf{L}^{(1)}\big)\big(\mathbf{L}_{-1}^{(2)}\big)^{-1}\mathbf{S}_{-1}^{(2)} + O(\iota) = \mathbf{0}, \tag{42}$$

where we have used the notations

$$\mathbf{T} = \tilde{\mathbf{L}}_0 - \big(1-c_0^{(2)}\big)^{-1}\mathbf{L}^{(1)}, \tag{43}$$

and $\tilde{\mathbf{L}}_0 = \tilde{\mathbf{L}}|_{\mathbf{L}^{(2)}\to\infty}$. Thus, expression (42) gives rise to the following system of equations

$$\mathbf{S}_{-1}^{(2)} = \bar{\mathbf{F}}_0^{(2)} - \big(\bar{\mathbf{F}}_0^{(2)}\big)^{-T} + \alpha\bar{J}_0^{(2)}\big(\bar{J}_0^{(2)} - 1\big)\big(\bar{\mathbf{F}}_0^{(2)}\big)^{-T} = \mathbf{0}, \tag{44}$$

$$\mathbf{T}\big(\bar{\mathbf{F}} - \bar{\mathbf{F}}_0^{(2)}\big) + c_0^{(2)}\big[\mathbf{S}^{(1)}\big(\bar{\mathbf{F}}_0^{(1)}\big) - \mathbf{S}_0^{(2)}\big] = \mathbf{0}. \tag{45}$$

Noting that Eq. (44) should be satisfied for an arbitrary constant α, it is deduced that the following equations must be satisfied

$$\bar{\mathbf{F}}_0^{(2)} - \big(\bar{\mathbf{F}}_0^{(2)}\big)^{-T} = \mathbf{0}, \quad \text{and} \quad \bar{J}_0^{(2)}\big(\bar{J}_0^{(2)} - 1\big)\big(\bar{\mathbf{F}}_0^{(2)}\big)^{-T} = \mathbf{0}. \tag{46}$$

The first equation implies that $\bar{\mathbf{F}}_0^{(2)}$ is an orthogonal matrix denoted by

$$\bar{\mathbf{F}}_0^{(2)} = \bar{\mathbf{R}}^{(2)}, \tag{47}$$

while, recalling the definition $\bar{J}_0^{(2)} = \det \bar{\mathbf{F}}_0^{(2)}$, it can be seen that the second equation is identically satisfied as well. This result implies that the reinforcement undergoes an average rigid rotation $\bar{\mathbf{R}}^{(2)}$, as expected on physical grounds. This result is also consistent with the expectation that the stress $\mathbf{S}^{(2)}$ given in (32) should remain bounded in the extreme case of rigid particles. In this connection, it is interesting to note that the average balance equation (36) is automatically satisfied due to the orthogonality result (47).

In turn, in the limit of rigid particles ($\iota \to 0$), the average deformation gradient in the matrix phase can be written as

$$\bar{\mathbf{F}}^{(1)} = \bar{\mathbf{F}}_0^{(1)} = \frac{1}{1-c}\big(\bar{\mathbf{F}} - c\bar{\mathbf{R}}^{(2)}\big), \tag{48}$$

where $c = c_0^{(2)}$. Accordingly, Eq. (45) reduces to

$$\mathbf{T}\big(\bar{\mathbf{F}} - \bar{\mathbf{R}}^{(2)}\big) + c\big[\mathbf{S}^{(1)}\big(\bar{\mathbf{F}}^{(1)}\big) - \mathbf{S}_0^{(2)}\big] = \mathbf{0}, \tag{49}$$

which can be solved for $\mathbf{S}_0^{(2)}$ to obtain the result that

$$\mathbf{S}_0^{(2)} = c^{-1}\mathbf{T}\left(\bar{\mathbf{F}} - \bar{\mathbf{R}}^{(2)}\right) + \mathbf{S}^{(1)}\big(\bar{\mathbf{F}}^{(1)}\big). \tag{50}$$

Making use of the above relation together with Eqs. (44), (47) and (50), the second-order estimate (38) can now be shown to reduce to

$$\widehat{W}(\bar{\mathbf{F}}) = (1-c)W^{(1)}\big(\bar{\mathbf{F}}^{(1)}\big) + \frac{1}{2}\left(\bar{\mathbf{F}} - \bar{\mathbf{R}}^{(2)}\right)\cdot\mathbf{T}\left(\bar{\mathbf{F}} - \bar{\mathbf{R}}^{(2)}\right). \tag{51}$$

In order to obtain the associated equation for the average rotation tensor $\bar{\mathbf{R}}^{(2)}$ of the rigid particles, we make use of (47) in (34) to find the following expression for $\mathbf{S}_0^{(2)}$

$$\mathbf{S}_0^{(2)} = \bar{\mathbf{F}}_1^{(2)} + \bar{\mathbf{R}}^{(2)}\big(\bar{\mathbf{F}}_1^{(2)}\big)^T\bar{\mathbf{R}}^{(2)} + \alpha\bar{J}_1^{(2)}\bar{\mathbf{R}}^{(2)}. \tag{52}$$

Substituting this expression in Eq. (49) and then multiplying it by $(\bar{\mathbf{R}}^{(2)})^T$ from left-hand side, we arrive at the following equation

$$\begin{aligned}&\big(\bar{\mathbf{R}}^{(2)}\big)^T\big[\mathbf{T}\big(\bar{\mathbf{F}} - \bar{\mathbf{R}}^{(2)}\big)\big] + c\big(\bar{\mathbf{R}}^{(2)}\big)^T\mathbf{S}^{(1)}\big(\bar{\mathbf{F}}^{(1)}\big)\\ &\quad = 2c\big\{\big(\bar{\mathbf{R}}^{(2)}\big)^T\bar{\mathbf{F}}_1^{(2)}\big\}_{Sym} + \alpha c\bar{J}_1^{(2)}\mathbf{I},\end{aligned} \tag{53}$$

where the subscript *Sym* stands for the symmetric part of the relevant tensor. (We also define the skew-symmetric part $\{\mathbf{A}\}_{Skew}$ of a second-order tensor $\mathbf{A}$ via the relation $\mathbf{A} = \{\mathbf{A}\}_{Sym} + \{\mathbf{A}\}_{Skew}$.) Thus, by taking the skew-symmetric part of both sides of expression (53), the tensorial equation for the three (generally) independent components of $\bar{\mathbf{R}}^{(2)}$ is easily obtained with the result that

$$\big\{\big(\bar{\mathbf{R}}^{(2)}\big)^T\big[\mathbf{T}\left(\bar{\mathbf{F}} - \bar{\mathbf{R}}^{(2)}\right)\big] + c\left(\bar{\mathbf{R}}^{(2)}\right)^T\mathbf{S}^{(1)}\big(\bar{\mathbf{F}}^{(1)}\big)\big\}_{Skew} = \mathbf{0}. \tag{54}$$

The resulting estimates (51) and (54) for the rigid-reinforced elastomers can be specialized for "particulate" microstructures [37, 40]. To this end, we make use of the following Willis-type estimate for the effective modulus tensor

$$\tilde{\mathbf{L}} = \mathbf{L}^{(1)} + \frac{c}{1-c}\mathbf{P}^{-1}, \tag{55}$$

where the subscript 0 has been dropped from $\tilde{\mathbf{L}}_0$ for convenience. Thus, substituting this estimate for the LCC, it follows that the second-order estimate (51) specializes to

$$\widehat{W}(\bar{\mathbf{F}}) = (1-c)W^{(1)}\big(\bar{\mathbf{F}}^{(1)}\big) + \frac{1}{2}\frac{c}{1-c}\big(\bar{\mathbf{F}} - \bar{\mathbf{R}}^{(2)}\big)\cdot\mathbf{E}\big(\bar{\mathbf{F}} - \bar{\mathbf{R}}^{(2)}\big), \tag{56}$$

where

$$\mathbf{E} = \mathbf{P}^{-1} - \mathbf{L}^{(1)}. \tag{57}$$

Accordingly, the associated kinematical equation (54) for $\bar{\mathbf{R}}^{(2)}$ can be written as

$$\big\{\big(\bar{\mathbf{R}}^{(2)}\big)^T\big[\mathbf{E}\big(\bar{\mathbf{F}} - \bar{\mathbf{R}}^{(2)}\big)\big] + (1-c)\big(\bar{\mathbf{R}}^{(2)}\big)^T\mathbf{S}^{(1)}\big(\bar{\mathbf{F}}^{(1)}\big)\big\}_{Skew} = \mathbf{0}. \tag{58}$$

Having computed the tensor $\bar{\mathbf{R}}^{(2)}$ from (58), the second-order estimate can be calculated via (56).

The second-order estimate (56) is completely specified, except for the choice of $\mathbf{L}^{(1)}$ in the LCC. Consistent with (10), in the earlier version of the TSO method [36], $\mathbf{L}^{(1)}$ was chosen to be equal to the tangent modulus tensor of the matrix phase, evaluated at the matrix average of the deformation $\bar{\mathbf{F}}^{(1)}$, i.e., $\mathbf{L}^{(1)} = \mathbf{L}_t^{(1)}(\bar{\mathbf{F}}^{(1)})$. In this work, the prescription

$$\mathbf{L}^{(1)} = \mathbf{L}_t^{(1)}(\bar{\mathbf{F}}) = \frac{\partial^2 W^{(1)}}{\partial\mathbf{F}\partial\mathbf{F}}(\bar{\mathbf{F}}) \tag{59}$$

will be adopted instead. This choice is motivated by the considerable simplification in the computation of $\tilde{\mathbf{L}}$, which is an essential element in the effective energy (51) (through $\mathbf{T}$). Indeed, the computation of $\mathbf{L}^{(1)}$ by means of the prescription (59) is completely explicit, and does not require the calculation of the tensor $\bar{\mathbf{R}}^{(2)}$, unlike the case for the earlier prescription. On the other hand, the resulting estimates can still be shown to be exact to second-order heterogeneity contrast (for non-rigid particles).

4.2 Energy Decomposition Approximation

The second-order method developed in the previous section can be applied to general compressible hyperelastic composites. For the special case of the composites made up of incompressible phases, the overall (exact) incompressibility constraint ($\bar{J} = \det(\bar{\mathbf{F}}) = 1$) must be satisfied. However, it can be verified that by taking the incompressibility limit of the effective energy function (51), the constraint $\bar{J} = 1$ is, in general, not satisfied. The failure to meet this constraint in the incompressibility limit, which is unacceptable, was already discussed in some detail by Ponte Castañeda and Tiberio [36]. In particular, for the special case of 2-D circular inclusions, they investigated the effect of the inclusion volume fraction on the deviation of the "approximate" macroscopic incompressibility constraint from the exact constraint $\bar{J} = 1$. The aim of this subsection is to propose a modification of method described in the last section to be able to ensure exact attainment of the exact constraint $\bar{J} = 1$ in the incompressibility limit for the composites. As mentioned before, in the earlier TSO method, the reference modulus tensor $\mathbf{L}^{(1)}$ in the LCC was set to be equal to $\mathbf{L}_t^{(1)}$. In this work, as described in the previous section, we will make use instead of the prescription (59) for $\mathbf{L}^{(1)}$. Indeed, making use of this prescription, it can be shown that the second term in the RHS of the estimate (51) is consistent with the constraint $\bar{J} = 1$ in the incompressibility limit. However, the first term in the estimate is still inconsistent with the exact incompressibility constraint. To address this issue, we propose to split up the energy functions of the constituent phases into "dilatational" and "distortional" parts, and homogenize

them, separately. In this way, the dilatational contribution to the effective energy function can be obtained *exactly*, while the distortional contribution may still be computed approximately using the tangent second-order procedure, presented in Sect. 3. Despite the fact that the splitting of the energy functional in general entails an approximation in the calculation of the effective stored-energy function, satisfaction of the *exact incompressibility constraint* can be ensured. With this objective in mind and without loss of generality, it proves helpful to introduce the following form for the strain-energy function of the constituent phases, namely,

$$W^{(r)}(\mathbf{F}) = W_{\mu}^{(r)}(\mathbf{F}) + \frac{1}{2}\mu'^{(r)}(J-1)^2, \tag{60}$$

where the parameter $\mu'^{(r)}$ denotes the Lamé modulus of the phases in the infinitesimal strain regime, which in order to recover incompressible behavior ($J \to 1$), will be taken to tend to infinity. Also, $W_{\mu}^{(r)}$ is that part of the stored-energy function $W^{(r)}$ not depending on $\mu'^{(r)}$. The effective stored-energy function of the nonlinear composite, defined by Eq. (3), may then be approximated as

$$\widehat{W}(\bar{\mathbf{F}}) \approx \widehat{W}_{\mu}(\bar{\mathbf{F}}) + \widehat{W}_{\mu'}(\bar{\mathbf{F}}), \tag{61}$$

where

$$\widehat{W}_{\mu}(\bar{\mathbf{F}}) = \underset{\mathbf{F}\in K(\bar{\mathbf{F}})}{\text{stat}} \sum_{r=1}^{N} c^{(r)} \left\langle W_{\mu}^{(r)}(\mathbf{F}) \right\rangle^{(r)}, \tag{62}$$

and

$$\widehat{W}_{\mu'}(\bar{\mathbf{F}}) = \frac{1}{2}\left(\underset{\mathbf{F}\in \mathrm{K}(\bar{\mathbf{F}})}{\text{stat}} \sum_{r=1}^{N} c^{(r)} \mu'^{(r)} \left\langle (J-1)^2 \right\rangle^{(r)} \right). \tag{63}$$

Making use of results from [32] for "elastic fluid" composites, the expression for $\widehat{W}_{\mu'}$ can be evaluated exactly as

$$\widehat{W}_{\mu'}(\bar{\mathbf{F}}) = \frac{1}{2}\tilde{\mu}'_R(\bar{J}-1)^2, \tag{64}$$

where

$$\tilde{\mu}'_R = \left[\sum_{r=1}^{N} c^{(r)} \left(\mu'^{(r)}\right)^{-1} \right]^{-1} \tag{65}$$

is the effective dilatational modulus in the ground state of the composite.

Now, by restricting attention to the two-phase rigidly reinforced composite, we apply the second-order procedure, developed in the prior subsection, to the distortional part of energy in (61). Thus, making use of the estimate (51) for $\widehat{W}_{\mu}(\bar{\mathbf{F}})$, it follows that

$$\widehat{W}_{\mu}(\bar{\mathbf{F}}) = (1-c) W_{\mu}^{(1)}\left(\bar{\mathbf{F}}^{(1)}\right) + \frac{1}{2}\left(\bar{\mathbf{F}} - \bar{\mathbf{R}}^{(2)}\right) \cdot \mathbf{T}\left(\bar{\mathbf{F}} - \bar{\mathbf{R}}^{(2)}\right), \tag{66}$$

where, by means of (54), the kinematical equation for $\bar{\mathbf{R}}^{(2)}$, associated with (62), can be written as

$$\left\{ \left(\bar{\mathbf{R}}^{(2)}\right)^T \left[\mathbf{T}\left(\bar{\mathbf{F}} - \bar{\mathbf{R}}^{(2)}\right)\right] + c\left(\bar{\mathbf{R}}^{(2)}\right)^T \mathbf{S}_{\mu}^{(1)}\left(\bar{\mathbf{F}}^{(1)}\right) \right\}_{Skew} = \mathbf{0}, \tag{67}$$

where $\mathbf{S}_{\mu}^{(1)}(\mathbf{F}) = \partial W_{\mu}^{(1)}(\mathbf{F})/\partial \mathbf{F}$. Moreover, we need an appropriate prescription for the modulus tensor $\mathbf{L}^{(1)}$ in the expression $\mathbf{T} = \tilde{\mathbf{L}} - (1-c)^{-1}\mathbf{L}^{(1)}$ used in the estimates (66) and (67). Motivated by the choice (59), here we will use the prescription

$$\mathbf{L}^{(1)} = \mathbf{L}_{\mu}^{(1)}(\bar{\mathbf{F}}) + \frac{1}{2}\mu'^{(1)}\frac{\partial^2[(J-1)^2]}{\partial \mathbf{F}\partial \mathbf{F}}\bigg|_{\mathbf{F}=\bar{\mathbf{F}}}, \tag{68}$$

where $\mathbf{L}_{\mu}^{(1)}(\mathbf{F}) = \partial^2 W_{\mu}^{(1)}(\mathbf{F})/\partial \mathbf{F}\partial \mathbf{F}$. Note that the second term (depending on $\mu'^{(1)}$) is needed to be able to enforce the incompressibility constraint in the LCC.

Next, specializing to rigid behavior for the inclusions in the "dilational" part of the effective stored-energy function of the two-phase composite, we have that $\tilde{\mu}'_R = (1-c)^{-1}\mu'^{(1)}$, and accordingly, the following estimate is obtained for $\widehat{W}_{\mu'}(\bar{\mathbf{F}})$

$$\widehat{W}_{\mu'}(\bar{\mathbf{F}}) = \frac{1}{2(1-c)}\mu'^{(1)}(\bar{J}-1)^2. \tag{69}$$

Finally, making use of expressions (66) and (69) for the two-phase, rigidly reinforced elastomers, the second-order estimate (61) reduces to

$$\widehat{W}(\bar{\mathbf{F}}) = (1-c)W_{\mu}^{(1)}\big(\bar{\mathbf{F}}^{(1)}\big) + \frac{1}{2}\big(\bar{\mathbf{F}}-\bar{\mathbf{R}}^{(2)}\big)\cdot\mathbf{T}\big(\bar{\mathbf{F}}-\bar{\mathbf{R}}^{(2)}\big) + \frac{1}{2(1-c)}\mu'^{(1)}(\bar{J}-1)^2. \tag{70}$$

Note that the approximate equality has been replaced here by a standard equality, and that the particle rotation $\bar{\mathbf{R}}^{(2)}$ is still given by (67). Naturally, the expression (70) for the effective stored-energy function of the reinforced elastomer can be used, in particular, together with the Willis estimate (55) for the LCC, to obtain the result

$$\widehat{W}(\bar{\mathbf{F}}) = (1-c)W_{\mu}^{(1)}\big(\bar{\mathbf{F}}^{(1)}\big) + \frac{1}{2}\frac{c}{1-c}\big(\bar{\mathbf{F}}-\bar{\mathbf{R}}^{(2)}\big)\cdot\mathbf{E}\big(\bar{\mathbf{F}}-\bar{\mathbf{R}}^{(2)}\big) + \frac{1}{2(1-c)}\mu'^{(1)}(\bar{J}-1)^2, \tag{71}$$

where

$$\big\{\big(\bar{\mathbf{R}}^{(2)}\big)^T\big[\mathbf{E}\big(\bar{\mathbf{F}}-\bar{\mathbf{R}}^{(2)}\big)\big] + (1-c)\big(\bar{\mathbf{R}}^{(2)}\big)^T\mathbf{S}_{\mu}^{(1)}\big(\bar{\mathbf{F}}^{(1)}\big)\big\}_{Skew} = \mathbf{0}, \tag{72}$$

and $\mathbf{E}$ is given by expression (57).

At this point, it is expedient to make the following remarks concerning some features of the estimates (71) and (72) for rigidly reinforced elastomers:

1. As was also the case for the earlier tangent second-order estimate in [36], the new estimate (71) may blow up at some finite values of $\bar{\mathbf{F}}$. Depending on the inclusion volume fraction and initial configuration of the microstructure, the quantity $\bar{J}^{(1)} = \det(\bar{\mathbf{F}}^{(1)})$ can become zero at finite values of the deformation (see relation (48)), causing certain terms in the expression $W_{\mu}^{(1)}(\bar{\mathbf{F}}^{(1)})$ for the estimate (71) to blow up. As discussed by Ponte Castañeda and Tiberio [36], this phenomenon can be interpreted as *lock up* for the composite, which is due to the fact that sufficiently large deformations would be expected to bring the rigid inclusions into contact with each other leading to strong stiffing of the composite.
2. In the limit of infinitesimal strains ($\bar{\mathbf{F}} \to \mathbf{I}$), the estimate (71) recovers the corresponding linear-elastic Willis estimate [37, 40]. The resulting energy can be written as $\widehat{W}(\bar{\mathbf{F}}) = 1/2\bar{\boldsymbol{\varepsilon}}.\,\tilde{\mathbf{L}}_L\cdot\bar{\boldsymbol{\varepsilon}}$, where $\bar{\boldsymbol{\varepsilon}}$ denotes the macroscopic infinitesimal strain tensor and $\tilde{\mathbf{L}}_L$ is the effective moduli tensor in the context of linear elasticity. Also, in this limit, the solution

of Eq. (72) agrees exactly with the corresponding prediction for the infinitesimal rotation of the particles [19], as given by

$$\bar{\mathbf{R}}_L^{(2)} = \mathbf{I} + \bar{\boldsymbol{\omega}} - \boldsymbol{R}_L \mathbf{P}_L^{-1} \bar{\boldsymbol{\varepsilon}}, \tag{73}$$

where $\bar{\boldsymbol{\omega}}$ stands for the macroscopic infinitesimal rotation tensor, and $\boldsymbol{R}_L$ and $\mathbf{P}_L$ are the well-known Eshelby tensors in the context of small strains and rotations (see Eqs. (15) and (19) in [19]).

4.2.1 Incompressible Matrix

The estimate (70), together with (67), and relation (68) for $\mathbf{L}^{(1)}$ (used in expression (43) for $\mathbf{T}$) holds for composites with a *compressible* matrix phase characterized by the stored-energy function (60). However, in the limit of *incompressible* behavior for the matrix, i.e., when $\mu'^{(1)} \to \infty$, the estimate (70) (unlike the earlier estimate (51)) is found to be consistent with the exact overall incompressibility constraint ($\bar{J} = 1$), and reduces to

$$\widehat{W}(\bar{\mathbf{F}}) = (1-c) W_\mu^{(1)}\big(\bar{\mathbf{F}}^{(1)}\big) + \frac{1}{2}\big(\bar{\mathbf{F}} - \bar{\mathbf{R}}^{(2)}\big) \cdot \mathbf{T}^I \big(\bar{\mathbf{F}} - \bar{\mathbf{R}}^{(2)}\big), \tag{74}$$

where

$$\mathbf{T}^I = \lim_{\mu'^{(1)} \to \infty} \big[\tilde{\mathbf{L}} - (1-c)^{-1} \mathbf{L}^{(1)}\big], \tag{75}$$

while the equation for $\bar{\mathbf{R}}^{(2)}$ reduces to

$$\big\{\big(\bar{\mathbf{R}}^{(2)}\big)^T \big[\mathbf{T}^I \big(\bar{\mathbf{F}} - \bar{\mathbf{R}}^{(2)}\big)\big] + c\,\big(\bar{\mathbf{R}}^{(2)}\big)^T \mathbf{S}_\mu^{(1)}\big(\bar{\mathbf{F}}^{(1)}\big)\big\}_{Skew} = \mathbf{0}. \tag{76}$$

For the special case of the Willis estimate for $\tilde{\mathbf{L}}$, the expression (74) further simplifies to

$$\widehat{W}(\bar{\mathbf{F}}) = (1-c) W_\mu^{(1)}\big(\bar{\mathbf{F}}^{(1)}\big) + \frac{1}{2}\frac{c}{1-c}\big(\bar{\mathbf{F}} - \bar{\mathbf{R}}^{(2)}\big) \cdot \mathbf{E}^I \big(\bar{\mathbf{F}} - \bar{\mathbf{R}}^{(2)}\big), \tag{77}$$

where

$$\mathbf{E}^I = \lim_{\mu'^{(1)} \to \infty} \big(\mathbf{P}^{-1} - \mathbf{L}^{(1)}\big), \tag{78}$$

while the corresponding equation for the rotation $\bar{\mathbf{R}}^{(2)}$ reduces to

$$\big\{\big(\bar{\mathbf{R}}^{(2)}\big)^T \big[\mathbf{E}^I \big(\bar{\mathbf{F}} - \bar{\mathbf{R}}^{(2)}\big)\big] + (1-c)\big(\bar{\mathbf{R}}^{(2)}\big)^T \mathbf{S}_\mu^{(1)}\big(\bar{\mathbf{F}}^{(1)}\big)\big\}_{Skew} = \mathbf{0}. \tag{79}$$

For completeness, we note that the macroscopic stress tensor $\bar{\mathbf{S}}(\bar{\mathbf{F}}) = \partial \widehat{W}(\bar{\mathbf{F}})/\partial \bar{\mathbf{F}}$ associated with the effective stored-energy function (77) may be written as

$$\begin{aligned}\bar{\mathbf{S}}(\bar{\mathbf{F}}) = {} & \mathbf{S}_\mu^{(1)}\big(\bar{\mathbf{F}}^{(1)}\big)\big(\boldsymbol{\mathcal{I}} - c\bar{\mathbf{g}}^{(2)}\big) + \cdots \\ & + \frac{c}{1-c}\left\{\big[\mathbf{E}^I\big(\bar{\mathbf{F}} - \bar{\mathbf{R}}^{(2)}\big)\big]\bar{\mathbf{G}}^{(2)} + \frac{1}{2}\big(\bar{\mathbf{F}} - \bar{\mathbf{R}}^{(2)}\big)\big[\big(\bar{\mathbf{F}} - \bar{\mathbf{R}}^{(2)}\big)\mathbf{Y}^I\big]\right\} - p\bar{\mathbf{F}}^{-T},\end{aligned} \tag{80}$$

where p stands for the arbitrary hydrostatic pressure associated with the incompressibility constraint, and $\mathbf{Y}^I$ is the sixth-order tensor with components

$$Y^I_{ijklpq} = \left.\frac{\partial E_{ijkl}}{\partial \bar{F}_{pq}}\right|_{\mu'^{(1)} \to \infty} = -\left.\left(P^{-1}_{ijmn}\frac{\partial P_{mnrs}}{\partial \bar{F}_{pq}} P^{-1}_{rskl} + \frac{\partial L^{(1)}_{ijkl}}{\partial \bar{F}_{pq}}\right)\right|_{\mu'^{(1)} \to \infty}. \tag{81}$$

In addition, $\bar{\mathbf{G}}^{(2)}$ is a fourth-order tensor with the following indicial representation

$$\bar{G}^{(2)}_{ijkl} = \mathcal{I}_{ikjl} - \bar{g}^{(2)}_{ijkl}, \tag{82}$$

where $\bar{g}^{(2)}_{ijkl} = \partial(\bar{R}^{(2)})_{ij}/\partial \bar{F}_{kl}$. Note that a tensorial equation for the components of the fourth-order tensor $\bar{\mathbf{g}}^{(2)}$ can be deduced from the kinematical equation (79), which can be written in indicial form as

$$\begin{aligned}\big\{&\bar{g}^{(2)}_{pikl} E^I_{pjrs}\big(\bar{F}_{rs} - \bar{R}^{(2)}_{rs}\big) + \bar{R}^{(2)}_{pi} Y^I_{pjrskl}\big(\bar{F}_{rs} - \bar{R}^{(2)}_{rs}\big) + \bar{R}^{(2)}_{pi} E^I_{pjrs} \bar{G}^{(2)}_{rskl} \\ &+ \big[(1-c)\bar{g}^{(2)}_{pikl}\big(S^{(1)}_{\mu}\big)_{pj} + \bar{R}^{(2)}_{pi}\big(L^{(1)}_{\mu}\big)_{pjrs}\big(\mathcal{I}_{rskl} - c\bar{g}^{(2)}_{rskl}\big)\big]\big\}\big|_{[ij]kl} = 0,\end{aligned} \tag{83}$$

where $A_{ijkl}|_{[ij]kl} = (A_{ijkl} - A_{jikl})/2$, and the tensors $\mathbf{S}^{(1)}_{\mu}$ and $\mathbf{L}^{(1)}_{\mu}$ are evaluated at $\bar{\mathbf{F}}^{(1)}$. On the other hand, the derivatives $\partial P_{ijkl}/\partial \bar{F}_{pq}$ in (81) are calculated via

$$\frac{\partial P_{ijkl}}{\partial \bar{F}_{pq}} = \frac{1}{4\pi |\mathbf{Z}_0|} \int_{|\boldsymbol{\xi}|=1} \frac{\partial H_{ijkl}}{\partial \bar{F}_{pq}} \big[\boldsymbol{\xi}^T \big(\mathbf{Z}_0^T \mathbf{Z}_0\big)^{-1} \boldsymbol{\xi}\big]^{\frac{-3}{2}} dS. \tag{84}$$

In turn, in this expression the derivatives $\partial H_{ijkl}/\partial \bar{\mathbf{F}}_{pq}$ can be evaluated by recalling the relation between the tensor $\mathbf{H}$ and $\mathbf{L}^{(1)}$ to obtain the result

$$\frac{\partial H_{ijkl}}{\partial \bar{F}_{pq}} = \frac{\partial B_{ik}}{\partial \bar{F}_{pq}} \xi_j \xi_l = -B_{im} \frac{\partial K_{mn}}{\partial \bar{F}_{pq}} B_{nk} \xi_j \xi_l = -B_{im} B_{nk} \mathcal{L}^{(1)}_{mrnspq} \xi_j \xi_l \xi_r \xi_s, \tag{85}$$

where $\boldsymbol{\mathcal{L}}^{(1)}$ is the sixth-order elastic modulus tensor defined by $\boldsymbol{\mathcal{L}}^{(1)}(\mathbf{F}) = \partial^3 W^{(1)}(\mathbf{F})/\partial \mathbf{F} \partial \mathbf{F} \partial \mathbf{F}$ [30] evaluated at $\bar{\mathbf{F}}$.

4.3 Dilute Concentrations

Relations (74) and (76) provide TSO estimates for (rigid) particle-reinforced elastomers under general loading in the finite concentration regime. In this subsection, we specialize these results for dilute concentrations of the particles, which is an important limiting case both for theoretical and practical reasons. Mathematically speaking, we carry out an asymptotic expansion of the estimates (74) and (76) for $c \ll 1$. To this end, we assume a regular perturbation expansion for $\bar{\mathbf{F}}^{(1)}$ in c, as given by

$$\bar{\mathbf{F}}^{(1)} = \bar{\mathbf{F}} + c\big(\bar{\mathbf{F}} - \bar{\mathbf{R}}^{(2)}_0\big) + c^2\big(\bar{\mathbf{F}} - \bar{\mathbf{R}}^{(2)}_0 - \bar{\mathbf{R}}^{(2)}_1\big) + O\big(c^3\big), \tag{86}$$

which is obtained by assuming that $\bar{\mathbf{R}}^{(2)} = \bar{\mathbf{R}}^{(2)}_0 + c\bar{\mathbf{R}}^{(2)}_1 + O(c^2)$ and employing Eq. (48) for $\bar{\mathbf{F}}^{(1)}$. In addition, keeping in mind that the tensor $\mathbf{L}^{(1)}$ is evaluated at $\bar{\mathbf{F}}$, and is therefore independent of the volume fraction, the tensor $\tilde{\mathbf{L}}$ can be assumed to have the following asymptotic expansion about $c = 0$:

$$\tilde{\mathbf{L}} = \mathbf{L}^{(1)} + c\,\tilde{\mathbf{L}}_1 + O\big(c^2\big). \tag{87}$$

Next, substituting (86) and (87) into (74), and expanding the resulting expression for small values of c, yields the result

$$\widehat{W}^{Dilute}(\bar{\mathbf{F}}) = W_\mu^{(1)}(\bar{\mathbf{F}}) + c\Big\{\big(\bar{\mathbf{F}} - \bar{\mathbf{R}}_0^{(2)}\big)\cdot \mathbf{S}_\mu^{(1)}(\bar{\mathbf{F}}) - W_\mu^{(1)}(\bar{\mathbf{F}}) + \frac{1}{2}\big[\big(\bar{\mathbf{F}} - \bar{\mathbf{R}}_0^{(2)}\big)\cdot\big(\tilde{\mathbf{L}}_1 - \mathbf{L}^{(1)}\big)\big(\bar{\mathbf{F}} - \bar{\mathbf{R}}_0^{(2)}\big)\big]\Big\} + O\big(c^2\big). \tag{88}$$

Similarly, the kinematical constraint (76) leads to

$$\big\{\big(\bar{\mathbf{R}}_0^{(2)}\big)^T\cdot\big[\big(\tilde{\mathbf{L}}_1 - \mathbf{L}^{(1)}\big)\big(\bar{\mathbf{F}} - \bar{\mathbf{R}}_0^{(2)}\big)\big] + \big(\bar{\mathbf{R}}_0^{(2)}\big)^T\mathbf{S}_\mu^{(1)}(\bar{\mathbf{F}})\big\}_{Skew} + O(c) = \mathbf{0}. \tag{89}$$

Moreover, using the Willis estimate (55) for the LCC, the TSO estimate (88) specializes to

$$\widehat{W}^{Dilute}(\bar{\mathbf{F}}) = W_\mu^{(1)}(\bar{\mathbf{F}}) + c\Big\{\big(\bar{\mathbf{F}} - \bar{\mathbf{R}}_0^{(2)}\big)\cdot \mathbf{S}_\mu^{(1)}(\bar{\mathbf{F}}) - W_\mu^{(1)}(\bar{\mathbf{F}}) + \frac{1}{2}\big[\big(\bar{\mathbf{F}} - \bar{\mathbf{R}}_0^{(2)}\big)\cdot\mathbf{E}^I\big(\bar{\mathbf{F}} - \bar{\mathbf{R}}_0^{(2)}\big)\big]\Big\} + O\big(c^2\big), \tag{90}$$

where the equation (89) for $\bar{\mathbf{R}}_0^{(2)}$ takes the form

$$\big\{\big(\bar{\mathbf{R}}_0^{(2)}\big)^T\big[\mathbf{E}^I\big(\bar{\mathbf{F}} - \bar{\mathbf{R}}_0^{(2)}\big)\big] + \big(\bar{\mathbf{R}}_0^{(2)}\big)^T\mathbf{S}_\mu^{(1)}(\bar{\mathbf{F}})\big\}_{Skew} + O(c) = \mathbf{0}. \tag{91}$$

It is worth mentioning that these results can be regarded as a generalization of Eshelby's results [11] for a composite material consisting of dilute concentrations of aligned, rigid ellipsoidal inclusions in a nonlinear hyperelastic matrix. As is well known, these dilute estimates depend only on the volume fraction (to first order), shape and orientation of the ellipsoidal inclusions, but not on the relative positions of the inclusions. In other words, the interactions between inclusions is neglected by the estimates (90) and (91). As a consequence, the effective stored-energy function (90) does not exhibit lock up at finite strains (unless the matrix does).

The corresponding expressions for the macroscopic stress tensor $\bar{\mathbf{S}}^{Dilute}(\bar{\mathbf{F}}) = \partial\widehat{W}^{Dilute}(\bar{\mathbf{F}})/\partial\bar{\mathbf{F}}$ are given by

$$\bar{\mathbf{S}}^{Dilute}(\bar{\mathbf{F}}) = \mathbf{S}_\mu^{(1)}(\bar{\mathbf{F}}) + \Big\{\big[\mathbf{S}_\mu^{(1)}(\bar{\mathbf{F}}) + \mathbf{E}^I\big(\bar{\mathbf{F}} - \bar{\mathbf{R}}_0^{(2)}\big)\big]\bar{\mathbf{G}}_0^{(2)} + \mathbf{L}_\mu^{(1)}(\bar{\mathbf{F}})\big(\bar{\mathbf{F}} - \bar{\mathbf{R}}_0^{(2)}\big) - \mathbf{S}_\mu^{(1)}(\bar{\mathbf{F}}) + \frac{1}{2}\big(\bar{\mathbf{F}} - \bar{\mathbf{R}}_0^{(2)}\big)\big[\big(\bar{\mathbf{F}} - \bar{\mathbf{R}}_0^{(2)}\big)\mathbf{Y}^I\big]\Big\}c - p\bar{\mathbf{F}}^{-T} + O\big(c^2\big), \tag{92}$$

where $(\bar{G}_0^{(2)})_{ijkl} = \mathcal{I}_{ikjl} - (\bar{g}_0^{(2)})_{ijkl}$, and where the quantities $(\bar{g}_0^{(2)})_{ijkl} = \partial(\bar{R}_0^{(2)})_{ij}/\partial\bar{F}_{kl}$ are determined by the equations

$$\big\{\big(\bar{g}_0^{(2)}\big)_{pikl}E^I_{pjrs}\big[\bar{F}_{rs} - \big(\bar{R}_0^{(2)}\big)_{rs}\big] + \big(\bar{R}_0^{(2)}\big)_{pi}Y^I_{pjrskl}\big[\bar{F}_{rs} - \big(\bar{R}_0^{(2)}\big)_{rs}\big] + \big(\bar{R}_0^{(2)}\big)_{pi}E^I_{pjrs}\big(\bar{G}_0^{(2)}\big)_{rskl} + \big(\bar{g}_0^{(2)}\big)_{pikl}\big(S_\mu^{(1)}\big)_{pj} + \big(\bar{R}_0^{(2)}\big)_{pi}\big(L_\mu^{(1)}\big)_{pjkl}\big\}\big|_{[ij]kl} = 0, \tag{93}$$

where the tensors $\mathbf{S}_\mu^{(1)}$ and $\mathbf{L}_\mu^{(1)}$ are now evaluated at $\bar{\mathbf{F}}$

4.4 Computation of the Tensor $\mathbf{E}^I$

The calculation of the effective stored-energy function for *incompressible*, particulate elastomeric composites, as well as the associated microstructure evolution (Eqs. (77) and (79))

under *general* (isochoric) loading conditions, requires the computation of the fourth-order, major-symmetric tensor $\mathbf{E}^I$. This tensor can in principle be estimated (approximately) by setting $\mu'^{(1)}$ sufficiently large (compared to the initial shear modulus of the matrix $\mu^{(1)}$) in the definition (78) for $\mathbf{E}^I$. Nevertheless, it is possible to perform a general asymptotic analysis for the computation of the tensor $\mathbf{E}^I$ in the incompressibility limit ($\mu'^{(1)} \to \infty$), as shown next. This analysis leads to closed-form expressions for the components of the tensor $\mathbf{E}^I$ for specific microstructures and/or loading conditions; more generally, numerical computation of the resulting integrals may be required.

Without loss of generality, and consistent with the definition of the stored-energy function for the matrix phase as given by (60), the modulus tensor $\mathbf{L}^{(1)}$ can be decomposed into incompressible and compressible parts, denoted by $\mathbf{L}^{(1)}_{\mu}$ and $\mathbf{L}^{(1)}_{-1}$ respectively, such that

$$\mathbf{L}^{(1)} = \varepsilon^{-1}\mathbf{L}^{(1)}_{-1} + \mathbf{L}^{(1)}_{\mu}, \tag{94}$$

where, by definition, $\varepsilon = 1/\mu'^{(1)}$ is a small parameter, $\mathbf{L}^{(1)}_{\mu} = \partial^2 W^{(1)}_{\mu}/\partial\mathbf{F}\partial\mathbf{F}(\bar{\mathbf{F}})$ and $\mathbf{L}^{(1)}_{-1}$ is given by

$$\mathbf{L}^{(1)}_{-1} = \left[J(2J-1)\mathbf{F}^{-T}\otimes\mathbf{F}^{-T} + J(J-1)\boldsymbol{\mathcal{X}}\right]\big|_{\mathbf{F}=\bar{\mathbf{F}}}. \tag{95}$$

It follows from (23) that the acoustic tensor associated with (94) takes the form

$$\mathbf{K} = \varepsilon^{-1}\mathbf{K}_{-1} + \mathbf{K}_{\mu}, \tag{96}$$

where $\mathbf{K}_{-1}$ and $\mathbf{K}_{\mu}$ are the parts of the acoustic tensor associated with $\mathbf{L}^{(1)}_{-1}$ and $\mathbf{L}^{(1)}_{\mu}$, respectively. The inverse of the (symmetric) acoustic tensor, $\mathbf{B} = \mathbf{K}^{-1}$, can then be calculated by means of the identity

$$B_{ik} = K^{-1}_{ik} = \frac{1}{2\det(\mathbf{K})}e_{irs}e_{kpq}K_{rp}K_{sq}, \tag{97}$$

where e_{ijk} is the permutating tensor of the third-order, and $\det(\mathbf{K})$ is given by

$$\det(\mathbf{K}) = \frac{1}{6}e_{ijk}e_{pqr}K_{ip}K_{jq}K_{kr}. \tag{98}$$

Substituting (96) into (97) together with (98), after some algebra, we find the following expression for $\mathbf{B}$,

$$\mathbf{B} = \frac{\varepsilon\mathbf{D}_1 + \mathbf{D}_0}{\varepsilon d_1 + d_0}, \tag{99}$$

where d_0 and d_1 are given by

$$\begin{aligned} d_0 &= \frac{1}{6}e_{ijk}e_{pqr}\left[(K_{\mu})_{ip}(K_{\mu})_{jq}(K_{-1})_{kr} + (K_{\mu})_{ip}(K_{-1})_{jq}(K_{\mu})_{kr} + (K_{-1})_{ip}(K_{\mu})_{jq}(K_{\mu})_{kr}\right], \\ d_1 &= \det(\mathbf{K}_{\mu}) = \frac{1}{6}e_{ijk}e_{pqr}(K_{\mu})_{ip}(K_{\mu})_{jq}(K_{\mu})_{kr}, \end{aligned} \tag{100}$$

and the tensors $\mathbf{D}_0$ and $\mathbf{D}_1$ have components

$$\begin{aligned}(D_0)_{ik} &= e_{irs}e_{kpq}(K_\mu)_{rp}(K_{-1})_{sq},\\ (D_1)_{ik} &= \frac{1}{2}e_{irs}e_{kpq}(K_\mu)_{rp}(K_\mu)_{sq}.\end{aligned} \tag{101}$$

Then, expanding Eq. (99) to second order in ε, we obtain

$$\mathbf{B} = \mathbf{B}_0 + \varepsilon\mathbf{B}_1 + \varepsilon^2\mathbf{B}_2 + O\left(\varepsilon^3\right), \tag{102}$$

from which it is straightforward to deduce that

$$\begin{aligned}\mathbf{B}_0 &= \frac{1}{d_0}\mathbf{D}_0,\\ \mathbf{B}_1 &= \frac{1}{d_0}\left(\mathbf{D}_1 - \frac{d_1}{d_0}\mathbf{D}_0\right),\\ \mathbf{B}_2 &= \frac{d_1}{(d_0)^3}(d_1\mathbf{D}_0 - d_0\mathbf{D}_1).\end{aligned} \tag{103}$$

The corresponding expansion for the tensor $\mathbf{P}$ can be obtained by making use of Eq. (102) in the definition (22) for $\mathbf{P}$, leading to

$$\mathbf{P} = \mathbf{P}_0 + \varepsilon\mathbf{P}_1 + \varepsilon^2\mathbf{P}_2 + O\left(\varepsilon^3\right), \tag{104}$$

where the tensors $\mathbf{P}_0$, $\mathbf{P}_1$, and $\mathbf{P}_2$ are given by

$$(P_q)_{ijkl} = \frac{1}{4\pi|\mathbf{Z}_0|}\int_{|\boldsymbol{\xi}|=1}(B_q)_{ik}\xi_j\xi_l\left[\boldsymbol{\xi}^T\left(\mathbf{Z}_0^T\mathbf{Z}_0\right)^{-1}\boldsymbol{\xi}\right]^{-\frac{3}{2}}dS, \quad q = 0, 1, 2. \tag{105}$$

In general, a Gaussian quadrature technique can be implemented for the numerical integration over the surface of the unit sphere, $|\boldsymbol{\xi}| = 1$. Note that the leading-order term in (104) is the limiting value of $\mathbf{P}$ in the incompressible matrix limit. Next, we turn to the computation the tensor $\mathbf{E}^I$, as defined by expression (78).

In this connection, it is important to remark that the tensor $\mathbf{P}_0$ is not of full-rank, meaning there is no fourth-order tensor $(\mathbf{P}_0)^{-1}$ such that $\mathbf{P}_0(\mathbf{P}_0)^{-1} = (\mathbf{P}_0)^{-1}\mathbf{P}_0 = \mathbf{I}$. Hence, to determine $\mathbf{E}^I$ it is necessary to carry out an asymptotic analysis for $\mathbf{Q} = \mathbf{P}^{-1}$, about $\varepsilon = 0$. For the sake of continuity, the pertinent derivations are given in Appendix A, and here we only spell out the final result of the asymptotic analysis, which is given by

$$\mathbf{E}^I = \mathbf{Q}_0 - \mathbf{L}_\mu^{(1)}, \tag{106}$$

where

$$\mathbf{Q}_0 = \mathbf{P}_0^\dagger(\boldsymbol{\mathcal{I}} - \mathbf{P}_1\mathbf{Q}_{-1}) + \sum_{i=1}^{3}\mathbf{W}_i \otimes \mathbf{V}_i^{(1)}, \tag{107}$$

with

$$\mathbf{Q}_{-1} = \sum_{i=1}^{3}\mathbf{W}_i \otimes \mathbf{V}_i^{(0)}. \tag{108}$$

In the above equations, $\{\mathbf{W}_1, \mathbf{W}_2, \mathbf{W}_3\}$ is a set of second-order tensor spanning the null space of $\mathbf{P}_0$, while the second order tensors $\mathbf{V}_i^{(0)}$ and $\mathbf{V}_i^{(1)}$ are defined by [4]

$$\mathbf{V}_i^{(0)} = \frac{1}{\mathbf{W}_i \cdot \mathbf{P}_1\mathbf{W}_i}\mathbf{W}_i \tag{109}$$

and

$$\mathbf{V}_i^{(1)} = -\frac{1}{\mathbf{W}_i \cdot \mathbf{P}_1 \mathbf{W}_i} \left\{ \left(\mathbf{P}_1 \mathbf{P}_0^{\dagger}\right)^T \mathbf{W}_i + \left[\mathbf{W}_i . \left(\mathbf{P}_2 - \mathbf{P}_1 \mathbf{P}_0^{\dagger} \mathbf{P}_1\right) \mathbf{W}_i\right] \mathbf{V}_i^{(0)} \right\}, \tag{110}$$

where $i = 1, 2, 3$ (no sum), and where the superscript T denotes the usual transpose of a fourth-order tensor (i.e., $(\cdot)^T_{ijkl} = (\cdot)_{klij}$). In addition, $\mathbf{P}_0^{\dagger}$ is the Moore-Penrose generalized inverse of $\mathbf{P}_0$ satisfying the properties

$$\begin{aligned} &\mathbf{P}_0 \mathbf{P}_0^{\dagger} \mathbf{P}_0 = \mathbf{P}_0, \qquad && \mathbf{P}_0^{\dagger} \mathbf{P}_0 \mathbf{P}_0^{\dagger} = \mathbf{P}_0^{\dagger}, \\ &\left(\mathbf{P}_0 \mathbf{P}_0^{\dagger}\right)^T = \mathbf{P}_0 \mathbf{P}_0^{\dagger}, \qquad && \left(\mathbf{P}_0^{\dagger} \mathbf{P}_0\right)^T = \mathbf{P}_0^{\dagger} \mathbf{P}_0. \end{aligned} \tag{111}$$

5 2-D Application: Reinforced Elastomers with Elliptical Fibers

In the previous section, we presented a general homogenization procedure to estimate the effective stored-energy function and the associated evolution of the microstructure for rigidly reinforced elastomeric composites in both the dilute and non-dilute concentration regimes. In this section and the next, we make use of this procedure to obtain some explicit estimates of the Willis-type for two specific classes of composites: (1) elastomers reinforced with aligned, cylindrical fibers subjected to general (transverse) plane-strain loading, and (2) elastomers reinforced with spherical particles subjected to general tri-axial loading. In this section, we will study the first class of composites, while the second class will be discussed in Sect. 6. (More general, non-spherical particle shapes will be considered elsewhere.) The variational estimates (77) and (79) can be employed for fairly general matrix behavior. Indeed, the stored-energy function $W^{(1)}$, characterizing the constitutive behavior of the matrix, is assumed to be objective, isotropic, strictly rank-one convex (strongly elliptic) function of the deformation gradient tensor $\mathbf{F}$. In this work, attention is restricted to stored-energy functions of the generalized neo-Hookean type

$$W^{(1)}(\mathbf{F}) = g(I) + h(J) + \frac{1}{2}\mu'^{(1)}(J-1)^2, \tag{112}$$

where $I = \mathrm{tr}(\mathbf{C})$ and the material functions $g(I)$ and $h(J)$ are assumed to be twice continuously differentiable satisfying the conditions: $g(3) = h(1) = 0$, $g_I(3) = \mu^{(1)}/2$, $h_J(3) = -\mu^{(1)}$, and $4g_{II}(3) + h_{JJ}(1) = \mu^{(1)}$, in which the subscripts I and J stand for partial differentiation with respect to the invariants I and J, respectively. The energy form (112) has been shown to provide reasonably good agreement with experimental data for rubberlike materials [30]. A well-known example of the general form (112), which captures the limiting chain extensibility of elastomers, is the (compressible) Gent model [13], expressed by

$$W^{(1)}(\mathbf{F}) = -\frac{J_m \mu^{(1)}}{2} \ln\left(1 - \frac{I-3}{J_m}\right) - \mu^{(1)} \ln(J) + \frac{1}{2}\left(\mu'^{(1)} - 2\frac{\mu^{(1)}}{J_m}\right)(J-1)^2, \tag{113}$$

where the dimensionless parameter J_m is the limiting value for $I - 3$ at which the elastomer locks up. It should be remarked that the strong ellipticity of the Gent model (113) is satisfied for all deformations by the conditions: $\mu^{(1)} > 0$, $J_m > 0$, $\mu'^{(1)} > 2\mu^{(1)}/J_m$. Note that the Gent model (113) reduces to the compressible neo-Hookean model, which never locks up, in the limit as $J_m \to \infty$.

It should be emphasized that, different from the previously discussed lock-up phenomenon for the composite, the lock up associated with the parameter J_m is due to the

elastomeric character of the matrix stemming from the fact that polymeric chains of the rubbery matrix become inextensible when they experience a certain strain level. Henceforth, for definiteness, we will refer to the former lock up as *geometric lock up* (GL), and to latter as *material lock up* (ML). By the same token, the macroscopic deformation gradients at which the geometric and material lock up occur are, respectively, denoted by $\bar{\mathbf{F}}^{\mathrm{GL}}$ and $\bar{\mathbf{F}}^{\mathrm{ML}}$. It is emphasized that the ML is already present in a homogeneous (Gent) matrix and enhanced with the reinforcement; however, the GL disappears in the limit of dilute particle concentration. It can be verified that the blow-up in the estimate (77) because of the GL or ML is caused only by the first term in (77), and, consequently, for a composite with a Gent matrix, the GL and ML respectively take place, when the following conditions are satisfied

$$\det\big(\bar{\mathbf{F}} - c\bar{\mathbf{R}}^{(2)}\big) = 0, \tag{114}$$

$$\mathrm{tr}\big[\bar{\mathbf{C}} - 2c\bar{\mathbf{F}}^T\bar{\mathbf{R}}^{(2)} + c^2\mathbf{I}\big] = (1-c)^2(J_m+3), \tag{115}$$

where $\bar{\mathbf{C}} = \bar{\mathbf{F}}^T\bar{\mathbf{F}}$. It should be remarked that both lock-up phenomena are affected by the microstructure evolution thorough $\bar{\mathbf{R}}^{(2)}$. It is obvious that the lock-up strain for the composite is determined by $\bar{\mathbf{F}}^{lock} = \min\{\bar{\mathbf{F}}^{\mathrm{GL}}, \bar{\mathbf{F}}^{\mathrm{ML}}\}$. In fact, depending on the underlying microstructure in the undeformed configuration and extensibility of the rubbery matrix (characterized by the parameter J_m), the composite may lock up because of either condition (114) or condition (115). It is remarked that for composites with a neo-Hookean matrix (where $J_m \to \infty$) $\bar{\mathbf{F}}^{lock} = \bar{\mathbf{F}}^{\mathrm{GL}}$. It is also worth mentioning that, for dilute concentration conditions, the effective stored-energy function (90) for reinforced Gent elastomers locks up at the same deformation as the Gent matrix, as given by the condition $\mathrm{tr}(\bar{\mathbf{C}}) = J_m + 3$.

5.1 Plane-Strain Loading of Fiber-Reinforced Elastomers

In this section, we obtain estimates for the effective behavior of hyperelastic composites made of a rubbery matrix and rigid and axially aligned fibers. It is assumed that the cylindrical fibers have an elliptical cross-section and are distributed with elliptical symmetry in the plane transverse to the fiber direction. Consistent with earlier discussions, the aspect ratio of both the fiber cross-section and distribution are taken to be given by ω. Furthermore, attention is restricted to macroscopic plane-strain deformation. Assume that the composite undergoes a *uniform* deformation gradient $\bar{\mathbf{F}}$ with the following matrix representation

$$\begin{aligned}[\bar{F}_{ij}] = &\begin{pmatrix} \cos(\bar{\psi}) & -\sin(\bar{\psi}) \\ \sin(\bar{\psi}) & \cos(\bar{\psi}) \end{pmatrix}\begin{pmatrix} \cos(\bar{\theta}) & -\sin(\bar{\theta}) \\ \sin(\bar{\theta}) & \cos(\bar{\theta}) \end{pmatrix} \\ &\times \begin{pmatrix} \bar{\lambda}_1 & 0 \\ 0 & \bar{\lambda}_2 \end{pmatrix}\begin{pmatrix} \cos(\bar{\theta}) & \sin(\bar{\theta}) \\ -\sin(\bar{\theta}) & \cos(\bar{\theta}) \end{pmatrix},\end{aligned} \tag{116}$$

with respect to the fixed Cartesian basis $\{\mathbf{e}_i\}$, $i = 1, 2$. In the above relation, $\bar{\lambda}_1$ and $\bar{\lambda}_2$ are the principal stretches and $\bar{\theta}$ denotes the angle (positive anticlockwise) of the in-plane Lagrangian stretch axes relative to the basis $\{\mathbf{e}_i\}$. Also, $\bar{\psi}$ serves to quantify the rigid-body rotation (or "continuum spin"). A schematic representation of the composite microstructure and loading parameters is depicted in Fig. 1a for $\bar{\psi} = 0$. The corresponding 3-D illustration, Fig. 1b shows a typical (embedded) long cylindrical fiber under the plane-strain loading.

It should be remarked that constitutive models for this class of fiber-reinforced elastomers have already been derived by Lopez-Pamies and Ponte Castañeda [26] making use of the second-order (GSO) homogenization theory. Analytical results were given for general

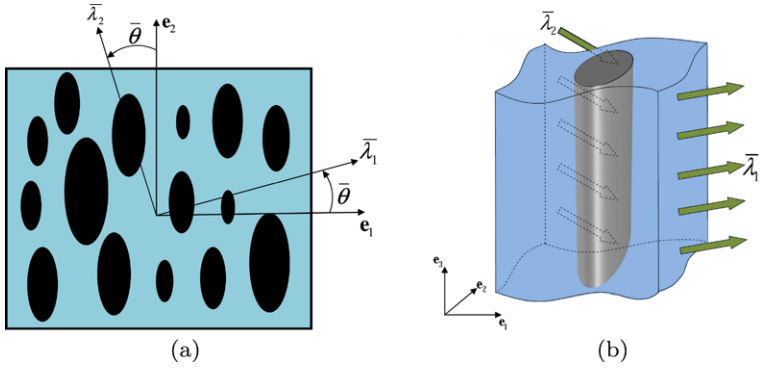

Fig. 1 Rigidly-reinforced composite under plane-strain loading. (**a**) Two-dimensional representation in the transverse plane. (**b**) Three-dimensional representation of a typical reinforcing fiber

matrix behavior of the form (112) in the limit of an incompressible matrix. These results, which will be spelled out later, have been shown to be in good agreement with corresponding FEM numerical results available in the literature for special types of loading conditions [29]. Hence, to gain some insight into the accuracy of the variational TSO estimates, described in the previous section, we will also show comparisons with the GSO estimates and FEM results for this class of composites in this section.

The constitutive behavior for the matrix phase is assumed to obey the Gent model given in (113). The computation of the TSO estimate (56), requires the calculation of the components of the tensor $\mathbf{P}$ for the cylindrical microstructure. The components of $\mathbf{P}$, in the rectangular Cartesian basis $\{\mathbf{e}_i\}$, $i = 1, 2, 3$, when the fibers are aligned in the direction $\mathbf{N} = \mathbf{e}_3$, are given by

$$P_{ijkl} = \frac{\omega}{2\pi} \int_0^{2\pi} \frac{H_{ijkl}(\xi_1, \xi_2, \xi_3 = 0)}{\xi_1^2 + \omega^2 \xi_2^2} \, d\theta \,, \tag{117}$$

where $H_{ijkl} = (L^{(1)}_{ipkq} \xi_p \xi_q)^{-1} \xi_j \xi_l$ with $\xi_1 = \cos(\theta)$, and $\xi_2 = \sin(\theta)$. In general, it is not possible to obtain analytical expressions for the components of the $\mathbf{P}$ tensor associated with matrix form (113) and loading condition (116). But it is easy to compute numerically the tensor $\mathbf{P}$, as well as the associated tensor $\mathbf{E}$.

In this section, we will focus our attention to *incompressible* Gent matrix phases obtained from expression (113) in the limit as $\mu'^{(1)} \to \infty$. This requires the computation of the tensor $\mathbf{E}^I$ via the procedure given in Sect. 4.3. Then, the calculated components of the tensor $\mathbf{E}^I$ can be substituted in Eqs. (77) and (79) to obtain the numerical values of the effective stored-energy function and the associated fiber rotation. It should be remarked that for the aligned loading case ($\bar{\theta} = 0$), the components of the tensor $\mathbf{E}^I$ can be expressed explicitly, since in this case the integrals in (105) can be calculated analytically. This leads to a closed-form expression for the effective energy, but the expression is quite lengthy and will not be included here for brevity. It is also important to mention that when the Gent behavior (113) is specialized to neo-Hookean behavior (equivalent to the limit of $J_m \to \infty$), the associated integrals in (105) can be performed analytically. In this case, derivations of closed-form expressions for the $\mathbf{E}^I$-tensor components and subsequently for the effective potential energy are feasible as discussed next.

5.2 Explicit Results for an Incompressible, neo-Hookean Matrix

In this subsection, we assume that the matrix phase behavior is characterized by a compressible neo-Hookean stored-energy function, given by

$$W^{(1)}(\mathbf{F}) = \frac{1}{2}\mu^{(1)}(I-2) - \mu^{(1)}\ln J + \frac{1}{2}\mu'^{(1)}(J-1)^2, \tag{118}$$

where the parameters $\mu^{(1)}$ and $\mu'^{(1)}$ denote the standard Lamé moduli of the matrix at zero strain. As mentioned earlier, (118) is the reduced form of (113) for the plane-strain loading when $J_m \to \infty$. In this case, all the in-plane components of the tensor $\mathbf{P}$ can be computed analytically and the results are provided in Appendix B. These results can then be used to perform an asymptotic expansion for the components of the tensor $\mathbf{E} = (\mathbf{P}^{-1} - \mathbf{L}^{(1)})|_{\mathbf{F}=\bar{\mathbf{F}}}$ in the incompressibility limit (i.e., $\mu'^{(1)} \to \infty$), leading to the following expressions for the components of $\mathbf{E}^I$, as defined by expression (78), namely,

$$\begin{aligned}
&E^I_{1111} = \frac{1}{2}\frac{\mu^{(1)}}{\bar{\lambda}_1\bar{\lambda}_2\omega}\Omega_1, \qquad E^I_{2222} = \frac{1}{2}\frac{\mu^{(1)}\omega}{\bar{\lambda}_1\bar{\lambda}_2}\Omega_2, \qquad E^I_{1212} = \frac{1}{2}\frac{\mu^{(1)}\omega}{\bar{\lambda}_1\bar{\lambda}_2}\Omega_1,\\
&E^I_{2121} = \frac{1}{2}\frac{\mu^{(1)}}{\bar{\lambda}_1\bar{\lambda}_2\omega}\Omega_2, \qquad E^I_{1121} = -\frac{1}{2}\frac{\mu^{(1)}}{\bar{\lambda}_1\bar{\lambda}_2\omega}\Omega_3, \qquad E^I_{2212} = -\frac{1}{2}\frac{\mu^{(1)}\omega}{\bar{\lambda}_1\bar{\lambda}_2}\Omega_3,
\end{aligned}$$

$$E^I_{1122} = E^I_{1221} = E^I_{1112} = E^I_{2221} = 0, \tag{119}$$

where

$$\begin{aligned}
\Omega_{1,2} &= (\bar{\lambda}_1+\bar{\lambda}_2)\big\{\bar{\lambda}_1+\bar{\lambda}_2 \mp (\bar{\lambda}_1-\bar{\lambda}_2)\cos\big[2(\bar{\psi}+\bar{\theta})\big]\big\},\\
\Omega_3 &= \big[(\bar{\lambda}_1)^2-(\bar{\lambda}_2)^2\big]\sin\big[2(\bar{\psi}+\bar{\theta})\big].
\end{aligned} \tag{120}$$

It then follows from expression (77) that the effective stored-energy function $\widehat{W}(\bar{\mathbf{F}})$ of the rigidly reinforced composite reduces to

$$\begin{aligned}
\widehat{W}(\bar{\mathbf{F}}) &= (1-c)W^{(1)}\big(\bar{\mathbf{F}}^{(1)}\big)\\
&\quad + \frac{\mu^{(1)}c(1+\bar{\lambda}_1^2)}{4\omega\,(1-c)\bar{\lambda}_1^2}\big\{2\big(1+\omega^2\big)\big(\bar{\lambda}_1^2 - 2\bar{\lambda}_1\cos(\phi)+1\big)\\
&\quad + \big(\omega^2-1\big)\big(\bar{\lambda}_1^2-1\big)\big[\cos(2\bar{\theta}-2\phi)-\cos(2\bar{\theta})\big]\big\},
\end{aligned} \tag{121}$$

where

$$\begin{aligned}
W^{(1)}\big(\bar{\mathbf{F}}^{(1)}\big) &= \mu^{(1)}\frac{\bar{\lambda}_1^4 - 2c\bar{\lambda}_1(1+\bar{\lambda}_1^2)\cos(\phi) - 2\bar{\lambda}_1^2 + 4c\bar{\lambda}_1^2 + 1}{2\bar{\lambda}_1^2(1-c)^2}\\
&\quad - \mu^{(1)}\ln\left[\frac{(1+c^2)\bar{\lambda}_1 - c(1+\bar{\lambda}_1^2)\cos(\phi)}{\bar{\lambda}_1(1-c)^2}\right].
\end{aligned}$$

In these relations, the angle ϕ, denoting the in-plane rigid body rotation of the fibers relative to the macroscopic rotation (i.e., $\phi = \bar{\psi}^{(2)} - \bar{\psi}$), is obtained from the kinematical relation

$$\begin{aligned}
&2\omega(1-c)\bar{\lambda}_1^2\cos(\phi)\Delta_1 + 2\bar{\lambda}_1\big[\big(\bar{\lambda}_1^2+1\big)\big(1+\omega^2\big) + \omega\,(1-c)\bar{\lambda}_1\Delta_2\big]\sin(\phi)\\
&\quad + \big(\bar{\lambda}_1^4-1\big)\big(\omega^2-1\big)\sin(2\bar{\theta}-2\phi) = 0,
\end{aligned} \tag{122}$$

where

$$\Delta_1 = -2c^2 \frac{\sin(\phi)[(1+\bar{\lambda}_1^2)\cos(\phi) - 2\bar{\lambda}_1]}{(1-c)[(1+c^2)\bar{\lambda}_1 - c(1+\bar{\lambda}_1^2)\cos(\phi)]},$$

$$\Delta_2 = c \frac{[\cos(\phi)(1+\bar{\lambda}_1^2) - 2\bar{\lambda}_1][2c\bar{\lambda}_1\cos(\phi) - \bar{\lambda}_1^2 - 1]}{(1-c)\bar{\lambda}_1[(1+c^2)\bar{\lambda}_1 - c(1+\bar{\lambda}_1^2)\cos(\phi)]}.$$

It is emphasized that the estimate (121) is consistent with the overall incompressibility constraint, which in this case reduces to $\bar{\lambda}_1\bar{\lambda}_2 = 1$. It is also remarked that the energy function (121) is independent of the angle $\bar{\psi}$, which is consistent with the objectivity of the energy function $\widehat{W}(\bar{\mathbf{F}})$, requiring that $\widehat{W}(\bar{\mathbf{F}}) = \widehat{W}(\bar{\mathbf{U}})$, where $\bar{\mathbf{U}} = (\bar{\mathbf{F}}^T\bar{\mathbf{F}})^{1/2}$ is the macroscopic stretch tensor.

The above results can be easily specialized for dilute concentrations by expanding about $c = 0$. Thus, keeping terms of order c in Eq. (121), the estimate for the effective stored-energy function $\widehat{W}(\bar{\mathbf{F}})$ is given by

$$\begin{aligned}
&\widehat{W}^{Dilute}(\bar{\mathbf{F}}) \\
&= \frac{1}{2}\mu^{(1)}\big(\bar{\lambda}_1^2 + \bar{\lambda}_1^{-2} - 2\big) \\
&\quad + \frac{1}{2}\mu^{(1)}\Bigg\{\frac{1}{\bar{\lambda}_1^2\omega}\big[2\omega\big(1+\bar{\lambda}_1^4\big) + \big(1+\omega^2\big)\big(1+\bar{\lambda}_1^2\big)\big[\big(1+\bar{\lambda}_1^2\big) - 2\bar{\lambda}_1\cos(\phi_0)\big] \\
&\quad + \big(\bar{\lambda}_1^4 - 1\big)\big(\omega^2 - 1\big)\sin(\phi_0)\sin(2\bar{\theta} - \phi_0) - 4\omega\bar{\lambda}_1^2\big] - \big(\bar{\lambda}_1^2 + \bar{\lambda}_1^{-2} - 2\big)\Bigg\}c + \mathrm{O}\big(c^2\big),
\end{aligned} \tag{123}$$

where $\phi_0 = \bar{\psi}_0^{(2)} - \bar{\psi}$ (where the angle $\bar{\psi}_0^{(2)}$ denotes the total in-plane rigid body rotation of fibers in the *dilute concentration regime*) is given by

$$2\bar{\lambda}_1\big(1+\omega^2\big)\sin(\phi_0) - \big(\bar{\lambda}_1^2 - 1\big)\big(\omega^2 - 1\big)\sin\big[2(\phi_0 - \bar{\theta})\big] + \mathrm{O}(c) = 0. \tag{124}$$

The estimates (123) and (124) are valid for arbitrary aspect ratios $\omega \geq 1$ of fibers. For the special case of the circular cross-section ($\omega = 1$) for the fibers (which also implies an isotropic distribution of the fibers), the in-plane behavior of the composite is isotropic and the stored-energy function (123) no longer depends on the loading angle $\bar{\theta}$. In this case, it is a simple matter to deduce that, the TSO estimate (123) reduces to

$$\widehat{W}^{Dilute}(\bar{\mathbf{F}}) = \frac{1}{2}\mu^{(1)}\big[\big(\bar{\lambda}_1^2 + \bar{\lambda}_1^{-2} - 2\big) + \big(2\bar{\lambda}_1^{-1} + 3\bar{\lambda}_1^{-2} + 3\big)(\bar{\lambda}_1 - 1)^2 c\big] + \mathrm{O}\big(c^2\big). \tag{125}$$

For comparison purposes, we recall in the next subsection the GSO results [26]. Although the GSO estimates are expected to be more accurate in general, they are more difficult to implement, and thus far results are only available for 2-D cases. On the other hand, as we will see in Sect. 6, the TSO can be used for general 3-D microstructures and loading conditions.

5.3 Generalized Second-Order Estimate

Lopez-Pamies and Ponte Castañeda [26] derived an expression for the effective stored-energy function of the class of fiber-reinforced composites described earlier with matrix

behavior (112) and transverse loading conditions (116). In the limit of incompressible behavior for the elastomeric matrix phase ($\mu'^{(1)} \to \infty$), the result simplifies to

$$\widehat{W}_{\mathrm{GSO}}(\mathbf{F}) = (1-c)g(\hat{I}), \tag{126}$$

where

$$\hat{I} = \frac{1}{(1-c)^2\bar{\lambda}_1^2\omega}\Big\{c\big(1+\bar{\lambda}_1^2\big)^2 + \big[1+2c(c-2)\bar{\lambda}_1^2+\bar{\lambda}_1^4\big]\omega + c\omega^2\big(1+\bar{\lambda}_1^2\big)^2 - c\big(\bar{\lambda}_1^4-1\big)\big(\omega^2-1\big)\sin(\phi)\sin(\phi-2\bar{\theta}) - 2c\bar{\lambda}\big(1+\bar{\lambda}_1^2\big)\big(1+\omega^2\big)\cos(\phi)\Big\}.$$

In this expression, the relative particle rotation angle ϕ is determined by

$$2\bar{\lambda}_1\big(1+\omega^2\big)\sin(\phi) - \big(\bar{\lambda}_1^2-1\big)\big(\omega^2-1\big)\sin\big[2(\phi-\bar{\theta})\big] = 0. \tag{127}$$

The GSO estimate (126) is known [26] to be consistent with the exact incompressibility constraint and expected to be fairly accurate for small to medium concentrations of fibers.

In the *dilute-concentration regime*, the GSO estimate (126) can be expanded about $c = 0$ to obtain the result that

$$\widehat{W}_{\mathrm{GSO}}^{Dilute}(\bar{\mathbf{F}}) = g(\bar{I}) + \left\{\frac{1}{\bar{\lambda}_1^2\omega}g'(\bar{I})\big[2\omega\big(1+\bar{\lambda}_1^4\big) + \big(1+\omega^2\big)\big(1+\bar{\lambda}_1^2\big)\big[\big(1+\bar{\lambda}_1^2\big) - 2\bar{\lambda}_1\cos(\phi_0)\big] + \big(\bar{\lambda}_1^4-1\big)\big(\omega^2-1\big)\sin(\phi_0)\sin(2\bar{\theta}-\phi_0) - 4\omega\bar{\lambda}_1^2\big] - g(\bar{I})\right\}c + \mathrm{O}\big(c^2\big), \tag{128}$$

where $\bar{I} = \mathrm{tr}(\bar{\mathbf{C}})$. The kinematical equation (127) is independent of the volume fraction of fibers and also provides the rotation of fibers in the dilute concentration regime.

Specializing the estimate (128) for a neo-Hookean matrix, the same second-order estimate is obtained as the dilute TSO estimate (123). Moreover, the estimates (124) and (127) for the particle rotation also agree exactly in this case. Consequently, the agreement of the TSO estimates (123) and (124) with the corresponding GSO results in the dilute concentration regime strongly suggests that the TSO estimates should be also be quite accurate for incompressible, rigidly-reinforced composites with more general microstructures (at least) in the dilute concentration regime. As we will see in the next subsection, differences can arise between the new TSO and GSO estimates for finite volume fractions, but only at sufficiently large stretches.

5.4 Discussion of the Results

In the remainder of this section, we present some illustrative results for the *new* TSO estimates for plane-strain loading of 2-D fiber-reinforced elastomers. For comparison purposes, the corresponding GSO results of Lopez-Pamies and Ponte Castañeda [26] are also included in the figures and shown with dashed curves. For simplicity, we restrict our attention to incompressible ($\mu'^{(1)} \to \infty$) Gent and neo-Hookean matrix phases, circular fibers ($\omega = 1$) and pure shear loading ($\bar{\theta} = \bar{\psi} = 0$, $\bar{\lambda}_1 = \bar{\lambda}_2^{-1} = \bar{\lambda}$). Results are provided for several volume fractions, c, and are normalized by $\mu^{(1)}$.

Figure 2 shows the new TSO estimates for the effective response of the reinforced neo-Hookean elastomers, as well as the corresponding GSO estimates. Results are shown for

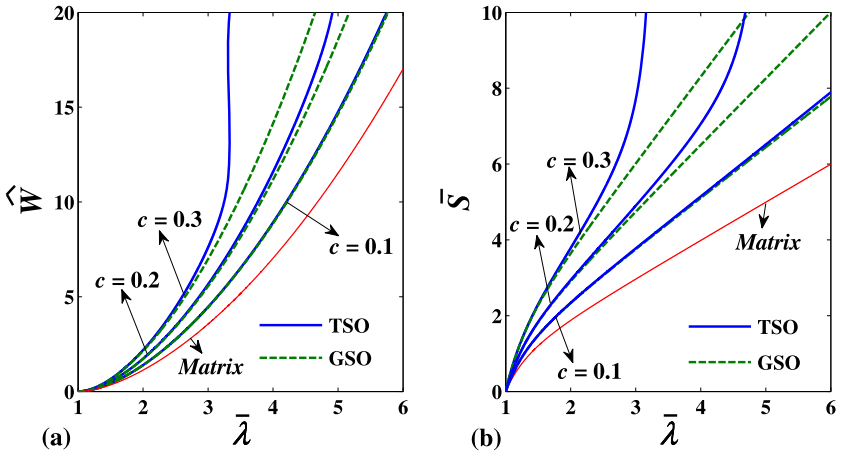

Fig. 2 New tangent second-order (TSO) and generalized second-order (GSO) estimates for the effective response of a rigidly fiber-reinforced elastomer with an incompressible neo-Hookean matrix under pure shear loading. The results are shown as a function of the applied stretch $\bar{\lambda}$ for different values of the fiber volume fraction. (**a**) The effective energy $\widehat{W}$. (**b**) The corresponding macroscopic stress $\bar{S} = d\widehat{W}/d\bar{\lambda}$

three different fiber volume fractions $c = 0.1, 0.2, 0.3$, as a function of the macroscopic stretch $\bar{\lambda}$. Part (a) shows the effective energy $\widehat{W}$, and part (b), the corresponding macroscopic stress $\bar{S} = d\widehat{W}/d\bar{\lambda}$. The new TSO results are seen to be quite close to the GSO estimates for a range of $\bar{\lambda}$, but they start to deviate from the GSO results, as the average stretch approaches the "geometric" lock-up condition (114) for the TSO estimates (i.e., $\bar{\lambda} \to 1/c$). For instance, it is seen for $c = 0.1$ (where the lock-up stretch is 10), the TSO model predicts very similar results for the effective energy as well as the macroscopic stress to those for the GSO in the range $1 \leq \bar{\lambda} \leq 6$. On the other hand, for $c = 0.3$ (where the lock-up stretch is 3.33), the agreement is very good only up to a stretch of 2.5.

Figure 3 shows a more detailed comparison of the new TSO estimates with earlier analytical estimates and numerical simulations for neo-Hookean elastomers reinforced by rigid fibers of circular cross section. Results are provided for two volume fractions: (a) $c = 0.2$, and (b) $c = 0.3$. The GSO (2006) estimates correspond to the stored-energy function (126), while the GSO (2004) and TSO (2000) estimates correspond to earlier versions of the GSO [24] and TSO [36] estimates, respectively. On the other hand, the LAM estimates refer to the sequentially laminated results of deBotton [9], while the FEM results refer to the finite element simulations of Moraleda et al. [29]. The main observation from these plots is that while the GSO estimate provides the best agreement with the FEM simulations, the new TSO estimate also provides excellent agreement with the FEM results (up to the point where the simulations were carried out), especially for the smaller fiber concentrations. For the higher volume fraction ($c = 0.3$) the new TSO estimates tend to overestimate the FEM results at sufficiently large stretches, but are still quite good for stretches of less than 1.5. On the other hand, the LAM estimates tend to underestimate the response of the reinforced elastomers for sufficiently large strains, even if the differences relative to the FEM are relatively small. Finally, it can be seen that the new TSO estimates are much improved relative to the earlier version [36] of the TSO estimates, and even compared to an earlier version [24] of the GSO estimates. The main conclusion from these comparisons is that the new way of handling the matrix incompressibility limit presented in Sect. 4.2 actually works quite well at least when the fiber concentrations and/or stretches are not too large.

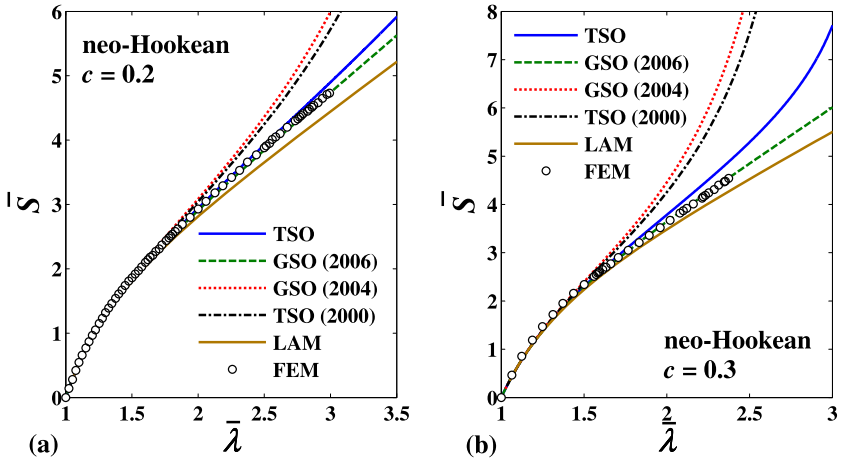

Fig. 3 The effective response of a rigidly fiber-reinforced elastomer with an incompressible neo-Hookean matrix under pure shear loading. The macroscopic stress $\bar{S} = d\widehat{W}/d\bar{\lambda}$ is plotted as a function of the applied stretch $\bar{\lambda}$ for (**a**) $c = 0.2$, and (**b**) $c = 0.3$. Comparisons between the new TSO estimate (121), the estimate (126) of Lopez-Pamies and Ponte Castañeda [26] "GSO (2006)", the earlier GSO results of Lopez–Pamies and Ponte Castañeda [24] "GSO (2004)", the earlier TSO results of Ponte Castañeda and Tiberio [36] "TSO (2000)", the laminate results of deBotton [9] "LAM", and the FE simulations of Moraleda et al. [29] "FEM"

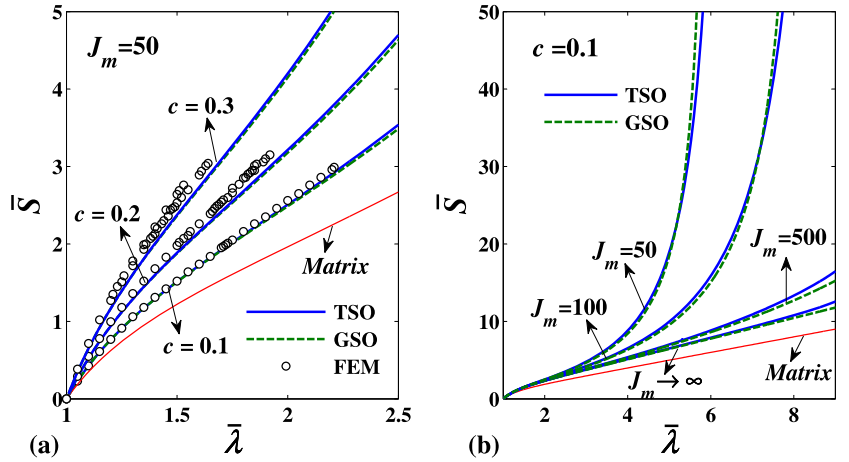

Fig. 4 New tangent second-order (TSO) estimate, generalized second-order (GSO) estimate (126), and the FE simulations of Moraleda et al. [29] (FEM) for the effective response of a fiber-reinforced elastomer with an incompressible Gent matrix under pure shear loading. The macroscopic stress $\bar{S} = d\widehat{W}/d\bar{\lambda}$ is depicted as a function of the applied stretch $\bar{\lambda}$, for (**a**) different values of the fiber volume fraction c with $J_m = 50$, and (**b**) different matrix lock-up parameters J_m with $c = 0.1$

Next, for completeness, we consider fiber-reinforced composites using the Gent model for the matrix and the same loading conditions as the previous case. The results for the macroscopic stress $\bar{S} = d\widehat{W}/d\bar{\lambda}$ are presented in Figs. 4a and 4b versus the applied stretch $\bar{\lambda}$. Figure 4a shows the results for composites with fiber concentrations $c = 0.1$, 0.2, 0.3 for

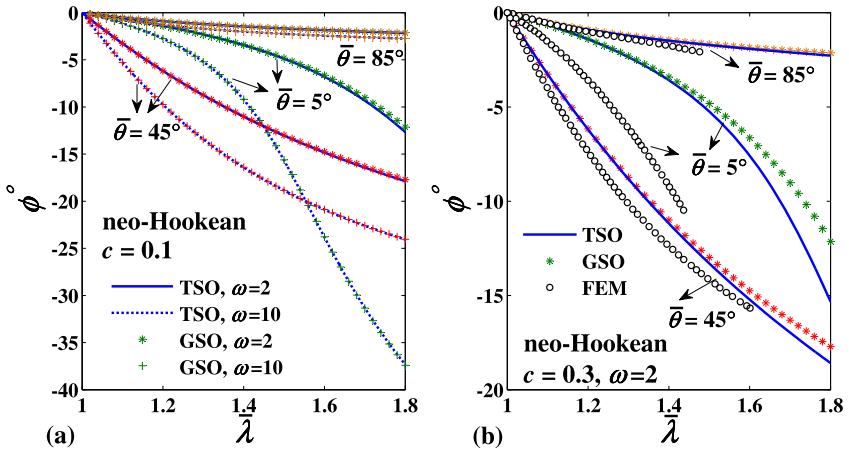

Fig. 5 The microstructure evolution in a rigidly fiber-reinforced elastomer with an incompressible neo-Hookean matrix under pure shear loading. The relative fiber rotation ϕ is plotted as a function of the applied stretch $\bar{\lambda}$ for three different stretching angles $\bar{\theta} = 5°,\ 45°,$ and $85°$. (**a**) Comparisons between the new TSO estimate (122) and the estimate (127) of Lopez-Pamies and Ponte Castañeda [26] for the volume fraction $c = 0.1$, and aspect ratios $\omega = 2$, and 10. (**b**) Comparisons between the new TSO estimate, the GSO estimate and the FEM simulations of Moraleda et al. [29] for $c = 0.3$, and $\omega = 2$

a fixed lock-up parameter ($J_m = 50$), while Fig. 4b shows results for Gent matrices with $J_m = 50, 100, 500, \infty$ for fixed volume fraction ($c = 0.1$). The responses of the unreinforced matrix with $J_m = 50$ and $J_m = \infty$ are included respectively in Figs. 4a and 4b for comparison purposes. In addition, the results of the finite element simulations of Moraleda et al. [29] for $J_m = 50$ are also included for comparison purposes. As can be seen from Fig. 4a, the agreement of the new TSO estimates for reinforced elastomers of the Gent type with the FEM results (and GSO estimates) is quite good for the range of deformations achieved in the numerical simulations. It should be noted, however, that the TSO (and GSO) predictions slightly underestimate the response, especially at the higher volume fractions. On the other hand, as show in Fig. 4b, the agreement of the new TSO and earlier GSO estimates for reinforced Gent elastomers is also quite good, even for fairly large stretches. However, the TSO estimates are slightly stiffer for intermediate stretches, but eventually become softer than the GSO estimates as the "constitutive" lock-up condition (115) is approached.

Finally, Fig. 5 presents results for the evolution of the particle orientation under non-aligned applied loadings for neo-Hookean elastomers reinforced by rigid fibers of elliptical cross section. Results for the (average) relative rotation ϕ (see Fig. 1) are shown for three different stretching angles ($\bar{\theta} = 5°,\ 45°,$ and $85°$). Figure 5a shows comparisons of the new TSO estimates with the GSO estimates [26] for two different fiber aspect ratios ($\omega = 2$ and 10), and given fiber volume fraction ($c = 0.1$). The results show that the largest rotations are generated for the larger aspect ratio (i.e., for $\omega = 10$), when the compressive direction is most closely aligned with the long fiber axis (i.e., for $\bar{\theta} = 5°$), although relatively large stretches are needed. In addition, the results show excellent agreement between the new TSO and GSO estimates at this fairly small value of c. This is consistent with the fact that the TSO and GSO equations ((127) and (124), respectively) for the fiber rotations agree precisely for a neo-Hookean matrix in the dilute concentration limit. Figure 5b presents additional comparisons of the new TSO estimates with the GSO estimates [26], as well as with the FEM numerical simulations of Moraleda et al. [29] for a volume fraction $c = 0.3$,

and aspect ratio $\omega = 2$. It can be seen from this plot that the agreement between the TSO homogenization results, on the one hand, and the FEM numerical results, on the other, is quite good for $\bar{\theta} = 45°$ and 85°, but less good for $\bar{\theta} = 5°$. This may be a consequence of the fact that the FEM results made use of equisized particles, which at this relatively high value of the fiber concentration may lead to stronger interactions among the fibers than the TSO results (corresponding to polydisperse distributions of fibers) can account for. In addition, it is not clear that a sufficiently large number of configurations has been used in the FEM simulations to generate accurate results by ensemble averaging. Be that as it may, the TSO homogenization estimates, which were also found to be consistent with the corresponding GSO results at this higher value of the fiber concentration, are at least *qualitatively* consistent with the results of the numerical simulations. Clearly, more extensive numerical work will be necessary to be able to assess the accuracy of the homogenization results in the future.

6 3-D Application: Reinforced Elastomers with Spherical Particles

As we have seen in the previous section, the new TSO procedure can be used to obtain accurate estimates for the macroscopic response and microstructure evolution for transverse loading of fiber-reinforced elastomers at finite strains, even when the fibers are rigid, corresponding to infinite contrast, and when the matrix is incompressible, leading to a strongly nonlinear *incompressibility constraint* for the composite (which can be recovered exactly by the theory). Although the GSO procedure [25] is expected to lead to even more accurate predictions, it is more difficult to implement because it makes use of additional information about the field fluctuations in the linear comparison composite. For this reason, it has not yet been implemented for general (3-D) ellipsoidal particles, especially in the limit of incompressible behavior for the matrix phase. On the other hand, the new TSO estimates of Sect. 4 for the effective stored-energy function of particle-reinforced (incompressible) elastomers are applicable for rigid particles with general ellipsoidal shape and distribution. However, for simplicity, in this section we will focus on an application of the TSO theory to particle-reinforced elastomers consisting of a random and isotropic distribution of spherical rigid inclusions in an isotropic, incompressible matrix phase, leaving for future work an in-depth investigation of more general ellipsoidal shapes for the particles.

We begin by remarking that, in view of objectivity and the assumed isotropy of the reinforced elastomer, it suffices to restrict attention to pure stretch deformations $\bar{\mathbf{F}} = \bar{\mathbf{U}}$ (i.e., $\bar{\mathbf{R}} = \mathbf{I}$), which, in the Cartesian basis $\{\mathbf{e}_i\}$, $i = 1, 2, 3$, can be expressed in the form

$$\bar{\mathbf{F}} = \bar{\mathbf{U}} = \bar{\lambda}_1 \mathbf{e}_1 \otimes \mathbf{e}_1 + \bar{\lambda}_2 \mathbf{e}_2 \otimes \mathbf{e}_2 + \bar{\lambda}_3 \mathbf{e}_3 \otimes \mathbf{e}_3, \tag{129}$$

where $\bar{\lambda}_i$ is the principal stretch in the $\mathbf{e}_i$-direction, and the overall incompressibility constraint $\bar{\lambda}_1 \bar{\lambda}_2 \bar{\lambda}_3 = 1$ holds. Under these hypotheses, it can be shown that $\bar{\mathbf{R}}^{(2)} = \mathbf{I}$ satisfies identically equation (79) for the particle rotation (as expected from the symmetry of the problem), and the TSO estimate (77) for the effective stored-energy function of the reinforced elastomer can be shown to reduce to

$$\begin{aligned} \widehat{W}(\bar{\mathbf{F}}) = (1-c) W_\mu^{(1)}\big(\bar{\mathbf{F}}^{(1)}\big) + \frac{c}{2(1-c)} \big[& \bar{\Lambda}_{11} E^I_{1111} + \bar{\Lambda}_{22} E^I_{2222} + \bar{\Lambda}_{33} E^I_{3333} \\ & + 2\big(\bar{\Lambda}_{12} E^I_{1122} + \bar{\Lambda}_{13} E^I_{1133} + \bar{\Lambda}_{23} E^I_{2233}\big)\big], \end{aligned} \tag{130}$$

where $\bar{\Lambda}_{ij} = (\bar{\lambda}_i - 1)(\bar{\lambda}_j - 1)$ $(i, j = 1, 2, 3)$.

In this section, we will confine our attention to stored-energy functions of the *generalized* neo-Hookean form (112) for the matrix phase. As discussed in Sect. 4.3, the computation of the microstructural tensor $\mathbf{E}^I$ requires the computation of the tensors $\mathbf{P}_i$ $(i = 0, 1, 2)$, as defined by (105), which in turn require the determination of the tensors $\mathbf{B}_i$ via the tensors $\mathbf{D}_0$, $\mathbf{D}_1$ and the scalars d_0, d_1, as provided by relations (103). After some algebraic manipulation, it is straightforward to deduce that the components of the symmetric, second-order tensors $\mathbf{D}_0$ and $\mathbf{D}_1$ for the matrix behavior (112) and the loading condition (129) reduce to

$$
\begin{aligned}
(D_0)_{11} &= 2\bar{\lambda}_1^2\big[\big(\bar{\lambda}_2^2\xi_3^2 + \bar{\lambda}_3^2\xi_2^2\big)g_I + 2\Delta_{23}^2 g_{II}\xi_2^2\xi_3^2\big],\\
(D_0)_{22} &= 2\bar{\lambda}_2^2\big[\big(\bar{\lambda}_1^2\xi_3^2 + \bar{\lambda}_3^2\xi_1^2\big)g_I + 2\Delta_{13}^2 g_{II}\xi_1^2\xi_3^2\big],\\
(D_0)_{33} &= 2\bar{\lambda}_3^2\big[\big(\bar{\lambda}_1^2\xi_2^2 + \bar{\lambda}_2^2\xi_1^2\big)g_I + 2\Delta_{12}^2 g_{II}\xi_1^2\xi_2^2\big],\\
(D_0)_{12} &= -2[\bar{\lambda}_3 g_I + 2\xi_3^2\Delta_{13}\Delta_{23}\bar{\lambda}_1\bar{\lambda}_2 g_{II}]\xi_1\xi_2,\\
(D_0)_{13} &= -2[\bar{\lambda}_2 g_I + 2\xi_2^2\Delta_{12}\Delta_{23}\bar{\lambda}_1\bar{\lambda}_3 g_{II}]\xi_1\xi_3,\\
(D_0)_{23} &= -2[\bar{\lambda}_1 g_I + 2\xi_1^2\Delta_{12}\Delta_{13}\bar{\lambda}_2\bar{\lambda}_3 g_{II}]\xi_2\xi_3,
\end{aligned}
$$

$$
\begin{aligned}
(D_1)_{11} &= 4g_I^2 + 8\big(\bar{\lambda}_2^2\xi_2^2 + \bar{\lambda}_3^2\xi_3^2\big)g_I g_{II} + h_{JJ}(D_0)_{11},\\
(D_1)_{22} &= 4g_I^2 + 8\big(\bar{\lambda}_1^2\xi_1^2 + \bar{\lambda}_3^2\xi_3^2\big)g_I g_{II} + h_{JJ}(D_0)_{22},\\
(D_1)_{33} &= 4g_I^2 + 8\big(\bar{\lambda}_1^2\xi_1^2 + \bar{\lambda}_2^2\xi_2^2\big)g_I g_{II} + h_{JJ}(D_0)_{33},\\
(D_1)_{12} &= -8\bar{\lambda}_3^{-1}\xi_1\xi_2 g_I g_{II} + h_{JJ}(D_0)_{12},\\
(D_1)_{13} &= -8\bar{\lambda}_2^{-1}\xi_1\xi_3 g_I g_{II} + h_{JJ}(D_0)_{13},\\
(D_1)_{23} &= -8\bar{\lambda}_1^{-1}\xi_2\xi_3 g_I g_{II} + h_{JJ}(D_0)_{23},
\end{aligned}
\tag{131}
$$

where $\Delta_{ij} = (\bar{\lambda}_i^2 - \bar{\lambda}_j^2)$, $i, j = 1, 2, 3$. In addition, the expressions for d_0 and d_1 are given by

$$
d_0 = 4\big(\bar{\lambda}_2^2\bar{\lambda}_3^2\xi_1^2 + \bar{\lambda}_1^2\bar{\lambda}_3^2\xi_2^2 + \bar{\lambda}_1^2\bar{\lambda}_2^2\xi_3^2\big)g_I^2 + 8\big[\bar{\lambda}_3^2\Delta_{12}^2\xi_1^2\xi_2^2 + \bar{\lambda}_2^2\Delta_{13}^2\xi_1^2\xi_3^2 + \bar{\lambda}_1^2\Delta_{23}^2\xi_3^2\xi_2^2\big]g_I g_{II},
$$

$$
d_1 = 8g_I^3 + h_{JJ}d_0 + 16\big(\bar{\lambda}_1^2\xi_1^2 + \bar{\lambda}_2^2\xi_2^2 + \bar{\lambda}_3^2\xi_3^2\big)g_I^2 g_{II}. \tag{132}
$$

For general matrix behavior, the integrals involved in the calculation of the tensors $\mathbf{P}_i$ in expressions (105) cannot be performed analytically. Therefore, the double integrals are computed numerically via Gaussian quadrature, with a sufficiently high numbers of Gauss points. Thus, using expressions (131) and (132), and setting $\mathbf{Z}_0 = \mathbf{I}$ for the spherical inclusions, the integrals may be easily computed by means of polar cylindrical coordinates

$$
\xi_1 = \sqrt{1 - z^2}\cos(\theta), \qquad \xi_2 = \sqrt{1 - z^2}\sin(\theta), \qquad \xi_3 = z, \tag{133}
$$

which vary over the intervals $0 \le \theta \le \pi$ and $0 \le z \le 1$. After calculation of the tensors $\mathbf{P}_i$, the tensor $\mathbf{E}^I$ can be calculated via the relations (106) to (110) (see also Appendix A). Finally, the computation of the effective stored-energy function (130) may be completed by means of the relevant components of the tensor $\mathbf{E}^I$.

Although the integrals (105) for the tensors $\mathbf{P}_i$ require numerical integration in general, they can actually be computed analytically at least for Gent behavior (113) for the matrix phase and axisymmetric loading conditions. In this case, a closed-form estimate may be

obtained for the macroscopic stored-energy function (130) of the particle-reinforced elastomer. However, the expressions are too lengthy to be included here. Instead, closed-form, analytical results are provided for the special case of neo-Hookean behavior for the matrix phase in the next subsection.

6.1 Analytical Results for (Incompressible) neo-Hookean Elastomers

In this section, we provide the specialization of the second-order estimate (130) for composite elastomers with *incompressible* neo-Hookean matrix phases. In fact, the microstructural tensors $\mathbf{P}$ and $\mathbf{E}$, as defined by expressions (22) and (57), respectively, can be computed analytically [27, 28] for *compressible* neo-Hookean behavior, and are given in Appendix C. Therefore, the incompressible limit ($\mu'^{(1)} \to \infty$) of the tensor $\mathbf{E}$ to obtain $\mathbf{E}^I$ can be evaluated directly in this case, without the more general procedure outlined in Sect. 4.3. In any event, having obtained the components of $\mathbf{E}^I$, the corresponding expression for the TSO estimate for the effective stored-energy function of the composite with incompressible neo-Hookean matrix phase is obtained by substitution into (130). The result may be written in the form

$$
\begin{aligned}
\widehat{W}(\bar{\mathbf{F}}) = (1-c)W_{\mu}^{(1)}\big(\bar{\mathbf{F}}^{(1)}\big) - \frac{c\mu^{(1)}}{2(1-c)}\Big\{ & \big\{\bar{\lambda}_1^2\bar{\lambda}_2^2\big[\bar{\lambda}_1^2+\bar{\lambda}_2^2+\bar{\lambda}_1\bar{\lambda}_2\big[2+\bar{\lambda}_1^7\bar{\lambda}_2^5+2\bar{\lambda}_1^6\bar{\lambda}_2^3 \\
& +\bar{\lambda}_1^5\bar{\lambda}_2(\bar{\lambda}_2+1)\big(\mathrm{I}_{1,0}^{\bar{1},1}+\mathrm{II}_{0,0}^{\bar{5},\bar{1}}+1\big)-2\bar{\lambda}_1^2\bar{\lambda}_2\big(1+\bar{\lambda}_1^2\bar{\lambda}_2\big)\big(\mathrm{I}_{0,0}^{\bar{3},2}-6\bar{\lambda}_2^2+2\big) \\
& +2\bar{\lambda}_1^3\bar{\lambda}_2^2\big(\mathrm{I}_{0,0}^{\overline{12},\bar{3}}+\mathrm{II}_{0,0}^{3,1}+6\big)+\bar{\lambda}_2\big(\bar{\lambda}_2^4-4\bar{\lambda}_2-6\big)\bar{\lambda}_1\big)\big]\big] \\
& \times\big[3\big(\bar{\lambda}_2^4\bar{\lambda}_1^2-1\big)\Xi_e^2+2\big(\bar{\lambda}_1^4\bar{\lambda}_2^2-2\bar{\lambda}_1^2\bar{\lambda}_2^4+1\big)\Xi_e\Xi_f-\bar{\lambda}_1^2\bar{\lambda}_2^2\big(\bar{\lambda}_1^2-\bar{\lambda}_2^2\big)\Xi_f^2\big] \\
& -\big(\bar{\lambda}_2^4\bar{\lambda}_1^2-1\big)\big(\bar{\lambda}_1^4\bar{\lambda}_2^2-1\big)\big[2\bar{\lambda}_1^2+2\bar{\lambda}_2^2+\bar{\lambda}_1\bar{\lambda}_2\big[\bar{\lambda}_2^3\big(3\bar{\lambda}_2^4-2\big)\bar{\lambda}_1^9 \\
& +2\bar{\lambda}_1^8\bar{\lambda}_2^3(2\bar{\lambda}_2+1)+\bar{\lambda}_1^7\bar{\lambda}_2^2\big(\mathrm{I}_{0,3}^{\bar{9},\bar{8}}+\mathrm{II}_{0,0}^{2,\bar{6}}+4\big)-2\bar{\lambda}_1^6\bar{\lambda}_2^2\big(\mathrm{I}_{3,0}^{\bar{2},\bar{3}}+\mathrm{II}_{0,0}^{3,\bar{6}}-1\big) \\
& -2\bar{\lambda}_1^5\bar{\lambda}_2^4\big(\mathrm{I}_{0,0}^{12,4}-3\bar{\lambda}_2^2-6\big)+2\bar{\lambda}_1^4\bar{\lambda}_2\big(\mathrm{I}_{\bar{3},2}^{\bar{2},3}+\mathrm{II}_{1,0}^{0,6}-1\big)+\bar{\lambda}_1^3\big(\mathrm{I}_{0,\bar{9}}^{9,\bar{2}}+\mathrm{II}_{4,2}^{\bar{2},0}-2\bar{\lambda}_2^9-4\big) \\
& +2\bar{\lambda}_1^2(\bar{\lambda}_2-1)\big(\mathrm{I}_{3,0}^{3,1}+\mathrm{II}_{2,0}^{0,3}+1\big) \\
& -\bar{\lambda}_1\bar{\lambda}_2^2(2\bar{\lambda}_2-1)(\bar{\lambda}_2-4)-4\bar{\lambda}_2^3-2\bar{\lambda}_2^2\big]\big]\big\}\sqrt{1-\bar{\lambda}_1^2\bar{\lambda}_2^4}+\bar{\lambda}_1\bar{\lambda}_2\big(\bar{\lambda}_2^4\bar{\lambda}_1^2-1\big) \\
& \times\big\{\big[-4+2\bar{\lambda}_1\bar{\lambda}_2\big[\bar{\lambda}_1^{11}\bar{\lambda}_2^5\big(3\bar{\lambda}_2^4-2\big)+\bar{\lambda}_1^{10}\bar{\lambda}_2^5\big(3\bar{\lambda}_2^2+4\bar{\lambda}_2+2\big)+\bar{\lambda}_1^9\bar{\lambda}_2^4\big(\mathrm{I}_{0,3}^{\bar{9},\overline{12}}+\mathrm{II}_{0,0}^{2,\bar{9}}+4\big) \\
& -\bar{\lambda}_1^8\bar{\lambda}_2^3\big(\mathrm{I}_{\overline{20},0}^{\bar{2},9}+\mathrm{II}_{9,0}^{\bar{4},\overline{10}}+3\big)+\bar{\lambda}_1^7\bar{\lambda}_2^3\big(\mathrm{I}_{10,3}^{3,20}+\mathrm{II}_{\overline{12},0}^{0,\overline{42}}+6\big)+\bar{\lambda}_1^6\bar{\lambda}_2^2\big(\mathrm{I}_{20,2}^{\bar{8},0}+\mathrm{II}_{\bar{9},4}^{\overline{16},10}+3\big) \\
& -\bar{\lambda}_1^5\bar{\lambda}_2^2\big(2\bar{\lambda}_2^9+\mathrm{I}_{0,9}^{\overline{33},\bar{6}}+\mathrm{II}_{\bar{4},\bar{2}}^{8,0}+16\big)+\bar{\lambda}_1^4\bar{\lambda}_2\big(\mathrm{I}_{\overline{16},2}^{\bar{8},18}+\mathrm{II}_{3,4}^{\overline{16},\bar{8}}+3\big) \\
& -\bar{\lambda}_1^3\bar{\lambda}_2\big(\mathrm{I}_{8,3}^{\bar{3},16}+\mathrm{II}_{6,0}^{0,\overline{33}}-6\big) \\
& +\bar{\lambda}_1^2\big(\mathrm{I}_{\overline{16},0}^{2,3}+\mathrm{II}_{3,0}^{4,\bar{8}}-3\big)+\bar{\lambda}_1\big(2\bar{\lambda}_2^2+3\bar{\lambda}_2^4+4+6\bar{\lambda}_2^3-12\bar{\lambda}_2\big)+4\bar{\lambda}_2-3\bar{\lambda}_2^2+2\big]\big]\Xi_e \\
& +\big[\bar{\lambda}_1^4+\bar{\lambda}_2^4+\bar{\lambda}_1\bar{\lambda}_2\big[\bar{\lambda}_2^7\bar{\lambda}_1^{13}+2\bar{\lambda}_2^5\bar{\lambda}_1^{12}-\bar{\lambda}_1^{11}\bar{\lambda}_2^3\big(4\bar{\lambda}_2^3+4\bar{\lambda}_2^2-1\big) \\
& -4\bar{\lambda}_1^{10}\bar{\lambda}_2^4\big(\mathrm{I}_{0,0}^{\bar{1},3}-2\bar{\lambda}_2^2+1\big)-\bar{\lambda}_1^9\bar{\lambda}_2^4\big(\mathrm{I}_{0,5}^{16,\bar{8}}+\mathrm{II}_{0,0}^{\bar{4},\overline{12}}-8\big)+2\bar{\lambda}_1^8\bar{\lambda}_2^3\big(\mathrm{I}_{\overline{12},0}^{2,3}+\mathrm{II}_{7,0}^{4,\bar{6}}+1\big) \\
& -\bar{\lambda}_1^7\bar{\lambda}_2\big(4\bar{\lambda}_2^9+\mathrm{I}_{24,12}^{0,4}+\mathrm{II}_{\overline{45},\overline{16}}^{8,0}+2\big)-2\bar{\lambda}_1^6\bar{\lambda}_2^2\big(\mathrm{I}_{12,2}^{\bar{2},\bar{2}}+\mathrm{II}_{\bar{7},4}^{\bar{4},6}-1\big)
\end{aligned}
$$

$$
\begin{aligned}
&+\bar{\lambda}_1^5\bar{\lambda}_2^2\big(4\bar{\lambda}_2^9+\mathrm{I}_{0,18}^{\bar{11},0}+\mathrm{II}_{\bar{8},\bar{4}}^{4,4}+8\big)-2\bar{\lambda}_1^4\bar{\lambda}_2\big(\mathrm{I}_{\bar{8},2}^{\bar{2},10}+\mathrm{II}_{1,4}^{\bar{4},\bar{4}}+2\big)\\
&+2\bar{\lambda}_1^3\bar{\lambda}_2\big(\mathrm{I}_{4,2}^{\bar{2},8}+\mathrm{II}_{\bar{2},0}^{0,\bar{17}}-2\big)+\bar{\lambda}_1^2\big(\mathrm{I}_{16,0}^{0,\bar{4}}+\mathrm{II}_{\bar{2},0}^{0,8}+2\big)-\bar{\lambda}_1\bar{\lambda}_2\big(\mathrm{II}_{1,0}^{8,0}+4\bar{\lambda}_2^3-2\big)\\
&+2\bar{\lambda}_2^2\big]\big]\Xi_f\Big\}\Big\{\bar{\lambda}_1^2\bar{\lambda}_2^2\Big[\big[9\bar{\lambda}_1^4\bar{\lambda}_2^4\big(\bar{\lambda}_1^2\bar{\lambda}_2^4-1\big)\Xi_e^2+6\bar{\lambda}_1^4\bar{\lambda}_2^4\big(\bar{\lambda}_1^4\bar{\lambda}_2^2-2\bar{\lambda}_2^4\bar{\lambda}_1^2+1\big)\Xi_e\Xi_f\\
&-3\bar{\lambda}_1^6\bar{\lambda}_2^6\big(\bar{\lambda}_1^2-\bar{\lambda}_2^2\big)\Xi_f^2-\bar{\lambda}_1^{12}\bar{\lambda}_2^8+\bar{\lambda}_1^{10}\bar{\lambda}_2^4\big(1-3\bar{\lambda}_2^6\big)+\bar{\lambda}_1^8\bar{\lambda}_2^6\big(5-\bar{\lambda}_2^6\big)-2\bar{\lambda}_1^6\bar{\lambda}_2^2\\
&+\bar{\lambda}_1^4\bar{\lambda}_2^4\big(\bar{\lambda}_2^6-5\big)+\bar{\lambda}_1^2\big(1-2\bar{\lambda}_2^6\big)+5\bar{\lambda}_2^8\bar{\lambda}_1^6+\bar{\lambda}_2^2\Big]\sqrt{1-\bar{\lambda}_1^2\bar{\lambda}_2^4}\\
&+2\bar{\lambda}_1\bar{\lambda}_2\big(\bar{\lambda}_2^4\bar{\lambda}_1^2-1\big)\Big[\big[\bar{\lambda}_1^8\bar{\lambda}_2^4+5\bar{\lambda}_1^6\bar{\lambda}_2^6+\bar{\lambda}_1^4\bar{\lambda}_2^2\big(\bar{\lambda}_2^6-4\big)-4\bar{\lambda}_1^2\bar{\lambda}_2^4+1\big]\Xi_e\\
&+\bar{\lambda}_1^2\bar{\lambda}_2^2\big[\bar{\lambda}_1^6\bar{\lambda}_2^2-3\bar{\lambda}_1^4\bar{\lambda}_2^4+\bar{\lambda}_1^2\big(1-\bar{\lambda}_2^6\big)+2\bar{\lambda}_2^2\big]\Xi_f\Big]\Big]\Big\}^{-1},
\end{aligned}
\tag{134}
$$

where

$$
W_\mu^{(1)}\big(\bar{\mathbf{F}}^{(1)}\big)=\frac{\mu^{(1)}}{2}\left[\sum_{i=1}^{3}\left(\frac{\bar{\lambda}_i-c}{1-c}\right)^2-3\right]-\mu^{(1)}\ln\left[\frac{(\bar{\lambda}_1-c)(\bar{\lambda}_2-c)(\bar{\lambda}_3-c)}{(1-c)^3}\right],
\tag{135}
$$

and the abbreviations

$$
\mathrm{I}_{c,d}^{a,b}=d\bar{\lambda}_2^7+c\bar{\lambda}_2^5+b\bar{\lambda}_2^3+a\bar{\lambda}_2,\qquad \mathrm{II}_{c,d}^{a,b}=d\bar{\lambda}_2^8+c\bar{\lambda}_2^6+b\bar{\lambda}_2^4+a\bar{\lambda}_2^2,
\tag{136}
$$

(a barred subscript/superscript indicates the corresponding negative coefficient) have been introduced for simplicity. In addition, Ξ_f and Ξ_e are given in terms of the incomplete elliptic integrals of the first and second kind [1], respectively, via

$$
\Xi_f=F\left(\sqrt{1-\bar{\lambda}_1^2\bar{\lambda}_2^4},\sqrt{\frac{\bar{\lambda}_1^4\bar{\lambda}_2^2-1}{\bar{\lambda}_1^2\bar{\lambda}_2^4-1}}\right),\qquad \Xi_e=E\left(\sqrt{1-\bar{\lambda}_1^2\bar{\lambda}_2^4},\sqrt{\frac{\bar{\lambda}_1^4\bar{\lambda}_2^2-1}{\bar{\lambda}_1^2\bar{\lambda}_2^4-1}}\right),
\tag{137}
$$

where the functions F and E are defined by

$$
F(a,b)=\int_0^a\frac{1}{\sqrt{1-t^2}\sqrt{1-b^2t^2}}dt,\qquad E(a,b)=\int_0^a\frac{\sqrt{1-b^2t^2}}{\sqrt{1-t^2}}dt.
\tag{138}
$$

It is emphasized for completeness that the above estimate is consistent with the macroscopic incompressibility constraint $\bar{\lambda}_1\bar{\lambda}_2\bar{\lambda}_3=1$, and linearizes properly. Note also that the estimate locks up whenever any of the stretches $\bar{\lambda}_i=c$. In addition, it is well worth considering the specializations of this expression for *Pure Shear*, *Uniaxial Tension* and *Equibiaxial Tension* loading conditions, as schematically represented in Fig. 6.

6.1.1 Pure Shear (PS)

For pure shear loading in the 1–3 plane (cf. Fig. 6a), $\bar{\lambda}_3=1$ and $\bar{\lambda}_2=1/\bar{\lambda}_1$, and the TSO estimate (134) for $\widehat{W}(\bar{\mathbf{F}})$ simplifies to

$$
\begin{aligned}
\widehat{W}(\bar{\mathbf{F}})=(1-c)W_\mu^{(1)}\big(\bar{\mathbf{F}}^{(1)}\big)-\frac{1}{2}\frac{c}{1-c}\frac{\mu^{(1)}}{\bar{\lambda}_1^2}\Big\{\Big\{2\big(\bar{\lambda}_1^2-1\big)\big[\big(\bar{\lambda}_1^2-1\big)^3\Xi_e+\Phi_{2,\bar{1}}^{0,1}\Xi_f\big]\\
+\big\{3\bar{\lambda}_1^4\big[3\Xi_e^2-2\big(\bar{\lambda}_1^2+2\big)\Xi_e\Xi_f+\big(\bar{\lambda}_1^2+1\big)\Xi_f^2\big]-\big(\bar{\lambda}_1^2-1\big)\Phi_{3,\bar{1}}^{1,\bar{1}}\big\}\sqrt{1-\bar{\lambda}_1^{-2}}\Big\}^{-1}
\end{aligned}
$$

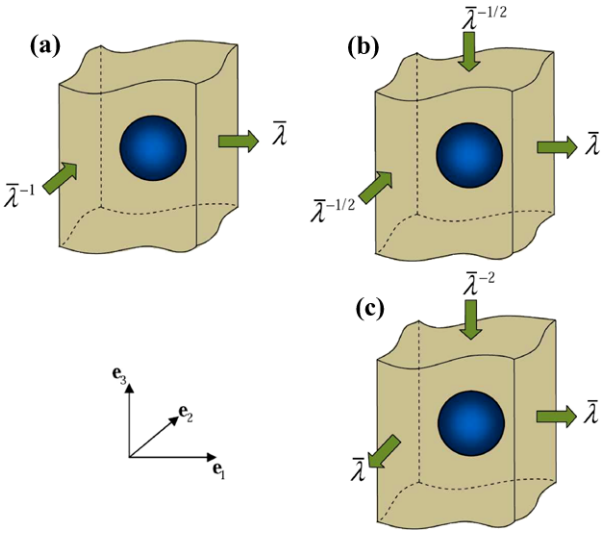

Fig. 6 Schematic representation of a matrix reinforced by spherical inclusions subjected to (**a**) Pure Shear (PS) loading, (**b**) Uniaxial Tension (UT) loading, and (**c**) Equibiaxial Tension (ET) loading

$$\times (\bar{\lambda}_1-1)^2\Big\{(\bar{\lambda}_1^2-1)\{[L_3(\bar{\lambda}_1^4-3)+2\bar{\lambda}_1\Phi_{1,5}^{2,3}]\Xi_f-2(2\bar{\lambda}_1^2+\bar{\lambda}_1+2)(\bar{\lambda}_1^2-1)^3\Xi_e\}$$
$$+\{\bar{\lambda}_1^2[\Phi_{1,1}^{0,1}+4\bar{\lambda}_1(\bar{\lambda}_1^4+\bar{\lambda}_1^2+1)][3\Xi_e^2-2(\bar{\lambda}_1^2+2)\Xi_e\Xi_f+(\bar{\lambda}_1^2+1)\Xi_f^2]$$
$$+(\bar{\lambda}_1^2-1)[L_3(2\bar{\lambda}_1^4-\bar{\lambda}_1^2+2)-2\bar{\lambda}_1\Phi_{0,2}^{1,2}]\}\sqrt{1-\bar{\lambda}_1^{-2}}\Big\}\Big\}, \tag{139}$$

where $L_3=(\bar{\lambda}_1^2-1)^2(\bar{\lambda}_1^2+1)$, and the compound symbols $\Phi_{c,d}^{a,b}=a\bar{\lambda}_1^8+b\bar{\lambda}_1^6+c\bar{\lambda}_1^4+d\bar{\lambda}_1^2+1$ are introduced for brevity (a,b,c,d are positive integer numbers, and a bar above the number indicates a negative sign). Also, Ξ_f and Ξ_e reduce to

$$\Xi_f=F\Big(\sqrt{1-\bar{\lambda}_1^{-2}},\sqrt{-\bar{\lambda}_1^2}\Big),\qquad \Xi_e=E\Big(\sqrt{1-\bar{\lambda}_1^{-2}},\sqrt{-\bar{\lambda}_1^2}\Big),$$

where the functions F and E have been defined in (138). (Note that although $b=\sqrt{-\bar{\lambda}_1^2}$ is complex, the actual integrals in these expressions depend on b through $b^2=-\bar{\lambda}_1^2$, which is real.)

6.1.2 Uniaxial Tension (UT)

For uniaxial loading in the $\mathbf{e}_1$-direction (cf. Fig. 6b), $\bar{\lambda}_2=\bar{\lambda}_3=\bar{\lambda}_1^{-1/2}$, and the TSO estimate (134) for $\widehat{W}(\bar{\mathbf{F}})$ reduces to

$$\widehat{W}(\bar{\mathbf{F}})=(1-c)W_\mu^{(1)}(\bar{\mathbf{F}}^{(1)})-\frac{c}{1-c}\mu^{(1)}$$
$$\times\{\bar{\lambda}_1^{7/2}[-3\bar{\lambda}_1^3\Upsilon\tanh^{-1}(\Upsilon)^2+(\bar{\lambda}_1^3-1)^2\tanh^{-1}(\Upsilon)+(\bar{\lambda}_1^3+\bar{\lambda}_1^6-2)\Upsilon]\}^{-1}$$
$$\times\{[2\bar{\lambda}_1^5(2\bar{\lambda}_1^3-6\bar{\lambda}_1^2-3\bar{\lambda}_1+1)-\bar{\lambda}_1^{7/2}(2\bar{\lambda}_1^6-3\bar{\lambda}_1^5+3\bar{\lambda}_1^4-15\bar{\lambda}_1^3+1)]\Upsilon\tanh^{-1}(\Upsilon)^2$$
$$+(\bar{\lambda}_1-1)^2(\bar{\lambda}_1^2+\bar{\lambda}_1+1)^2[2\bar{\lambda}_1^2(\bar{\lambda}_1+1)(2\bar{\lambda}_1-1)$$
$$-\sqrt{\bar{\lambda}_1}(\bar{\lambda}_1^5-\bar{\lambda}_1^4+5\bar{\lambda}_1^3-1)]\tanh^{-1}(\Upsilon)$$

$$+(\bar{\lambda}_1-1)\big(\bar{\lambda}_1^2+\bar{\lambda}_1+1\big)\big[2\bar{\lambda}_1^3\big(2\bar{\lambda}_1^4+\bar{\lambda}_1^3-3\bar{\lambda}_1^2+4\bar{\lambda}_1+2\big)$$
$$-\bar{\lambda}_1^{7/2}\big(\bar{\lambda}_1^5-\bar{\lambda}_1^4+3\bar{\lambda}_1^3+2\bar{\lambda}_1^2-2\bar{\lambda}_1+9\big)\big]\Upsilon\big\} \tag{140}$$

where $\Upsilon=\sqrt{(\bar{\lambda}_1^3-1)/\bar{\lambda}_1^3}$.

6.1.3 Equibiaxial Tension (ET)

For equibiaxial loading (cf. Fig. 6c), $\bar{\lambda}_3=\bar{\lambda}_2^{-2}=\bar{\lambda}_1^{-2}$, and the TSO estimate (134) reduces to

$$\widehat{W}(\bar{\mathbf{F}})=(1-c)W_\mu^{(1)}\big(\bar{\mathbf{F}}^{(1)}\big)-\frac{c}{1-c}\mu^{(1)}\bar{\lambda}_1^{-4}$$
$$\times\Big\{3\bar{\lambda}_1^6\sqrt{\bar{\lambda}_1^6-1}\Big[\tan^{-1}\Big(\sqrt{\bar{\lambda}_1^6-1}\Big)\Big]^2+\big(\bar{\lambda}_1^6-1\big)^2\Big[\tan^{-1}\Big(\sqrt{\bar{\lambda}_1^6-1}\Big)\Big]$$
$$-\big(\bar{\lambda}_1^6-1\big)^{3/2}\big(2\bar{\lambda}_1^6+1\big)\Big\}^{-1}\Big\{\bar{\lambda}_1^4\sqrt{\bar{\lambda}_1^6-1}\big(\bar{\lambda}_1^{12}-2\bar{\lambda}_1^9+6\bar{\lambda}_1^7-15\bar{\lambda}_1^6+12\bar{\lambda}_1^5+3\bar{\lambda}_1^4$$
$$-4\bar{\lambda}_1^3-3\bar{\lambda}_1^2+2\big)\Big[\tan^{-1}\Big(\sqrt{\bar{\lambda}_1^6-1}\Big)\Big]^2$$
$$+\big(\bar{\lambda}_1^6-1\big)^2\big(\bar{\lambda}_1^{10}-2\bar{\lambda}_1^7+2\bar{\lambda}_1^5-5\bar{\lambda}_1^4+4\bar{\lambda}_1^3+\bar{\lambda}_1^2-1\big)\Big[\tan^{-1}\Big(\sqrt{\bar{\lambda}_1^6-1}\Big)\Big]$$
$$-\big(\bar{\lambda}_1^6-1\big)^{3/2}(\bar{\lambda}_1-1)^2\big(4\bar{\lambda}_1^9-\bar{\lambda}_1^8+2\bar{\lambda}_1^7+7\bar{\lambda}_1^6+6\bar{\lambda}_1^5+3\bar{\lambda}_1^4$$
$$+2\bar{\lambda}_1^3-2\bar{\lambda}_1^2-2\bar{\lambda}_1-1\big)\Big\}. \tag{141}$$

It is worth emphasizing that for UT and ET loadings, the expressions for the effective stored-energy functions do not contain elliptic integrals. Moreover, it should be mentioned that the effective stored-energy functions (139) to (141) are all strongly elliptic (strictly rank-one convex). This observation can be verified by means of the conditions provided by Zee and Stenberg [41] for strong ellipticity of isotropic hyperelastic materials.

6.2 Results for Gent Elastomers and Discussion

In this subsection, we present some specific results for the stress-stretch relations arising from the TSO estimates for general triaxial loading of elastomeric composites consisting of Gent (or neo-Hookean) elastomers reinforced by isotropic distributions of spherical particles. As discussed in the previous section for the three particular loadings (PS, UT, ET), there is only one loading parameter, and we will depict all results here as functions of $\bar{\lambda}_1=\bar{\lambda}$. The results correspond to several volume fractions, $c=0.1,\ 0.2,\ 0.3$, lock-up parameters, $J_m=50,\ 100,\ 500,\ \infty$, and are normalized by the ground-state shear moduli ($\mu^{(1)}=1$). It is recalled that the case $J_m\to\infty$ corresponds to an incompressible neo-Hookean matrix, so that the corresponding results are calculated by making use of the explicit expressions (139) to (141).

Figures 7, 8 and 9 show plots for the new TSO estimates for the macroscopic stress $\bar{S}=\partial\widehat{W}/\partial\bar{\lambda}$ in the particles-reinforced elastomers, as functions of the applied stretch $\bar{\lambda}$, for pure shear, uniaxial tension and equibiaxial tension, respectively. Parts (a) of the figures show the results for composites with neo-Hookean matrices at various particle volume fractions, while parts (b) shows the corresponding results for composites with Gent matrices with

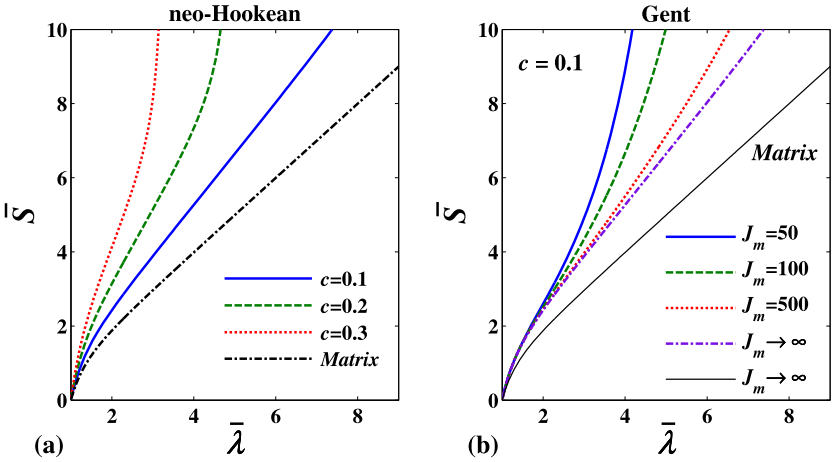

Fig. 7 New tangent second-order (TSO) estimates for the macroscopic stress $\bar{S} = d\widehat{W}/d\bar{\lambda}$ in particle-reinforced elastomers under pure shear loading ($\bar{\lambda}_3 = 1$, $\bar{\lambda}_2 = 1/\bar{\lambda}_1$), as functions the applied stretch $\bar{\lambda}_1 = \bar{\lambda}$. (**a**) neo-Hookean matrix for different values of the fiber volume fraction. (**b**) Gent matrix for different matrix lock-up parameters

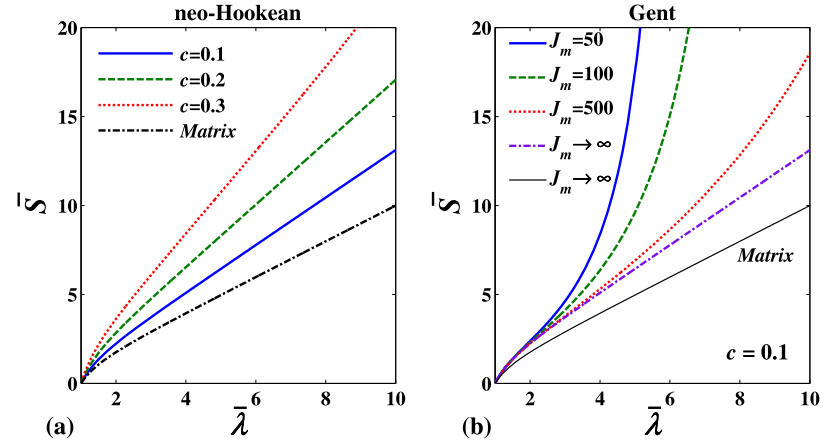

Fig. 8 New TSO estimates for the macroscopic stress $\bar{S} = d\widehat{W}/d\bar{\lambda}$ in particle-reinforced elastomers under uniaxial tension loading ($\bar{\lambda}_2 = \bar{\lambda}_3 = \bar{\lambda}_1^{-1/2}$), as functions the applied stretch $\bar{\lambda}_1 = \bar{\lambda}$. (**a**) neo-Hookean matrix for different values of the fiber volume fraction. (**b**) Gent matrix for different matrix lock-up parameters

several values of J_m, for a given volume fraction of particles $c = 0.1$. It is seen from these figures that the volume fraction of the reinforcing particles has a strong effect on the overall response of the reinforced elastomer, for all three loading types. On the other hand, the strain-locking parameter J_m in the Gent elastomers can also be seen to have a strong effect on the macroscopic response of the reinforced elastomer. In addition, it should be emphasized that the differences observed in the response of the three different loadings are due in part to the different ways in which the results are presented. Of course, the results are consistent in the limit of small strains with the results of linear elasticity, and therefore independent

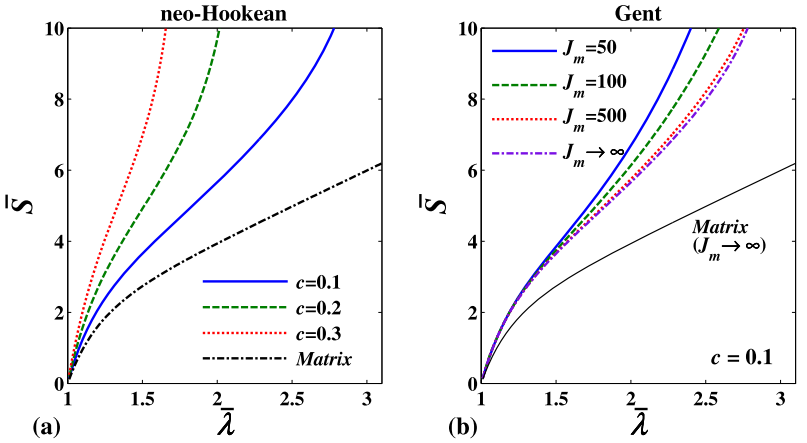

Fig. 9 New TSO estimates for the macroscopic stress $\bar{S} = d\widehat{W}/d\bar{\lambda}$ in particle-reinforced elastomers under equibiaxial tension loading ($\bar{\lambda}_3 = \bar{\lambda}_2^{-2} = \bar{\lambda}_1^{-2}$), as functions the applied stretch $\bar{\lambda}_1 = \bar{\lambda}$. (**a**) neo-Hookean matrix for different values of the fiber volume fraction. (**b**) Gent matrix for different matrix lock-up parameters

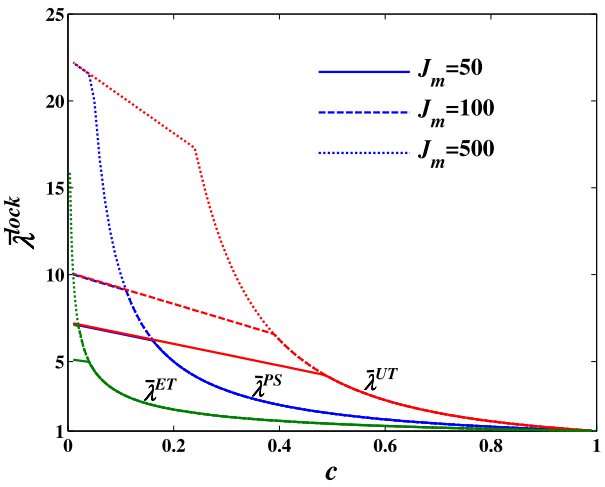

Fig. 10 TSO estimates for the macroscopic stretch, $\bar{\lambda}_1^{lock}$, at which an particle-reinforced incompressible Gent elastomer locks up under three different loadings: Pure shear (PS), Uniaxial tension (UT) and Equibiaxial tension (ET). The results are shown as a function of particle concentration c for different values of the matrix lock-up parameter J_m

of the loading conditions. However, as we will see below, there is an intrinsic effect of the loading conditions for large strains.

Figure 10 shows plots for the "lock-up" stretch in particle-reinforced, Gent elastomers. As already mentioned in the context of the fiber-reinforced elastomers in Sect. 5, the composite may undergo either "geometric" or "material" lock up. Thus, Fig. 10 shows plots of the stretch $\bar{\lambda}_1^{lock}$ at which lock up first takes place for a given loading path. The results are given for three particular loadings: Pure shear (PS), Uniaxial tension (UT) and Equibiaxial tension (ET). The corresponding geometric lock up condition are given by $\bar{\lambda}_1 = c^{-1}$, $\bar{\lambda}_1 = c^{-2}$ and $\bar{\lambda}_1 = c^{-1/2}$, respectively, while those for material lock up are given by

$$\begin{aligned}
&\bar{\lambda}_1^4 - 2\bar{\lambda}_1^3 c - \left[(1-c)^2 J_m - 4c + 2\right]\bar{\lambda}_1^2 - 2\bar{\lambda}_1 c + 1 = 0,\\
&\bar{\lambda}_1^3 - 2\bar{\lambda}_1^2 c - \left[(1-c)^2 J_m - 6c + 3\right]\bar{\lambda}_1 - 4c\sqrt{\bar{\lambda}_1} + 2 = 0,\\
&2\bar{\lambda}_1^6 - 4\bar{\lambda}_1^5 c - \left[(1-c)^2 J_m + 3 - 6c\right]\bar{\lambda}_1^4 - 2c\bar{\lambda}_1^2 + 1 = 0,
\end{aligned} \tag{142}$$

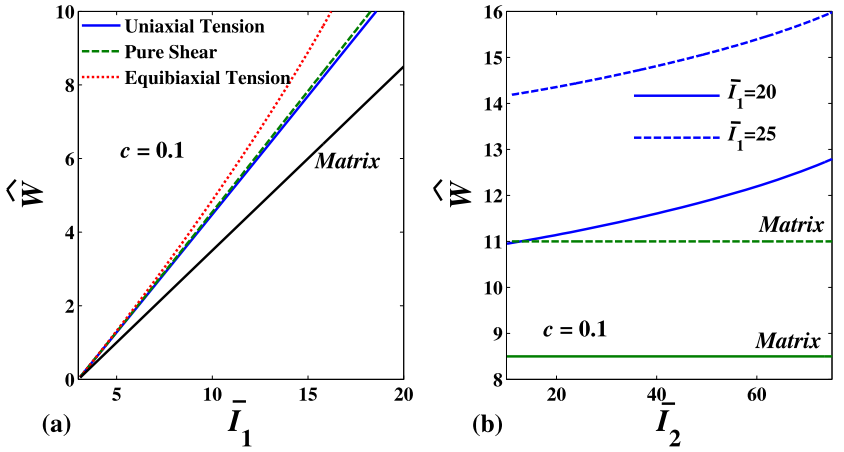

Fig. 11 NewTSO estimates for the effective response of a rigidly particle-reinforced elastomer with an incompressible neo-Hookean matrix. (**a**) The effective energy $\widehat{W}$ versus the macroscopic invariant $\bar{I}_1$ under three different loadings: Pure shear (PS), Uniaxial tension (UT) and Equibiaxial tension (ET). (**b**) The effective energy $\widehat{W}$ versus the invariant $\bar{I}_2$ for two different values of the invariant $\bar{I}_1$

respectively. The results are shown as functions of the particle volume fraction, for fixed values of the Gent lock-up parameter $J_m = 50, 100, 500$. The main observation in this figure is the transition from material lock up to geometric lock up as the particle concentration is increased. Thus, for smaller volume fraction the lock-up stretch is associated with the material lock up (depicted as "straight" lines). On the other hand, for sufficiently large volume fraction (depending on the specific loading), the lock up switches to the geometric (curved lines). It is also seen that the addition of rigid particles enhances the material lock-up effect, with respect to the homogeneous matrix phase. This is related to the fact that the rigid phase cannot deform under deformation and all the deformation must be "concentrated" in the matrix, leading to a smaller effective lock-up stretch for the composite.

As discussed in Sect. 5.4, the accuracy of the TSO results is expected to deteriorate as geometric and material lock-up conditions are approached. For this reason, Fig. 10 could be interpreted as providing an estimate for the range of validity of the TSO results in terms of the maximum applied stretch $\bar{\lambda}$ for given particle concentration and loading condition. Clearly, the range of validity of the estimates decreases with increasing the particle volume fraction. Thus, it is evident from the plot that UT loading has a relatively larger range of validity, while the range of validity for ET loading is more restricted with increasing values of c. For instance, for composites with a Gent matrix and fixed particle volume fraction $c = 0.2$ and lock-up parameter $J_m = 500$, the range of validity for PS, UT and ET loadings can be estimated as $1 \leq \bar{\lambda} \leq 4.5$, $1 \leq \bar{\lambda} \leq 17$ and $1 \leq \bar{\lambda} \leq 2.3$, respectively.

Finally, Figs. 11a and 11b present plots of the effective stored-energy function of the composite versus the macroscopic invariants $\bar{I}_1 = \bar{\lambda}_1^2 + \bar{\lambda}_2^2 + \bar{\lambda}_3^2$ and $\bar{I}_2 = \bar{\lambda}_1^2\bar{\lambda}_2^2 + \bar{\lambda}_2^2\bar{\lambda}_3^2 + \bar{\lambda}_3^2\bar{\lambda}_1^2$ of the deformation, respectively. The matrix is assumed to be neo-Hookean and results for a non-reinforced matrix are also included for comparison. It is observed in Fig. 11a that the effective behavior for the composite differs noticeably for the three particular loading conditions (i.e., for PS, UT and ET loadings), while the corresponding behaviors for a homogeneous neo-Hookean matrix are all identical. More specifically, it can be seen that the response for ET loading becomes increasingly stiffer with the deformation, while the responses for PS and UT loadings remain close to each other and are more compliant. Given

that the material response (as gauged by the matrix response) is the same, the differences observed in the response of the composite must be attributed to the differences in the evolution of the microstructures for the different loading conditions. Figure 11b shows results for the effective stored-energy function of the composite as a function of the second invariant $\bar{I}_2$, for two different, fixed values of the first invariant $\bar{I}_1$. The corresponding results for the matrix phase are also included for comparison purposes. Thus, it can be seen that $\bar{I}_2$ has a strong effect on the macroscopic response of the composite, while the matrix material exhibits no such effect. This phenomenon is a consequence of the nonlinear response of the composite, leading to dependence on the second invariant of the deformation. (Note that dependence on third invariant would also be expected in general, but it is excluded here due to overall incompressibility of material.)

7 Concluding Remarks

In this paper, we have developed new constitutive models for the macroscopic response of composites with hyperelastic phases and particulate microstructures, subjected to general, three-dimensional, finite deformations. For this purpose, we have made use of a suitable extension of the tangent second-order (TSO) homogenization theory of Ponte Castañeda and Tiberio [36], which is capable of accounting for the strongly nonlinear overall incompressibility constraint (for incompressible behavior of the phases), as well as for the reorientation of the particles with the deformation. Thus, for incompressible elastomers reinforced with random distributions of aligned, ellipsoidal, rigid inclusions, the expression (77) was derived for the macroscopic stored-energy function $\widehat{W}(\bar{\mathbf{F}})$ in terms of Eq. (79) for the evolution of the particle orientation $\bar{\mathbf{R}}^{(2)}$, the stored-energy function $W_{\mu}^{(1)}$ of the elastomeric phase (with ground-state shear modulus $\mu^{(1)}$), the initial concentration of the particles c, and a certain microstructural tensor $\mathbf{E}^{I}$, serving to characterize the particle shape, and defined by expression (106). In particular, closed-form, analytical results were obtained for neo-Hookean rubbers reinforced by isotropic distributions of spherical particles under general loading conditions (see expressions (134) to (141)). For this case, it was found that the macroscopic stored-energy function exhibits dependence on the second invariant of the right Cauchy–Green deformation tensor (even when the matrix response is assumed to depend only on the first invariant), in agreement with theoretical expectations. In addition, it was also found that the macroscopic response of Gent-type elastomers reinforced with isotropic distributions of spherical particles is strongly elliptic, and therefore shear-band localization instabilities of the type found by Lopez-Pamies and Ponte Castañeda [26] and Agoras et al. [3] for fiber-reinforced composites loaded in compression along the long axis of the fibers were not found in this case.

The TSO theory was also tested for a model 2-D problem consisting of transverse shear loading of elastomers reinforced with cylindrical fibers of elliptical cross-section, where it was found to recover exactly the generalized second-order (GSO) results of Lopez-Pamies and Ponte Castañeda [25] for dilute concentration of elliptical fibers in a neo-Hookean elastomeric matrix. For more general material behavior (e.g., Gent) and non-dilute conditions, the new TSO theory is still in relatively good agreement with the GSO predictions, although it can lead to much stiffer predictions for neo-Hookean matrix behavior, when the TSO theory predicts "geometric" lock up, at sufficiently large deformations. However, for more realistic situations, when lock up due to the matrix behavior is present, the differences are relatively minor. In any case, comparisons with FEM simulations for realistic values of the

matrix locking strain and macroscopic stretches, are in excellent agreement even for relatively high concentrations (i.e., up to 30 %).

It should be emphasized that while there are presently other homogenization theories for hyperelastic composites (e.g., the GSO [25] and sequentially laminated [9] homogenization methods), the new TSO method developed in this work offers a good balance of generality and accuracy. Indeed, to the best of our knowledge, the TSO estimates developed in this work are the first homogenization estimates for reinforced elastomers with *general* particle shape. While only the case of spherical inclusions has been developed in detail here, results are also available for the response of elastomers reinforced with ellipsoidal inclusions under general (non-aligned) loading conditions. Due to the anisotropy of these material systems and the important effects of particle reorientation, which can lead to loss of ellipticity of the macroscopic response, the analysis of these results is quite a bit more involved and will be considered in detail in a future publication.

Acknowledgements This material is based upon work supported by the National Science Foundation under Grant No. CMMI-0969570.

Appendix A: On the Calculation of the Tensor $\mathbf{E}_I$

In this appendix, we present a brief outline of the asymptotic analysis associated with obtaining the limiting value of the tensor $\mathbf{E}$ $(= \mathbf{P}^{-1} - \mathbf{L}^{(1)})$ in the incompressibility limit (i.e., in the limit as $\varepsilon \to 0$). We first spell out the main steps necessary to carry out the asymptotic expansion for $\mathbf{Q} = \mathbf{P}^{-1}$ about $\varepsilon = 0$. For this purpose, we assume that the incompressibility constraint holds, and that the tensor $\mathbf{Q}$ can be expanded in the form

$$\mathbf{Q} = \varepsilon^{-1}\mathbf{Q}_{-1} + \mathbf{Q}_0 + \varepsilon\mathbf{Q}_1 + O\left(\varepsilon^2\right), \tag{A.1}$$

where $\mathbf{Q}_{-1} \neq \mathbf{0}$. In order to compute the unknown, tensorial coefficients $\mathbf{Q}_{-1}$ and $\mathbf{Q}_0$, we need to first find the null-space of $\mathbf{P}_0$ (the first term in the expansion (104)), defined by

$$\operatorname{null}\mathbf{P}_0 = \{\mathbf{N} | \mathbf{P}_0\mathbf{N} = \mathbf{0}\}. \tag{A.2}$$

By solving $\mathbf{P}_0\mathbf{N} = \mathbf{0}$ for the second-order tensor $\mathbf{N}$, we will have

$$\operatorname{null}\mathbf{P}_0 = \operatorname{span}\{\mathbf{W}_1, \mathbf{W}_2, \mathbf{W}_3\}, \tag{A.3}$$

where $\{\mathbf{W}_1, \mathbf{W}_2, \mathbf{W}_3\}$ stands for an orthogonal basis for the set of skew-symmetric, second-order tensors such that $\mathbf{W}_i + \mathbf{W}_i^T = \mathbf{0}$ and $\mathbf{W}_i \cdot \mathbf{W}_j = 0$ $(i \neq j)$, $i, j = 1, 2, 3$. Using the major symmetry of the tensor $\mathbf{P}_0$ $((P_0)_{ijkl} = (P_0)_{klij})$, Eq. (A.3) indicate that

$$(P_0)_{ijkl}(W_p)_{kl} = (P_0)_{klij}(W_p)_{kl} = 0, \quad p = 1, 2, 3. \tag{A.4}$$

By substituting the asymptotic expansions (104) and (A.1) into the identity $\mathbf{PQ} = \mathbf{QP} = \boldsymbol{\mathcal{I}}$, and collecting coefficients of the same power as ε, the following system of equations is obtained

$$\mathbf{Q}_{-1}\mathbf{P}_0 = \mathbf{P}_0\mathbf{Q}_{-1} = \mathbf{0}, \tag{A.5}$$

$$\mathbf{P}_0\mathbf{Q}_0 + \mathbf{P}_1\mathbf{Q}_{-1} = \mathbf{Q}_0\mathbf{P}_0 + \mathbf{Q}_{-1}\mathbf{P}_1 = \boldsymbol{\mathcal{I}}, \tag{A.6}$$

$$\mathbf{P}_0\mathbf{Q}_1 + \mathbf{P}_1\mathbf{Q}_0 + \mathbf{P}_2\mathbf{Q}_{-1} = \mathbf{Q}_1\mathbf{P}_0 + \mathbf{Q}_0\mathbf{P}_1 + \mathbf{Q}_{-1}\mathbf{P}_2 = \mathbf{0}. \tag{A.7}$$

Thus, this system of linear equations for $\mathbf{Q}_{-1}$, $\mathbf{Q}_0$, and $\mathbf{Q}_1$ uniquely determines the coefficients in the expansion (A.1). Noting that $\det(\mathbf{Q}_{-1}) = 0$, the general solution to the tensorial equation (A.5) can be written as [4]

$$\mathbf{Q}_{-1} = \sum_{i=1}^{3} \mathbf{W}_i \otimes \mathbf{V}_i^{(0)}, \tag{A.8}$$

where the arbitrary matrices $\mathbf{V}_i^{(0)}$ are determined using (A.6). To this end, by transposing (A.6) (meaning $(\cdot)_{ijkl}^T = (\cdot)_{klij}$) and then right-multiplying it with $\mathbf{W}_i$, it follows that

$$(P_1)_{ijkl}(Q_{-1})_{klrs}(W_p)_{ij} = (W_p)_{rs}, \quad p = 1, 2, 3, \tag{A.9}$$

where use has been made of the relations (A.4). Substituting (A.8) into (A.9), it leads to

$$\left[(P_1)_{ijkl}(W_p)_{ij}(W_p)_{kl}\right]\left(V_p^0\right)_{rs} = (W_p)_{rs}, \quad p = 1, 2, 3, \tag{A.10}$$

from which it is concluded that

$$\mathbf{V}_i^{(0)} = \frac{1}{\mathbf{W}_i \cdot \mathbf{P}_1 \mathbf{W}_i} \mathbf{W}_i, \quad i = 1, 2, 3. \tag{A.11}$$

Next, the general solution of (A.6) can be represented as [4]

$$\mathbf{Q}_0 = \mathbf{P}_0^{\dagger}(\boldsymbol{\mathcal{I}} - \mathbf{P}_1\mathbf{Q}_{-1}) + \sum_{i=1}^{3} \mathbf{W}_i \otimes \mathbf{V}_i^{(1)}, \tag{A.12}$$

By the same token, in order to find $\mathbf{V}_i^{(1)}$, we take the transpose of (A.7) and then right-multiply it with $\mathbf{W}_i$, which leads to

$$(P_1)_{ijkl}(Q_0)_{klrs}(W_p)_{ij} + (P_2)_{ijkl}(Q_{-1})_{klrs}(W_p)_{ij} = 0, \quad p = 1, 2, 3, \tag{A.13}$$

where, again, use has been made of relations (A.4). Substituting (A.12) and (A.8) into the above equation, and doing some algebra, Eqs. (110) for $\mathbf{V}_i^{(1)}$ are obtained. Finally, in the limit as $\varepsilon \to 0$, we recover $\mathbf{Q}_{-1} = \mathbf{L}_{-1}^{(1)}$ (when the isochoric deformation condition is satisfied), and the tensor $\mathbf{E}^I = (\mathbf{P}^{-1} - \mathbf{L}^{(1)})|_{\mu'^{(1)} \to \infty}$ reduces to $\mathbf{E}^I = \mathbf{Q}_0 - \mathbf{L}_{\mu}^{(1)}$.

Appendix B: In-plane Components of the Tensor P for Cylindrical Inclusions with Elliptical Cross-Section Embedded in a Compressible neo-Hookean Matrix

In this appendix, we present explicit expressions for the (in-plane) components of the tensor $\mathbf{P}$, associated with a cylindrical fiber of elliptical cross-section embedded in a generalized linear-elastic material with modulus tensor $\mathbf{L}^{(1)}$. It is recalled that the tensor $\mathbf{P}$, defined by (117), makes use of the tangent modulus tensor $\mathbf{L}^{(1)} = (\partial^2 W^{(1)}/\partial \mathbf{F}\,\partial \mathbf{F})|_{\mathbf{F}=\bar{\mathbf{F}}}$. Since $\mathbf{L}^{(1)}$ is characterized by the objective and isotropic stored energy function $W^{(1)}$, the following condition is known [26] to be satisfied by $\mathbf{L}^{(1)}$

$$L_{ijkl}^{(1)}(\bar{\mathbf{F}}) = \bar{Q}_{rm}\bar{Q}_{jn}\bar{Q}_{sp}\bar{Q}_{lq}\bar{R}_{ir}\bar{R}_{ks}L_{mnpq}^{*}(\bar{\mathbf{D}}), \tag{B.1}$$

where $\bar{\mathbf{R}}$ and $\bar{\mathbf{Q}}$ are the macroscopic orthogonal tensors in the decompositions $\bar{\mathbf{F}} = \bar{\mathbf{R}}\bar{\mathbf{U}} = \bar{\mathbf{R}}\bar{\mathbf{Q}}\bar{\mathbf{D}}\bar{\mathbf{Q}}^T$, given by $\bar{\mathbf{Q}} = \cos(\bar{\theta})\,(\mathbf{e}_1 \otimes \mathbf{e}_1 + \mathbf{e}_2 \otimes \mathbf{e}_2) + \sin(\bar{\theta})(\mathbf{e}_2 \otimes \mathbf{e}_1 - \mathbf{e}_1 \otimes \mathbf{e}_2)$ and $\bar{\mathbf{R}} = \cos(\bar{\psi})\,(\mathbf{e}_1 \otimes \mathbf{e}_1 + \mathbf{e}_2 \otimes \mathbf{e}_2) + \sin(\bar{\psi})(\mathbf{e}_2 \otimes \mathbf{e}_1 - \mathbf{e}_1 \otimes \mathbf{e}_2)$, with respect to the 2-D laboratory frame of reference, and $\bar{\mathbf{D}}$ is a diagonal, second-order tensor with matrix representation $\bar{\mathbf{D}} = \bar{\lambda}_1\,\mathbf{e}_1 \otimes \mathbf{e}_1 + \bar{\lambda}_2\,\mathbf{e}_2 \otimes \mathbf{e}_2$. The tensor $\mathbf{L}^*$ is orthotropic relative to $\{\mathbf{e}_i\}$ and, recalling that it exhibits major symmetry $L^*_{ijkl} = L^*_{klij}$, it follows that it generally has five in-plane, independent components. However, in order to obtain simple analytical expressions for the $\mathbf{P}$ tensor components, following Lopez-Pamies and Ponte Castañeda ([26]), we take advantage of the following constraint for the components of $\mathbf{L}^{(1)}$

$$L^{(1)}_{1221} = \sqrt{\left(L^{(1)}_{1111} - L^{(1)}_{1212}\right)\left(L^{(1)}_{2222} - L^{(1)}_{1212}\right)} - L^{(1)}_{1122}, \tag{B.2}$$

which is satisfied by the tangent modulus of a neo-Hookean material (but not for more general hyperelastic materials including Gent).

Following Lopez-Pamies and Ponte Castañeda [24, 26], the four independent components of $\mathbf{L}^{(1)}$ are chosen to be $L^{(1)}_{1111} = l^*_1$, $L^{(1)}_{2222} = l^*_2$, $L^{(1)}_{1122} = l^*_3$, $L^{(1)}_{1212} = l^*_4$. It can then be deduced from relation (B.1) that

$$P_{ijkl}(\bar{\mathbf{F}}) = \bar{R}_{ip}\bar{R}_{kq}\,P^*_{pjql}(\bar{\mathbf{U}}). \tag{B.3}$$

Now, making use of this choice of $\mathbf{L}^{(1)}$ along with the constraint (B.2), it follows that the in-plane components of $\mathbf{P}^*$, after some algebra, can be expressed in terms of the variables C_j $(j = 1, \ldots, 13)$, and the functions P_i $(i = 1, 2, 3)$, via

$$P^*_{1111} = P_1(C_1, C_2, C_3), \qquad P^*_{2222} = P_2(C_4, C_5, C_6), \qquad P^*_{1122} = P_3(C_7, C_8, C_9)$$

$$P^*_{1212} = P_2(C_1, C_2, C_{10}), \qquad P^*_{1112} = P_3(C_1, C_2, C_{11}), \qquad P^*_{1121} = P_1(C_7, -C_8, C_{12})$$

$$P^*_{2212} = P_2(C_7, -C_8, C_{12}), \qquad P^*_{2221} = P_3(C_4, C_5, C_6),$$

$$P^*_{1221} = P_3(C_7, C_8, -C_2/2), \qquad P^*_{2121} = P_1(C_4, C_5, C_{13})$$

where

$$C_1 = 2L^*\cos^4(\bar{\theta}) + \left(3l^*_1 - 4l^*_4 + l^*_2 - 4l^*\right)\cos^2(\bar{\theta}) + l^*_4 - l^*_1,$$

$$C_2 = \left[L^*\cos^2(\bar{\theta}) + l^*_1 - l^* - l^*_4\right]\sin(2\bar{\theta}),$$

$$C_3 = -L^*\cos^4(\bar{\theta}) + 2\left(l^*_1 - l^* - l^*_4\right)\cos^2(\bar{\theta}) + l^*_1,$$

$$C_4 = 2L^*\cos^4(\bar{\theta}) + \left(3l^*_2 - 4l^*_4 + l^*_1 - 4l^*\right)\cos^2(\bar{\theta}) + l^*_4 - l^*_2,$$

$$C_5 = \left[L^*\cos^2(\bar{\theta}) + l^*_2 - l^* - l^*_4\right]\sin(2\bar{\theta}),$$

$$C_6 = L^*\sin^2(\bar{\theta})\cos^2(\bar{\theta}) - l^*_4,$$

$$C_7 = L^*\sin(4\bar{\theta})/4, \qquad C_8 = L^*\sin^2(2\bar{\theta})/2 - l^*,$$

$$C_9 = \left[l^*_1 - l^* - l^*_4 - L^*\cos^2(\bar{\theta})\right]\sin(\bar{\theta})\cos(\bar{\theta}),$$

$$C_{10} = L^*\cos^4(\bar{\theta}) + 2\left(l^*_4 + l^* - l^*_1\right)\cos^2(\bar{\theta}) + l^*_1,$$

$$C_{11} = 2\left(l^*_4 + l^* - l^*_1\right)\cos^2(\bar{\theta}) - L^*\cos^4(\bar{\theta}) + l^*_1,$$

$$C_{12} = \left[L^* \cos^2(\bar{\theta}) + l_1^* - l^* - l_4^*\right] \sin(\bar{\theta}) \cos(\bar{\theta}),$$
$$C_{13} = L^* \sin^2(2\bar{\theta})/4 - l_4^*,$$

and

$$\begin{aligned}
&P_1(A_1, A_2, A_3)\\
&\quad = \vartheta \big\{ \big\{ \varpi (A_1 a_1 + A_2 a_2) s_2 - k\big(a_1^2 + a_2^2\big)\big[(ka_1 - 1)A_3 + k(ka_1 - 1)A_1\\
&\qquad + k(ka_2 - a_2)A_2\big]\big\} s_1\\
&\qquad + \big\{\big(a_1^2 + a_2^2\big)\big[k\big(2a_1 + a_2^2\big) - 2\big]A_3 - a_2\big[3ka_1^2 - a_2^2 k + \big[\big(a_2^2 - 4\big)k - 1\big]a_1 + 2\big]A_2\\
&\qquad + \big[2ka_1^2 + 2\big(2a_2^2 k - 1\big)a_1 + ka_2^4 - (2k+1)a_2^2\big]A_1\big\} s_2\big\},\\
&P_2(A_1, A_2, A_3)\\
&\quad = -\vartheta \big\{ \big\{ \varpi (A_1 a_1 + A_2 a_2) s_2 - (k-1)\big(a_1^2 + a_2^2\big)\big[(ka_1 - 1)A_3 + k(ka_1 - 1)A_1\\
&\qquad + k(ka_2 - a_2)A_2\big]\big\} s_1 + \big\{\big(a_1^2 + a_2^2\big)\big[k\big(2a_1 - 2a_1^2 - a_2^2\big) + 2a_1 + a_2^2 - 2\big]A_3\\
&\qquad + a_2\big[ka_1^3 + (1-5k)a_1^2 + (1+4k)a_1 + (1-k)a_2^2 - 2\big]A_2\\
&\qquad + \big[\big(2 + 2k - ka_2^2\big)a_1^2 + 2\big(ka_2^2 - 1\big)a_1 + (1-2k)a_2^2 - 2a_1^3 k\big]A_1\big\} s_2\big\},\\
&P_3(A_1, A_2, A_3)\\
&\quad = \vartheta \big\{ \big\{ \varpi (A_1 a_2 - A_2 a_1) s_2 - k(k-1)\big(a_1^2 + a_2^2\big)\big[a_2 k A_1 + (1 - ka_1)A_2 + a_2 A_3\big]\big\} s_1\\
&\qquad + \big\{a_2\big[2a_1^3 k + \big(a_2^2 k - 2 - 2k\big)a_1^2 + 2\big(1 - a_2^2 k\big)a_1 + (2k-1)a_2^2\big]A_2\\
&\qquad - a_2\big[3a_1^2 k + \big(a_2^2 k - 4k - 1\big)a_1 + 2 - a_2^2 k\big]A_1 - a_2\big(a_1^2 + a_2^2\big)(ka_1 - 2k + 1)A_3\big\} s_2\big\}.
\end{aligned}$$

In the above expressions,

$$a_1 = \big(l_1^* - l_2^*\big)\cos(2\bar{\theta})/a, \qquad a_2 = \big(l_1^* - l_2^*\big)\sin(2\bar{\theta})/a, \qquad a = -\big[l_1^* \sin^2(\bar{\theta}) + l_2^* \cos^2(\bar{\theta})\big]$$
$$\varpi = (ka_1 - 1)^2 + k(k-1)a_2^2, \qquad \vartheta = 2\pi a \big\{\varpi \big(a_1^2 + a_2^2\big) s_1 s_2\big\}^{-1},$$
$$L^* = 2l_4^* + 2l^* - l_2^* - l_1^*, \qquad s_1 = \sqrt{4 - 4a_1 - a_2^2}, \qquad s_2 = \sqrt{k(k-1)},$$
$$l^* = \sqrt{\big(l_1^* - l_4^*\big)\big(l_2^* - l_4^*\big)}, \quad k = \omega^2 \big/ \big(\omega^2 - 1\big).$$

For the special case of compressible neo-Hookean materials, the expression for the components of the tensor $\mathbf{P}$ are obtained by substituting the following expressions for $l_1^*, \ldots, l_4^*$ into the above relations

$$\begin{aligned}
&l_i^* = \bar{\lambda}_i^{-2}\big[\mu^{(1)}\big(\bar{\lambda}_i^2 + 1\big) + \mu'^{(1)}\bar{J}^2\big] \quad (i = 1, 2),\\
&l_3^* = \mu'^{(1)}(2\bar{J} - 1), \quad \text{and} \quad l_4^* = \mu^{(1)},
\end{aligned} \tag{B.4}$$

where $\bar{J} = \det(\bar{\mathbf{F}}) = \bar{\lambda}_1 \bar{\lambda}_2$.

Appendix C: The Tensors P and E for Spherical Inclusions Embedded in a Compressible neo-Hookean Matrix

In this appendix, explicit analytical expressions are given for the components of the tensors **P** and **E** for spherical inclusions embedded in generalized linear-elastic material with moduli tensor $\mathbf{L}^{(1)}$, whose components are assumed to satisfy [2] the constraints

$$L^{(1)}_{1212} = L^{(1)}_{1313} = L^{(1)}_{2323}$$

$$\begin{aligned} &L^{(1)}_{1221} = \sqrt{\left(l^*_1 - l^*_7\right)\left(l^*_2 - l^*_7\right)} - l^*_4, \qquad L^{(1)}_{1331} = \sqrt{\left(l^*_1 - l^*_7\right)\left(l^*_3 - l^*_7\right)} - l^*_5, \\ &L^{(1)}_{2332} = \sqrt{\left(l^*_2 - l^*_7\right)\left(l^*_3 - l^*_7\right)} - l^*_6, \end{aligned} \tag{C.1}$$

where the variables l^*_i $(i = 1, \ldots, 7)$ have been identified with the seven remaining "independent" components of $\mathbf{L}^{(1)}$ (relative to the basis $\{\mathbf{e}_i\}$) via

$$\begin{aligned} &l^*_1 = L^{(1)}_{1111}, \qquad l^*_2 = L^{(1)}_{2222}, \qquad l^*_3 = L^{(1)}_{3333}, \qquad l^*_4 = L^{(1)}_{1122}, \qquad l^*_5 = L^{(1)}_{1133}, \\ &l^*_6 = L^{(1)}_{2233}, \qquad l^*_7 = L^{(1)}_{1212}. \end{aligned} \tag{C.2}$$

In this connection, it should be noted that the conditions (C.1) are satisfied by the tangent modulus of a neo-Hookean material, but not more generally.

Recalling that the composite is statistically isotropic in the undeformed configuration, the expression for **P** in the basis $\{\mathbf{e}_i\}$ can be expressed as

$$P_{ijkl} = \frac{1}{4\pi}\int_0^{\pi}\int_0^{2\pi} \left(L^{(1)}_{imkn}\xi_m\xi_n\right)^{-1}\xi_j\xi_l \, d\theta \, d\phi, \tag{C.3}$$

where $\xi_1 = \sin(\phi)\cos(\theta)$, $\xi_2 = \sin(\phi)\sin(\theta)$, and $\xi_3 = \cos(\phi)$. Now, making use of the above choice for $\mathbf{L}^{(1)}$, it can be shown that the components of the microstructural tensor **P** are given by the analytical expressions

$$\begin{aligned} P_{1111} = &-\frac{1}{3l^*_7(l^*_1 - l^*_3)^{3/2}(l^*_1 - l^*_2)^2}\Big\{\sqrt{l^*_2}\left(l^*_1 - l^*_7\right)\left\{2\chi_1\Xi_e + l^*_3\left(l^*_2 - l^*_1\right)\Xi_f\right\} \\ &- \sqrt{l^*_1 - l^*_3}\Big\{\left(l^*_3 + l^*_7 + l^*_2\right)\left(l^*_1\right)^2 - \left[\left(3l^*_2 + 2l^*_3\right)l^*_7 - \left(l^*_2\right)^2 + 2l^*_3l^*_2\right]l^*_1 \\ &+ l^*_2l^*_3\left(4l^*_7 - l^*_2\right)\Big\}\Big\}, \\ P_{2222} = &-\frac{1}{3l^*_2l^*_7(l^*_2 - l^*_1)^2(l^*_2 - l^*_3)^2\sqrt{l^*_1 - l^*_3}} \\ &\times\Big\{\left(l^*_2 - l^*_7\right)\sqrt{l^*_2}\left\{2l^*_2\left(l^*_1 - l^*_3\right)\chi_2\Xi_e + l^*_3\left(l^*_2 - l^*_1\right)\left[2l^*_3l^*_2 + l^*_1\left(l^*_2 - 3l^*_3\right)\right]\Xi_f\right\} \\ &- l^*_2\left(l^*_2 - l^*_3\right)\sqrt{l^*_1 - l^*_3}\Big\{\left(l^*_1 + l^*_7 + l^*_3\right)\left(l^*_2\right)^2 - \left[\left(3l^*_1 + 2l^*_3\right)l^*_7 + 2l^*_3l^*_1 - \left(l^*_1\right)^2\right]l^*_2 \\ &- l^*_1l^*_3\left(l^*_1 - 4l^*_7\right)\Big\}\Big\}, \\ P_{3333} = &\frac{1}{3l^*_7(l^*_2 - l^*_3)^2(l^*_1 - l^*_3)^{(3/2)}}\Big\{\sqrt{l^*_2}\left(l^*_7 - l^*_3\right)\left\{2\chi_3\Xi_e - \left[l^*_1l^*_3 + l^*_2\left(2l^*_3 - 3l^*_1\right)\right]\Xi_f\right\} \\ &+ \sqrt{l^*_1 - l^*_3}\left(l^*_2 - l^*_3\right)\left[\left(l^*_7 - l^*_1 - l^*_2\right)l^*_3 + l^*_1l^*_2\right]\Big\}, \end{aligned}$$

$$P_{1122} = \frac{1}{3l_7^*(l_2^*-l_1^*)^2(l_2^*-l_3^*)\sqrt{l_1^*-l_3^*}}\big(l_4^* + L_{1221}^{(1)}\big)$$
$$\times \Big\{\sqrt{l_2^*}\big\{l_3^*\big(l_2^*-l_1^*\big)\Xi_f - \chi_3\Xi_e\big\} + \big(l_1^*+l_2^*\big)\big(l_3^*-l_2^*\big)\sqrt{l_1^*-l_3^*}\Big\},$$
$$P_{1133} = \frac{l_1^*-l_7^*}{3l_7^*(l_1^*-l_2^*)(l_2^*-l_3^*)(l_1^*-l_3^*)^{3/2}(l_4^*+L_{1221}^{(1)})}$$
$$\times \Big\{\sqrt{l_2^*}\chi_2\Xi_e - \sqrt{l_2^*}l_3^*\big(l_2^*-l_1^*\big)\Xi_f - l_1^*\big(l_2^*-l_3^*\big)\sqrt{l_1^*-l_3^*}\Big\},$$

$$P_{2233} = -\frac{l_6^* + L_{2332}^{(1)}}{3l_7^*(l_1^*-l_2^*)(l_2^*-l_3^*)^2\sqrt{l_1^*-l_3^*}}$$
$$\times \Big\{\sqrt{l_2^*}\big[\chi_1\Xi_e + 2l_3^*\big(l_2^*-l_1^*\big)\Xi_f\big] - l_2^*\big(l_2^*-l_3^*\big)\sqrt{l_1^*-l_3^*}\Big\}, \tag{C.4}$$

where

$$\Xi_f = F\left(\sqrt{\frac{l_1^*-l_3^*}{l_1^*}}, \sqrt{\frac{l_1^*(l_2^*-l_3^*)}{l_2^*(l_1^*-l_3^*)}}\right), \qquad \Xi_e = E\left(\sqrt{\frac{l_1^*-l_3^*}{l_1^*}}, \sqrt{\frac{l_1^*(l_2^*-l_3^*)}{l_2^*(l_1^*-l_3^*)}}\right),$$

and $\chi_{1,2,3} = l_{1,2,3}^*(l_{2,1,1}^* + l_{3,3,2}^*) - 2l_{2,1,1}^* l_{3,3,2}^*$. The functions F and E denote the incomplete elliptic integrals of the first and second kinds, respectively [1] which are defined in (138). It is also remarked that the other non-zero components of the tensor $\mathbf{P}$ do not enter the TSO expression (130).

Then, the components of the tensor $\mathbf{E}$ may be computed from the corresponding components of the tensor $\mathbf{P}$ by means of the following relations

$$E_{1111} = \big(P_{2222}P_{3333} - P_{2233}^2\big)\Pi - l_1^*, \qquad E_{2222} = \big(P_{1111}P_{3333} - P_{1133}^2\big)\Pi - l_2^*$$
$$E_{3333} = \big(P_{1111}P_{2222} - P_{1122}^2\big)\Pi - l_3^*, \qquad E_{1122} = (P_{2233}P_{1133} - P_{1122}P_{3333})\Pi - l_4^*$$
$$E_{1133} = (P_{1122}P_{2233} - P_{1133}P_{2222})\Pi - l_5^*, \qquad E_{2233} = (P_{1122}P_{1133} - P_{2233}P_{1111})\Pi - l_6^*, \tag{C.5}$$

where

$$\Pi = \big(P_{1111}P_{2222}P_{3333} + 2P_{1122}P_{1133}P_{2233} - P_{1111}P_{2233}^2 - P_{2222}P_{1133}^2 - P_{3333}P_{1122}^2\big)^{-1}.$$

Next, it is noted that the seven independent components $l_1^*, l_2^*, \ldots, l_7^*$ (defined by (C.2)) for a compressible neo-Hookean material are given by

$$l_i^* = \bar{\lambda}_i^{-2}\big[\mu^{(1)}\big(\bar{\lambda}_i^2+1\big) + \mu'^{(1)}\bar{J}^2\big], \quad i = 1,2,3,$$
$$l_i^* = \mu'^{(1)}\bar{\lambda}_i(2\bar{J}-1), \quad i = 4,5,6, \tag{C.6}$$

and $l_7^* = \mu^{(1)}$, where $\bar{J} = \det(\bar{\mathbf{F}}) = \bar{\lambda}_1\bar{\lambda}_2\bar{\lambda}_3 = 1$.

Finally, the expression for the relevant components of the tensor $\mathbf{E}^I$ may be obtained by substituting the expressions (C.6) for the l_i^* $(i = 1, \ldots, 7)$ into the components of the tensor $\mathbf{E}$ (C.5) and taking the limit as $\mu'^{(1)} \to \infty$. The final expressions are not included here for brevity.

References

1. Abramowitz, M., Stegun, I.: Handbook of Mathematical Functions with Formulas, Graphs, and Mathematical Tables. Dover, New York (1965)
2. Agoras, M., Lopez-Pamies, O., Ponte Castañeda, P.: A general hyperelastic model for incompressible fiber-reinforced elastomers. J. Mech. Phys. Solids **57**, 268–286 (2009)
3. Agoras, M., Lopez-Pamies, O., Ponte Castañeda, P.: Onset of macroscopic instabilities in fiber-reinforced elastomers at finite strain. J. Mech. Phys. Solids **57**, 1828–1850 (2009)
4. Avrachenkov, K.E., Haviv, M., Howlett, P.G.: Inversion of analytic matrix functions that are singular at the origin. SIAM J. Matrix Anal. Appl. **22**, 1175–1189 (2001)
5. Bergstrom, J.S., Boyce, M.C.: Mechanical behavior of particle-filled elastomers. Rubber Chem. Technol. **72**, 633–656 (1999)
6. Bouchart, M., Brieu, V., Bhatnagar, N., Kondo, D.: A multiscale approach of nonlinear composites under finite deformation: experimental characterization and numerical modeling. Int. J. Solids Struct. **47**, 1737–1750 (2010)
7. Brun, M., Lopez-Pamies, O., Ponte Castañeda, P.: Homogenization estimates for fiber-reinforced elastomers with periodic microstructures. Int. J. Solids Struct. **44**, 5953–5979 (2007)
8. Chen, H., Liu, Y., Zhao, X., Lanir, Y., Kassab, G.S.: A micromechanics finite-strain constitutive model of fibrous tissue. J. Mech. Phys. Solids **59**, 1823–1837 (2011)
9. deBotton, G.: Transversely isotropic sequentially laminated composites in finite elasticity. J. Mech. Phys. Solids **53**, 1334–1361 (2005)
10. deBotton, G., Hariton, I., Socolsky, E.A.: Neo-Hookean fiber-reinforced composites in finite elasticity. J. Mech. Phys. Solids **54**, 533–559 (2006)
11. Eshelby, J.D.: The determination of the elastic field of an ellipsoidal inclusion and related problems. Proc. R. Soc. Lond. A **241**, 376–396 (1957)
12. Finlay, H.M., Whittaker, P., Canham, P.B.: Collagen organization in branching region of human brain arteries. Stroke **29**, 1595–1601 (1998)
13. Gent, A.N.: A new constitutive relation for rubber. Rubber Chem. Technol. **69**, 59–61 (1996)
14. Geymonat, G., Müller, S., Triantafyllidis, N.: Homogenization of nonlinearly elastic materials, microscopic bifurcation and macroscopic loss of rank-one convexity. Arch. Ration. Mech. Anal. **122**, 231–290 (1993)
15. Hariton, I., deBotton, G.: The nearly isotropic behaviour of high-rank nonlinear sequentially laminated composites. Proc. R. Soc. Lond. A **459**, 157–174 (2003)
16. Hill, R.: On constitutive macro-variables for heterogeneous solids at finite strain. Proc. R. Soc. Lond. Ser. A, Math. Phys. Sci. **326**, 131–147 (1972)
17. Honeker, C.C., Thomas, E.L.: Impact of morphological orientation in determining mechanical properties in triblock copolymers. Chem. Mater. **8**, 1702–1714 (1996)
18. Idiart, M.I.: Modeling the macroscopic behavior of two-phase nonlinear composites by infinite rank laminates. J. Mech. Phys. Solids **56**, 2599–2617 (2008)
19. Kailasam, M., Ponte Castañeda, P.: A general constitutive theory for linear and nonlinear particulate media with microstructure evolution. J. Mech. Phys. Solids **46**, 427–465 (1998)
20. Lahellec, N., Mazerolle, F., Michel, J.-C.: Second-order estimate of the macroscopic behavior of periodic hyperelastic composites: theory, experimental validation. J. Mech. Phys. Solids **52**, 27–49 (2004)
21. Levin, V.M.: Thermal expansion coefficients of heterogeneous materials. Mekh. Tverd. Tela **2**, 83–94 (1967)
22. Lopez-Pamies, O., Idiart, M.I.: Fiber-reinforced hyperelastic solids: a realizable homogenization constitutive theory. J. Eng. Math. **68**, 57–83 (2010)
23. Lopez-Pamies, O., Ponte Castañeda, P.: Second-order estimates for the macroscopic response and loss of ellipticity in porous rubbers at large deformations. J. Elast. **76**, 247–287 (2004)
24. Lopez-Pamies, O., Ponte Castañeda, P.: Second-order homogenization estimates incorporating field fluctuations in finite elasticity. Math. Mech. Solids **9**, 243–270 (2004)
25. Lopez-Pamies, O., Ponte Castañeda, P.: On the overall behavior, microstructure evolution, and macroscopic stability in reinforced rubbers at large deformations: I—Theory. J. Mech. Phys. Solids **54**, 807–830 (2006)
26. Lopez-Pamies, O., Ponte Castañeda, P.: On the overall behavior, microstructure evolution, and macroscopic stability in reinforced rubbers at large deformations: II—Application. J. Mech. Phys. Solids **54**, 831–863 (2006)
27. Lopez-Pamies, O., Ponte Castañeda, P.: Homogenization-based constitutive models for porous elastomers and implications for macroscopic instabilities: I—Analysis. J. Mech. Phys. Solids **55**, 1677–1701 (2007)

28. Lopez-Pamies, O., Ponte Castañeda, P.: Homogenization-based constitutive models for porous elastomers and implications for macroscopic instabilities: II—Results. J. Mech. Phys. Solids **55**, 1702–1728 (2007)
29. Moraleda, J., Segurado, J., Llorca, J.: Finite deformation of incompressible fiber-reinforced elastomers: A computational micromechanics approach. J. Mech. Phys. Solids **57**, 1596–1613 (2009)
30. Ogden, R.W.: Non-linear Elastic Deformations. Dover, New York (1997)
31. Park, C., Yoon, J., Thomas, E.L.: Enabling nanotechnology with self-assembled block copolymer patterns. Polymer **44**, 6725–6760 (2003)
32. Ponte Castañeda, P.: The overall constitutive behavior of nonlinearly elastic composites. Proc. R. Soc. Lond. A **422**, 147–171 (1989)
33. Ponte Castañeda, P.: The effective mechanical properties of nonlinear isotropic composites. J. Mech. Phys. Solids **39**, 45–71 (1991)
34. Ponte Castañeda, P.: Bounds and estimates for the properties of nonlinear heterogeneous systems. Philos. Trans. R. Soc. Lond. A **340**, 531–567 (1992)
35. Ponte Castañeda, P.: Exact second-order estimates for the effective mechanical properties of nonlinear composite materials. J. Mech. Phys. Solids **44**, 827–862 (1996)
36. Ponte Castañeda, P., Tiberio, E.: A second-order homogenization method in finite elasticity and applications to black-filled elastomers. J. Mech. Phys. Solids **48**, 1389–1411 (2000)
37. Ponte Castañeda, P., Willis, J.R.: The effect of spatial distribution on the effective behavior of composite materials and cracked media. J. Mech. Phys. Solids **43**, 1919–1951 (1995)
38. Ponte Castañeda, P., Willis, J.R.: Variational second-order estimates for nonlinear composites. Proc. R. Soc. Lond. A **455**, 1799–1812 (1999)
39. Racherla, V., Lopez-Pamies, O., Ponte Castañeda, P.: Macroscopic response and stability in lamellar nanostructured elastomers with "oriented" and "unoriented" polydomain microstructures. Mech. Mater. **42**, 451–468 (2010)
40. Willis, J.R.: Bounds and self-consistent estimates for the overall moduli of anisotropic composites. J. Mech. Phys. Solids **25**, 185–202 (1977)
41. Zee, L., Sternberg, E.: Ordinary and strong ellipticity in the equilibrium theory of incompressible hyperelastic solids. Arch. Ration. Mech. Anal. **83**, 53–90 (1983)